Electrical Safety in Hazardous Environments: Ignition Studies.

by

Neil Pennington

Thesis submitted in accordance with the requirements of the University of Liverpool for the degree of Doctor in Philosophy.

August 1990

Department of Electrical Engineering & Electronics.

BRITISH LIBRARY

IMAGING SERVICES NORTH

Boston Spa, Wetherby
West Yorkshire, LS23 7BQ
www.bl.uk

VOLUME CONTAINS CLEAR OVERLAYS

OVERLAYS HAVE BEEN SCANNED SEPERATELY AND THEN AGAIN OVER THE RELEVANT PAGE

For My Late Father,

Thomas Pennington.

ABSTRACT

The work described in this thesis had, as its principal aim, the development of an understanding of the mechanisms influencing the electrical ignition safety of cellulosic materials in hazardous environments.

Two systems were employed in the experimental programme, firstly a short-arc apparatus in which an electrical arc between two carbon electrodes was used as an ignition source, and a laser system which employed a carbon dioxide laser as an ignition source. The short-arc ignition source was mounted inside a pressure vessel to allow experiments to be carried out under conditions of increased gas pressure.

The arc system was used to provide the majority of the experimental data. The behaviour of the combustion characteristics of standard paper samples were examined with particular attention being paid to the flammability, burn time and time to visible flame of the samples. These quantities were investigated as a function of the arc electrical input power over the range from 50W to 100W for various values of gas pressure and oxygen concentration. The pressure in the combustion chamber was varied from 1 to 5 atm. and oxygen concentrations of between 16% and 36% by volume (with the balance being nitrogen) were employed. The effect of dividing the arc radiation into discrete pulses of energy with a variable delay between the two pulses was investigated and the concept of a 'Critical Pulse Delay' was developed. The effects of variations of pulse energy, power level, pressure and oxygen concentration on the critical pulse delay were investigated. It was found that increases of oxygen concentration and/or gas pressure increase the flammability of the samples, decrease the sample burn time, and lengthen

the critical pulse delay. Increasing the power level of the pulses results in a decrease of the critical pulse delay.

The laser system was developed as an alternative ignition source to the arc, and the effect of sample thickness on the penetration time of the laser under conditions of a constant radiant flux of 5W and normal atmospheric conditions was investigated.

A qualitative physical model of the combustion process for cellulosic materials based on the existence of an unique growth/decay balance of flammable species near the surface of the target material has been developed and its application to the results obtained using the experimental apparatus is described. The properties of the arc and the laser as ignition sources are summarised, followed by suggestions for future work which will help to test further the ideas of the combustion model.

Finally, the implications of the experimental results reported in the thesis, and in particular the existence of a critical delay between successive ignition pulses, are put into a wider context in considering electrical safety in hazardous environments.

ACKNOWLEDGEMENTS.

In a work of this kind, in which so many people have been involved, it is difficult to acknowledge every individual, and therefore, I would like to apologise if any one feels that they have been omitted.

I would like to thank my supervisor, Dr. J.A. Rees, for his guidance during the period of research and for his useful suggestions during the preparation of this thesis.

I am grateful to the Ministry of Defence for financing the research; Dr. L. Virr for his support during the first two years; Dr. J. Livesey, and Mr. A. Thomas for their encouragement and support during the final period of research.

I am also grateful to the University of Liverpool for the provision of laboratory facilities for the experimental work.

I would also like to thank the staff in the office and the lads in the mechanical, electronics, glass and instrument workshops, and the stores for their generous assistance; Mrs. Sandra Collins for preparing the drawings and Mr. Alan Evans and Mr. A. West for preparing the photographs contained in the thesis.

Thanks must also go to Mike Feeney for introducing me to the complexities of word processing and to my colleagues in the department, in particular Phil Mellor and the lads in DSP, for the sport, beers, and conversation that help relieve the pressures of work.

I would also like to thank my Mother and sister, Suzanne, for their encouragement and support.

Thankyou Diane for your support and patience in putting up with my swings of mood and the long hours associated with the production of this thesis; without you this work would have been much harder to complete.

LIST OF PRINCIPAL SYMBOLS.

DC	Direct Current.
DTA	Differential Thermal Analysis.
HSE	Health and Safety Executive.
IR	Infra Red.
MTA	Mass spectrometric Thermal Analysis.
NBS	National Bureau of Standards.
NML	Naval Materials Laboratory.
RX	Receiver.
TGA	Thermogravimetric Analysis.
TX	Transmitter.
USNRDL	United States National Radiological Defense Laboratory.
UV	Ultra Violet.
a	absorptivity.
A	Arrhenius pre-exponential factor.
A	area. (m^2)
Bi	Biot Number.
c	specific heat capacity. ($J/kg.K$)
d	electrode gap. (mm)
E	input energy. (J)
E_a	irradiance of arc. (W/mm^2)
E_b	irradiance of laser. (W/mm^2)
E_A	activation energy. ($J/mole$)
E_T	irradiance incident at thermopile. (W/m^2)
f	fraction of heat feedback from flame.
f_c	convective component of heat feedback.

f_r	radiative component of heat feedback.
F_o	Fourier Number.
h	convective heat transfer coefficient. $(W/m.K)$
I	arc current. $(Amps)$
I_A	arc radiant intensity. (W/Sr)
l	length of chamber. (cm)
L	thickness or half thickness. (m)
L_v	latent heat of vaporisation. (J/g)
m	mass of material. (g)
$\dot{m}_b$	rate of mass loss due to burning. (g/s)
$\dot{m}_{cr}$	critical volatile flow rate. (J/g)
$\dot{m}_e$	rate of evaporation of material. (J/g)
n	number of measurements (statistical).
n_C	number of moles of carbon.
n_G	number of moles of gas.
n_{O_2}	number of moles of oxygen.
P	pressure. $(p.s.i.)$ or $(atm.)$
P_A	electrical input power for arc. (W)
$\dot{q}$	rate of heat transfer. (W)
Q	exothermicity of reaction. (W)
$\dot{Q}$	heat generation term (Frank-Kamenetskii) (W)
$\dot{Q}_C$	rate of heat release. (W)
$\dot{Q}_E$	rate of energy supply. (W)
$\dot{Q}_L$	rate of heat loss. (W)
$\dot{Q}_R$	radiative heat flux per unit area. (W/m^2)
r	radial distance. (m)
r_0	characteristic dimension. (m)

R	universal gas constant.
S	area of heat loss. (m^2)
t	time. (s)
t_1	duration of pulse one. (s)
t_2	duration of pulse 2. (s)
t_d	pulse delay time. (s)
T	temperature. (K)
T_a	ambient temperature. (K)
T_{cr}	critical ambient temperature. (K)
T_i	ignition temperature. (K)
T_0	initial temperature. (K)
T_∞	final temperature. (K)
U	firepoint condition.
v	volume of chamber. (m^3)
V	volume. (m^3)
V_A	anode voltage. ($Volts$)
V_C	cathode voltage. ($Volts$)
x	distance. (m)
X	single measurement (statistical).
$\overline{X}$	arithmetic mean (statistical).
α	thermal diffusivity. (m^2/s)
β	thermopile calibration factor. (W/Vcm^2)
δ	dimensionless rate of heat production.
δ_{cr}	critical dimensionless rate of heat production.
$\Delta A, \Delta B$	error on a measurement.
ΔH_c	heat of combustion. (kJ/g) or (kJ/mol)
θ	temperature difference. (K)
K	thermal conductivity. ($W/m.K$)

ρ	density.(g/cm^3)
σ_{n-1}	standard deviation (statistical).
τ	slab thickness. (m)
ϕ_A	arc radiant flux. (W)
ϕ_T	radiant flux incident at thermopile. (W)
ψ	maximum value of heat feedback fraction.
Ω	solid angle. (Sr)

TABLE OF CONTENTS

CHAPTER 1. INTRODUCTION.

The concept of safety engineering when applied to human working conditions is, arguably, a relatively young science; concieved during, and born after, the industrial revolution of the late 19th, and early 20th, century. It was during this turbulent period that mankind first realised the true potential of the environment in which he lived - the seemingly limitless supplies of fossil fuels and metallic ore deposits. However, this new-found wealth brought with it a tendency to over exploit natural reserves and, increasingly, man has had to look to the stars and, perhaps more realistically, to the sea for potential additional sources of fuel reserves.

This move to exploit sea-bed resources has introduced problems for the safety engineer however, particularly when considering the possible electrical hazards associated with working in laboratories or factories[1] in deep sea conditions. A very real consequence of working under the conditions of increased pressure and oxygen concentration typical of sub sea conditions, is that the potential for electrical ignition of materials used in such surroundings can be much greater when compared with the potential under normal atmospheric conditions.

At first glance, it may appear that, in order to operate effectively and without risk, all that is necessary is to find co-existing regions of safe pressure and oxygen concentration in which to operate. There are, however, physiological limits to safe working conditions, as the gas mixtures necessary to support life are highly pressure dependent and an

atmosphere which may offer no risk of electrical ignition may not be capable of life support.

There may also be a problem with the accumulation of gas pockets and variations in the mixing of the gases within the chamber; the assumption that an atmosphere is safe under conditions of electrical ignition will be compromised by their existence.

The provision of safe power levels for the electrical ignition of materials within high pressure, high oxygen environments also provides the engineer with problems. The work contained within this thesis will show, through a comprehensive experimental programme, that when electrical energy is supplied in short pulses, as opposed to a continuous burst, previous ideas concerning safe power levels will have to be reconsidered.

1.1 THE PHYSIOLOGICAL ASPECTS OF HYPERBARIC WORKING CONDITIONS.

The thorax of an unprotected human diver can be compressed to one fifth of its normal size at atmospheric pressure[1], before major problems are encountered. Since a descent through 10m of sea water produces an increase in external pressure of 1atm., this means that the normal human diver can descend to a maximum depth of 50m whilst holding his breath. For a diver to descend to a depth greater than 50m, it is necessary for him to breathe a gas that has a pressure equal to that of the surrounding water; a problem usually solved by the use of a diving suit or a hyperbaric chamber, such as a diving bell.

Although increasing the gas pressure, to compensate for the increase in water pressure due to the depth of dive, has the desired effect on lung "squeeze", another problem is introduced; for a given percentage of oxygen in the inspired gas, the partial pressure of oxygen increases with external pressure. Thus, when breathing air at a pressure of 5atm., a diver is exposed to an oxygen partial pressure equivalent to that of breathing approximately 100% oxygen at atmospheric pressure. When breathed at too high a partial pressure, oxygen is toxic; affecting the lungs and the central nervous system - both effects are a function of time and pressure.

The solution to oxygen toxicity is to dilute the oxygen with inert gases. Diluents commonly used are nitrogen and helium, however both diluents have problems associated with them. The problems incurred when using nitrogen are well documented[2]; principally, as the partial

pressure of nitrogen is increased (due to depth of dive) it has a narcotic effect on the diver, commonly known as "rhapsody of the deep", causing the diver's judgement to become impaired - often with fatal consequences. In addition, because of its high density, a significant nitrogen content in a hyperbaric atmosphere may lead to breathing difficulties. The alternative diluent, helium, has a density one-seventh that of nitrogen, causing far less resistance to breathing, and also eliminates the problem of narcosis. The main drawback when using helium as a diluent is that a diver's speech becomes distorted (the amount of distortion increasing with increase in depth) impeding effective communication. However, this is an acceptable problem that can, to some extent, be resolved using an electronic communication system.

These are some of the many consequences of using gas mixtures in hyperbaric chambers. The implications for ignition safety are wide ranging: a gas mixture containing 1.5% oxygen at atmospheric pressure offers a very low risk of ignition, however, when breathed at a depth of 200m its partial pressure is equivalent to 30% oxygen at atmospheric pressure - an environment which has a high fire risk.

1.2 ELECTRICAL FAILURE: POTENTIAL IGNITION HAZARDS.

Having established that there is an increased fire risk under hyperbaric conditions, it is important to identify the electrical connections typical of a hyperbaric chamber which, under conditions of failure, may lead to the start of a fire.

A comprehensive summary of the electrical equipment employed in the normal operation of hyperbaric sub sea intervention was produced by Virr[3]. Typical appliances are; general life support systems such as heating, lighting and electric fans used in the circulation of gas through CO_2 scrubbers; electric motors used for propulsion; electronic systems such as those used in communications and navigation, and hand-held equipment. All such equipment could, under varying conditions, experience electrical failure leading to ignition of the surrounding gas or materials such as clothing or bedding[2] in the chamber. Another potential electrical hazard comes in the form of electrical cables and connections within a hyperbaric chamber. Virr reported that, at high gas pressures, cables experience "swelling and damage on decompression unless depressurisation proceeds slowly". Clearly this could well result in an electrical fault such as a discharge to ground.

Other applications involving hyperbaric chambers include hospital operating theatres used, for example, when a diver is involved in an accident underwater and has not been able to undergo decompression, or when atmospheres of pure oxygen are required in the treatment of burns. This type of application introduces added ignition hazards such as those involved with ventricular defibrillation - the spark produced, under the right conditions, could have fatal consequences.

Potential ignition sources having been identified, it is now necessary to discuss the incidence and type of fire problems already encountered; many involving loss of human life.

1.3 ELECTRICAL FAILURE: THE CONSEQUENCES.

Three major incidents involving hyperbaric chambers have been reported[4,5,6], each involving the loss of human life.

The first incident, discussed by Dorr[4], occured at the US. Navy Experimental Diving Unit in 1965. Two men were killed when fire broke out in a decompression chamber. The source of ignition was believed to have been an electric motor which overheated and ignited a paper filter situated next to the motor; fire then spread quickly to mattresses and clothing resulting in a complete burn-out of the interior of the chamber. The atmosphere within the chamber was not, at the time, considered hazardous; consisting mainly of 20% O_2, 36% N_2, and *He* at a total pressure of 55 p.s.i.

The second incident, reported by Swan[5], occured at Brooks Air Force Base in 1967 resulting in the deaths of two airmen who were carrying out maintenance work within a space environment simulator. The electrical failure believed to have caused the accident was the fracture of a table lamp cord which shorted to the aluminium chamber floor - the resulting arc causing ignition of the clothing worn by the men. The atmosphere of 100% oxygen at 0.5atm. pressure contributed to an increase in chamber temperature of 800 *'F* in 14 seconds, which led to complete burn-out of the chamber within 32 seconds.

The third incident, reported by Tanaka and Ichikawa[6] occured in a Tokyo hospital in 1969. It is believed that an accidental electrical spark was the cause of the ignition of flammable solid materials within a hyperbaric operating theatre, resulting in burn-out of the chamber.

The above examples clearly indicate that there is a need to carry out research into the electrical ignition of materials under hyperbaric conditions. However, experience shows us that it is not only hyperbaric conditions that can lead to fatal accidents; the incident of November 1987 at King's Cross Underground Station[7] clearly shows that ignition can occur under normal conditions provided that sufficient ignitable fuel is available for exposure to a heat source. One of the many tests performed by the H.S.E. involved using a thermal analyser to give information on the volatiles evolved from certain materials removed from the site of the fire. The flammability of these vapours was then tested using a hot plate to pre-heat the sample, and a pilot flame to heat the vapours produced by the degradation process. The sample was in contact with the plate for 10s, at which point a propane burner flame was applied for 5s; the process was repeated until ignition occured. It was found that, for a plate temperature of 350 $^{\circ}C$, the third application of the burner resulted in ignition with a flame persisting for a short time (refered to as "flash ignition"). However, for a plate temperature of 400 $^{\circ}C$, ignition occured on the second application of the pilot flame. This burning process lasted longer than that described above, and was refered to as "stable burning". Clearly, the distribution of energy with respect to time is an important factor in the ignition safety of materials and we have a need, therefore, to consider normal atmospheric conditions in parallel with those typical of a hyperbaric chamber.

The research programme reported here aims to simulate the conditions, both normal and hyperbaric, which may cause ignition of a flammable material on exposure to an energy source, and to see how the

distribution of that energy, with respect to time, affects the combustion behaviour of the material under test.

1.4 REFERENCES.

[1] Hamilton, R.W. Jr., and Schreiner, H.R., "Putting and Keeping Man in the Sea." Chemical Engineering. (June 1968)

[2] Department of Energy, "Suggested Limits For Contaminants in Hyperbaric Chambers." Offshore Technology Report, OTH86262, H.M.S.O. Books. (1987)

[3] Virr, L.E., "The Role of Electricity in Sub Sea Intervention." I.E.E. Proceedings. Vol.134, Pt.A, No.6. (June 1987)

[4] Dorr, V.A., "Final Report on Combustion Safety in Diving Atmospheres." Contract N00014-66-C-0149, Office of Naval Research, US. Navy. (1971)

[5] Swan, A.G., "Two Man Space Environment Simulator Accident." Proceedings of Fire Hazards and Extinguishment Conference, Brooks Air Force Base. (1967)

[6] Tanaka, R., and Ichikawa,K., "Ignition of Flammable Solid Materials by Electrical Discharges Under Artificial Atmospheres." 2nd International Conference - Electrical Safety in Hazardous Environments. (Dec. 1975)

[7] Wharton, K.R., "Fire at King's Cross Underground Station, 18th November 1987. Part5: Ignition Tests and Characterisation of Samples." H.S.E. Research and Laboratory Services Division, RI/FR/1/87. (March 1988)

CHAPTER 2. THE IGNITION OF MATERIALS: A LITERATURE REVIEW.

There have, perhaps, been two major milestones in the study of the ignition properties of materials. The first was the work of Semenov[1] and, later, Frank-Kamenetskii[2], which provided the first comprehensive studies of the ignition of gaseous systems; the second was the Second World War (1939-1945).

Following the bombing of Hiroshima and Nagasaki, which saw the end of World War II, it was recognised that there was a need to investigate the possibility of the ignition of cellulosic fuels exposed to the intense thermal radiation emitted by a nuclear detonation. Among the groups actively involved in extensive experimental work on the subject were The Naval Materials Laboratory (N.M.L.), The National Bureau of Standards (N.B.S.) and, principally, The National Radiological Defense Laboratory (U.S.N.R.D.L.). Sauer[3], in 1956, attempted to unify all the data available on the charring of semi-infinite slabs of wood exposed to thermal radiation, and found that data from N.M.L., N.B.S., and U.S.N.R.D.L., correlated well when examined by the transient heat conduction equation.

There have since been other comprehensive reviews, notably by Martin[4], Welker[5], and Kanury[6,7].

Martin summarised work performed at U.S.N.R.D.L. His conclusions were that, when cellulose is heated slowly, a large fraction of the original weight remains as carbonaceous residue (char) after the evolu-

tion of highly oxygenated products such as H_2O and CO_2, whilst rapid heating leaves little or no char and the volatile products are, on average, correspondingly richer in carbon. Measurements of volatile products of cellulose exposed to intense radiant energy showed a maximum in the rate of evolution at a time close to the instant of ignition. Levoglucosan, the main volatile component, increases in yield from 25% on exposure to 75% at ignition, these values depending on irradiance levels.

Welker comprehensively discussed the ignition of cellulosic materials by considering the techniques employed by a wide range of experimentors and correlated data using several ignition models. His conclusions were that, although thermal degradation and ignition studies had led to an understanding of the fundamental processes involved, it was not possible to predict, without the benefit of experimental results, whether or not, or when, ignition would occur for a given set of conditions.

Kanury's first review concentrated on unifying the data obtained by a number of investigators in order to find critical surface temperatures for spontaneous and piloted ignition, under conditions of radiative and convective heating. His second review was concerned with the conditions governing the development of hostile fires. He made use of experimental data from a 20 year period to discuss the factors influencing ignition, propagation and growth, and control and extinction phenomena. One of his many salient comments concerned the modelling of a fire; he said that two fires under seemingly similar circumstances, are seldom similar in their behaviour: the material alone has many variables such as thermal conductivity, specific heat capacity, density, and heat of combustion.

Thus, in order to conduct systematic observations on destructive fires, resort is taken to simulating them.

The following review will attempt to highlight some of the important conclusions drawn by a wide range of investigators concerning the thermal degradation and ignition of cellulosic samples, fire retardancy, and the influence of hazardous environments on ignition behaviour.

2.1 THERMAL DEGRADATION.

Martin[8] postulated that the combustion of cellulose involves first, decomposition of the solid into volatiles, and, second, gas phase oxidation of the products after mixing with air. Two competitive reactions were proposed; one consisting of pyrolysis to carbon and oxygenated volatile products, at low heating rates; the second consisting of pyrolysis entirely to volatile products, largely oxygen free, at higher heating rates. Both reactions are first order.

Lipska and Parker[9] studied the volatilisation and decomposition of α- cellulose, without ignition, and postulated that there are three distinct chronological phases of pyrolysis at each temperature studied. After the initial decomposition and weight loss period, both the volatilisation and the decomposition obey an apparent zero order expression, followed by a kinetically first order phase for the weight loss, resulting in a residual char deposit which does not undergo further pyrolysis. They used a single valued activation energy of 42 *kCal/mole* to describe decomposition and volatilisation rates over the temperature range 250 $^{\circ}C$ to 298 $^{\circ}C$.

Two temperature ranges, 200 $^{\circ}C$ to 280 $^{\circ}C$, and 280 $^{\circ}C$ to 340 $^{\circ}C$, were studied by Kilzer and Broido[10] using Differential Thermal Analysis (D.T.A.), Thermogravimetric Analysis (T.G.A.), and Mass spectrometric Thermal Analysis (M.T.A.). It was proposed that in the range 200 $^{\circ}C$ to 280 $^{\circ}C$ cellulose degrades initially to "dehydrocellulose" and H_2O, and then to char, H_2O, CO, CO_2, and other volatile gases. In the range 280

$^{\circ}C$ to 340 $^{\circ}C$ there is a tar-forming reaction (levoglucosan) which is highly reactive, forming char at 320 $^{\circ}C$ with the evolution of volatile gases.

Lincoln[11] also provided useful data on the quantity and type of volatile products obtained from the pyrolysis of cellulose. A carbon arc was used giving irradiances of 1.5 to 11.0 $Cal/cm^2/$ sec and pulse durations of between less than 0.1s and several minutes, in order to study the decomposition products from blackened α-cellulose. The principal products found were H_2O, CO_2, CO, twelve volatile organic compounds, char and tar.

Lincoln came to several interesting conclusions: slow heating of the cellulose produced primarily water and char, whilst rapid heating yielded more tar; also the average molecular weight of pyrolysis products from flash heating was much lower than that found for longer duration pulses. Observations of considerable importance to fire research were that the higher irradiances yield much larger amounts of CO and organic volatiles, all of which are quite combustible, and that short lived species are produced from the flash pyrolysis of cellulose.

Cullis et al.[12] used a furnace/gas-flow system at a maximum temperature of 1300K and an average heating rate of 12°/ sec to study the pyrolysis of 1mm thick cellulose strips. The gaseous products detected over the temperature range 523K to 823K were N_2, CO, CO_2, O_2, H_2, CH_4, C_2H_4, and C_3H_6.

Motivated by the need to understand the source of pollutant species in wood-burning stoves, Ohlemillar et al.[13] examined the products generated when wood is heated, without flaming, in atmospheres of varying

oxygen concentration. Small wood samples were exposed to varying radiant heat fluxes (2 - 7.8 W/cm^2) and varying oxygen concentration (0 - 21% O_2 in N_2). Sample weight was monitored in some tests, and temperature, using five embedded thermocouples, in others. In all tests, the gaseous products were monitored; principally H_2O, CO, CO_2, and tar. It was found that the mass flux for a sample degrading in air is twice as large as in nitrogen, and that the amounts of CO and CO_2 increase with an increase in ambient oxygen concentration.

Although the majority of combustion studies are concerned with the application of thermal energy to the surface of the sample, conclusions similar to those illustrated above were drawn by Flynn et al.[14] when considering the photochemical degradation of cellulose. Sheets of cotton were dried and irradiated in a vacuum, at 40 $^{\circ}C$, by light having a wavelength of 253.7 nanometers. The composition and rate of evolution of gaseous products were measured. It was found that H_2 (87.5 mole%), CO_2 (4.3 mole%), and CO (8.2 mole%) were evolved during irradiation, and that the fraction of H_2 decreased with increase in irradiation time; the fraction of CO to CO_2 remaining approximately constant.

We have seen the conclusions drawn by a variety of investigators as to what happens to cellulose when it degrades under a radiant flux. However, nothing has been mentioned concerning the process of ignition for such a solid material. Ignition phenomena are considered in the following section.

2.2 IGNITION PHENOMENA.

There have been many investigations into the ignition behaviour of solid materials, both mathematical and experimental. Since the nature of the present research is experimental, we will concentrate on the latter category.

Gross and Robertson[15] proposed that ignition depends on a critical temperature balance; where the heat generated in a material, over a long period of time, is equal to the heat lost. At this condition, a slight increase in either the "critical" bulk size or the "critical" ambient temperature (effectively the ignition temperature) results in self (or spontaneous) ignition.

Martin and Lai[16] studied the ignition behaviour of blackened α-cellulose exposed to thermal pulses typical of those produced by a nuclear blast. They found that the ignition behaviour showed three different regions: sustained glowing ignition at low irradiances and long exposures; sustained flaming ignition at shorter exposures and higher irradiances; unsustained flaming ignition at very short times and high peak irradiances.

Akita[17] proposed that a criterion for the ignitability of a solid should be the ignition lag: the time elapsed between the application of heat and the formation of a flame. During his studies he made use of a Tesla coil spark and a hot surface to divide the ignition of wood into auto ignition (spontaneous), kindled ignition (pilot), and self ignition.

A significant contribution to the discussion of the radiative ignition of cellusic fuels has been made by Simms[18,19,20], at the Fire Research Station, Borehamwood. Simms made use of three sources of radiation: a 1ft. square gas-fired radiant panel, and two sources from which the radiation is focussed by an ellipsoid mirror; one being a tungsten filament lamp; the other a carbon arc.

In his first study, Simms was concerned with spontaneous ignition, that is, the ignition of the volatile gases without the presence of an extraneous igniting source. He found that ignition first occurs in the gas phase; flame is seen to appear well away from the surface. Of the factors affecting ignition, external draughts and the supply of volatiles are likely to determine whether ignition can occur. Using the same ignition sources, he went further in his second study in which he found that ignition of the volatiles occurs when the stream of volatiles becomes turbulent. If turbulence does not occur within a short distance of the point of emission of the volatiles, ignition does not occur, even though the temperatures of the solid and the volatile stream are the same as when ignition does occur. One explanation for this was that this may be due to turbulence increasing the size of the reacting zone, and by increasing the rate of mixing with air. However, Simms also found that even though an external draught, by making the volatile stream turbulent, reduces the ignition threshold, if ignition originally occurs in the absence of a draught, its imposition does not affect the ignition time.

Pilot ignition by radiation was the subject of Simms's third study, where the volatiles produced during the degradation process are ignited by a pilot flame, or spark, and the flame flashes back to the surface. A

number of woods were subjected to radiation from a gas-fired radiant panel. A pilot flame was placed above the surface, and its position varied in order to study the variation of ignitability with position and size of pilot flame. The conclusions reached, were that the pilot ignition time depends, not only upon the intensity of radiation and the density of the wood, but also upon the position and possibly upon the size of the pilot flame, also.

Koohyar et al.[21] studied both the spontaneous and pilot ignition characteristics of five species of wood; fir, mahogany, oak, pine, and redwood, using a line buoyant diffusion flame having an irradiance level between 0.275 and 0.855 $Cal/cm^2/$ sec. Their conclusions agreed with those of Simms, in that they found that, in order for an irradiated cellulosic material to ignite, it is necessary to form a combustible mixture in the volatile stream at a point where the temperature is high enough for this mixture to ignite.

The effect of moisture levels on the ignition behaviour of cellulosic fuels was studied by Simms and Law[22]. Specimens of wood were oven-dried and conditioned to moisture content. The specimens were exposed to decreasing levels of radiation until it was reasonable to assume that ignition would not take place because the evolution of volatiles was too low. Both pilot and spontaneous ignition data were taken and the ignition time recorded. It was found that the effect of moisture, for any wood, is to increase the ignition time, the total ignition energy required, and the minimum intensity necessary for both spontaneous and pilot ignition.

The effect of sample orientation on ignition was investigated by Kashiwagi[23]. A CO_2 laser and a gas-fired radiant panel were used as radiant heat sources in order to study the radiative ignition of vertical and horizontal samples (1.5cm thick). It was found that the vertically mounted sample forms a thinner buoyant boundary layer of decomposition products, and the interaction of the plume with the horizontal external radiation source is much less than that for a horizontal sample.

A xenon lamp was employed by Yoshizawa and Kubota[24] to clarify the mechanism of the gas phase ignition of a cellulosic solid. The 1kW xenon lamp was focussed on small cellulose bricks using an ellipsoid mirror to give a heat flux of 30 W/cm^2. The time and space variations of the temperature and fuel concentration, in the gas phase, were examined precisely during ignition, by means of a Mach-Zender interferometer and a gas sampler. The ignition point where the flame kernel first appeared was determined, and the transition from ignition to quasi-steady flame was followed by means of a Schlieren system. It was found that when the cellulose is irradiated, it first produces CO and CO_2 by endothermic reactions, and then generates small amounts of hydrocarbons by exothermic reactions. Ignition follows in the region where the gaseous fuel concentration is extremely high, and is controlled by gas phase reactions of the minor species.

As can be seen above, the study of the thermal degradation, and the subsequent ignition behaviour of cellulosic materials, has been extensive. It is not surprising, therefore, to find that the nature of flame spread, and, in particular, the property of fire retardancy, has been the subject of a variety of investigations.

2.3 FIRE RETARDANCY AND THE SPREAD OF FLAME.

Ignition, and the spread of flame, can be inhibited in several ways: principally by the addition of inorganic retardants, removal of the ignition source, and by the reduction of pressure or ambient oxygen concentration.

Laible[25] studied the ignition behaviour of textile fabrics, mainly cellulose, treated with fire retardants. His most persuasive argument, concerning the action of a fire retardant, was based on the production of levoglucosan, an intermediate product of the degradation of pure cellulose. It was found that modifying cellulose to reduce the formation of levoglucosan (which degrades to tar and volatiles) had the desired flame retardation effect.

Schwenker and Pacsu[26] also came to the conclusion that the formation of levoglucosan is an important intermediate stage, and that flammability is due to the further breakdown of levoglucosan to give flammable gases and tars. A series of halogens were tested as potential retardants, and it was concluded that the relative efficiency was: Iodine > Bromine > Chlorine > Fluorine.

A similar conclusion was drawn by Kilzer and Broido[10], who observed that fire retarding agents in cellulose, catalyse a dehydration and char forming reaction at the expense of a de-polymerisation reaction, of which levoglucosan is the product.

Sibulkin and Tewari[27] studied samples prepared from pure cellulose, and from cellulose that had been treated with *NaOH* and

Na_2CO_3. The samples were burned at atmospheric pressure in mixtures of oxygen and nitrogen. Measurements of burning rates for pure and retarded cellulose, show the rates to increase with ambient oxygen concentration. The amount of retardant required to cause extinction is found to increase sharply as the oxygen concentration is increased.

Rasbash and Langford[28] also found that the ambient oxygen concentration was a vital factor in extinction and fire retardancy observations. Wooden dowels were burned in atmospheres of reduced oxygen concentration, using N_2 and CO_2 as diluents. It was found that flames were extinguished as the oxygen concentration was reduced, and a lower limit of oxygen concentration in N_2 of 11.3% by volume was found for a constant radiant flux.

Itoh and Kurosaki[29], rather than measuring the inhibition of flame spread, were concerned with the effect of flame spread on several parallel sheets of paper in close proximity to one another. It was found that the flame spread rate increases with the number of sheets, and approaches a constant value.

Martin and Broido[30] identified several factors influencing fire control during their studies on high altitude nuclear detonations. They identified dried leaves, grasses, and furniture fabrics (all cellulose based) as the most fire-prone fuels. The main factors influencing fire extinction were: reduction of potential ignition sources, provision for rapid extinguishment, and the reduction of fire spread potential.

We have been concerned, above, with the combustion behaviour of cellulosic fuels under atmospheric or sub-atmospheric pressures, and

normal or reduced oxygen concentrations. Clearly, these conditions serve to reduce the potential for ignition hazards. Any review into the combustion behaviour of a cellulosic solid, particularly with safety in mind, should, however, include a discussion of the behaviour of solids under conditions of increased pressure (hyperbaric) and increased oxygen concentration, i.e. in hazardous environments.

2.4 IGNITION IN HAZARDOUS ENVIRONMENTS.

The ignition of, and flame spread over, several fabrics and paper were studied by Woods and Johnson[31], under pressures from 315p.s.i., down to the limiting pressures for ignition. It was found that the minimum total pressure limit for ignition of the standard filter paper used, is much lower at 41% O_2 than at 21% O_2 in oxygen/nitrogen mixtures. It was also found that, in general, materials have a faster burning rate in mixtures of oxygen with helium than in mixtures of oxygen with nitrogen. The nature of the material under test was also shown to have a marked influence on the effect that variables such as oxygen content and diluent have on the rate of burning.

A significant contribution to research into combustion in hazardous environments was made by Dorr[32,33]. The first study was divided into three phases; firstly, to determine the effect of pressure, oxygen concentration, and diluent gas, on the burning rate of standard materials such as filter paper; secondly, to determine the minimum oxygen concentration required to burn flammable solids in the presence of nitrogen and helium; thirdly, to define a new fire resistance scale for fabrics. The tests

were conducted in a 15x51cm cylinder, with the burning rates of filter paper determined over a pressure range of 1 to 10atm., in mixtures of 15 to 100% oxygen in helium or nitrogen. It was found that raising the pressure, or increasing the oxygen concentration, always raises the burning rate; accelerated burning rates are evident when helium is substituted for nitrogen as the diluent gas at the same partial pressure.

Upon extending his study to consider safe working conditions, it was found that, at high pressure, the oxygen partial pressure is limited physiologically; because of this the region where no combustion can occur is limited. When helium is used as the diluent gas, this region is expanded compared with that for nitrogen. Clearly, when it is impractical to work in these regions, it is important to reduce any ignition risks to a minimum.

Dorr's second study was concerned with the ignition behaviour of materials suggested for use in hyperbaric decompression chambers. The ignition sources used were designed to simulate possible electrical hazards, such as the spark produced when removing a plug from a socket, and the failure of an electrical motor. The same conclusions on burning rate were reached as in the previous study, but difficulties were found in relating small scale test results to those obtained using a full size decompression chamber.

Johnson and Woods[34] also made use of two chambers; one, 12.6 litres in volume, was used for atmospheric pressure tests; another, 142 litres in volume, was used to an upper pressure limit of 75p.s.i. The specimens were exposed to a "hot" nichrome wire, and observed through a viewing port. It was observed that there was a greater ignition delay,

and difficulty of igniting the samples, in an oxygen/helium mixture than for an oxygen/nitrogen mixture; this was explained on the basis of helium having a greater thermal conductivity than nitrogen. It was also observed that there is an increase in flammability with increase in oxygen concentration, and to a lesser degree with increased pressure, although it was concluded that no simple multiplying factor can be applied in predicting flammability in unusual atmospheres, from data obtained under normal conditions.

Bartels and Howes[35], although concerned with the ignition of gases using an inductive circuit, provided some interesting observations on the effects of pressure and oxygen concemtration on minimum igniting currents. It was found that the minimum igniting current was reduced with increased pressure. A reduction of 37% in current, when the pressure is doubled, was compared with the work of Lewis and Von Elbe[36], in which a 60% reduction in minimum energy was observed for the same pressure change. It was found that, since the circuit used was inductive, the reductions were consistent when considering minimum energy. Thus, the flammability did not depend on the absolute value of circuit parameter; only on the value of energy supplied to the system. It was also observed that oxygen enrichment reduces the minimum igniting current; a result which was again consistent with the findings of Lewis and Von Elbe.

Tanaka and Ichikawa[37] also found that the minimum igniting currents and the minimum igniting voltages, for inductive and capacative circuits respectively, decrease with increasing oxygen concentration and

the total pressure. However, it was seen that the effect of the oxygen concentration is much larger than that of the pressure.

The trends illustrated above were also observed by Brennan[38] using, primarily, a carbon arc as a source of radiant energy. It was found that the ignitability of thin cellulosic samples was drastically increased with increase in oxygen concentration, and, to a smaller extent, pressure. However, care must be taken when refering to the absolute values of minimum ignition time, due to the variability of the energy supply.

The nature of the combustion behaviour of materials, under varying environmental conditions, has been the subject of extensive research. However, the Author agrees with the conclusions drawn by Welker[5], that, 20 years further on, even though a great deal is understood about the processes involved, we are still unable to predict when, or whether or not, ignition will occur.

The following theoretical study, contained in Chapter3, does not attempt to predict the ignition behaviour of a solid material, but attempts to identify the various parameters, and the role taken by these parameters, in the combustion process.

2.5 REFERENCES.

[1] Semenov, N.N., "Theories of Combustion Processes." Z, Phys. Chem., 48, pp.571-582 (1928)

[2] Frank-Kamenetskii, D.A., "Temperature Distribution in Reaction Vessel and Stationary Theory of Thermal Explosion." Journal of Phys. Chem. (USSR), 13, pp738-755. (1939)

[3] Sauer, F.M., "The Charring of Wood During Exposure to Thermal Radiation: Correlation Analysis for Semi-Infinite Solids." U.S.D.A. Forest Service. (1956)

[4] Martin, S., "Ignition of Organic Materials by Radiation." Fire Research Abstracts and Reviews, 7, pp.85-97. (1965)

[5] Welker, J.R., "The Pyrolysis and Ignition of Cellulosic Materials: A Literature Review." J. Fire & Flammability, 1, pp.12-29. (1970)

[6] Kanury, A.M., "Ignition of Cellulosic Solids-A Review." Fire Research Abstracts and Reviews, 14, pp.24-52. (1972)

[7] Kanury, A.M., "The Science and Engineering of Hostile Fires." Fire Research Abstracts and Reviews, 18, pp. 72-96. (1976)

[8] Martin, S.B., "The Mechanisms of Ignition of Cellulosic Materials by Intense Thermal Radiation." Research and Development Technical Report, USNRDL-TR-102. (1956)

[9] Lipska, A.E., and Parker, W.J., "Kinetics of the Pyrolysis of Cellulose Over the Temperature Range 250 °C to 300 °C." USNRDL-TR-928. (Nov. 1965)

[10] Kilzer, F.J., and Broido, A., "Speculations on the Nature of Cellulose Pyrolysis." Pyrodynamics, 2, pp.151-163. (1965)

[11] Lincoln, K.A., "Flash Pyrolysis of Solid Fuel Materials by Thermal Radiation." Pyrodynamics, 2, pp.133-143. (1965)

[12] Visanuvimol, V., "Pyrolysis of Cellulose Under Conditions of Rapid Heating." Combustion & Flame, 49, pp.235-248. (1983)

[13] Ohlemillar, T.J., Kahiwagi, T., and Werner, K., "Wood Gasification at Fire Level Heat Fluxes." Combustion & Flame, 69, pp.155-170. (1987)

[14] Flynn, J.H., Wilson, W.K., and Morrow, W.L., "Degradation of Cellulose in a Vacuum with Ultra-Violet Light." Journal of Research-N.B.S., 60, pp.229-233. (1958)

[15] Gross, D., and Robertson, A.F., "Self Ignition Temperatures of Materials from Kinetic Reaction Data." Journal of Research-N.B.S., 61, pp.413-417. (1958)

[16] Martin, S.B., and Lai, W., "Thermal Radiation Damage to Cellulosic Materials." Research and Development Technical Report, USNRDL-TR-252, (1958)

[17] Akita, K., "Studies on the Mechanism of Ignition of Wood." Report of the Fire Research Institute of Japan, 9, pp.1-44,51-54,77-83,99-105. (1959)

[18] Simms, D.L., "Ignition of Cellulosic Materials by Radiation." Combustion & Flame, 4, pp.293-300. (1960)

[19] Simms, D.L., "Experiments on the Ignition of Cellulosic Materials by Thermal Radiation." Combustion & Flame, 5, pp.369-375. (1961)

[20] Simms, D.L., "On the Pilot Ignition of Wood by Radiation." Combustion & Flame, 7, pp.253-261. (1963)

[21] Koohyar, A.N., Welker, J.R., and Sliepevich, C.M., "The Irradiation and Ignition of Wood by Flame." Fire Technology, 4, pp.291-294. (1968)

[22] Simms, D.L., and Law, M., "The Ignition of Wet and Dry Wood by Radiation." Combustion & Flame, 11, pp.377-388. (1967)

[23] Kashiwagi, T., "Effects of Sample Orientation on Radiative Igntion." Combustion & Flame, 44, pp.223-245. (1982)

[24] Yoshizawa, Y., and Kubota, H., "Experimental Study on Gas-Phase Ignition of Cellulose Under Thermal Radiation." Nineteenth Symposium(International) on Combustion, pp.787-795. (1982)

[25] Laible, R.C., "Recent Work on the Mechanism of the Thermal Degradation of Cellulose." American Dyestuff Reporter, 46, pp.173-178. (1958)

[26] Schwenker, R.F., Jr., and Pacsu, E., "Chemically Modifying Cellulose for Flame Resistance." Industrial and Engineering Chemistry, 50, pp.91-96. (1958)

[27] Sibulkin, M., and Tewari, S.S., "Measurements of Flaming Combustion of Pure and Fire-Retarded Cellulose." Combustion & Flame, 59, pp.31-42. (1985)

[28] Rasbash, D.J., and Langford, B., "Burning of Wood in Atmospheres of Reduced Oxygen Concentration." Combustion & Flame, 12, pp.13-40. (1968)

[29] Itoh, A., and Kurosaki, Y., "Dowmward Flame Spread Along Several Vertical, Parallel Sheets of Paper." Combustion & Flame, 60, pp.269-277. (1985)

[30] Martin, S., and Broido, A., "Thermal Radiation and Fire Effects of Nuclear Detonations." USNRDL Technical Report 652. (May, 1963)

[31] Woods, F.J., and Johnson, J.E., "Flammability in Unusual Atmospheres, Part2. Selected Materials in Oxygen-Nitrogen and Oxygen-Helium Mixtures at Pressures up to 315p.s.i.a." NRL Report 6606. (Sept., 1967)

[32] Dorr, V.A., "Fire Studies in Oxygen-Enriched Atmospheres." The Journal of Fire and Flammability, 1, pp.91-106. (1970)

[33] Dorr, V.A., "Effects of Environmental Parameters Upon Combustion of Fire-Resistant Materials, Potential Electrical Sources of Ignition and Analysis of Combustion Products." Annual Report on Combustion Safety in Diving Atmospheres. (1971)

[34] Johnson, J.E., and Woods, F.J., "Flammability in Unusual Atmospheres, Part1. Preliminary Studies of Materials in Hyperbaric Atmospheres Containing Oxygen, Nitrogen, and/or Helium." NRL Report 6470. (Oct. 1966)

[35] Bartels, A.L., and Howes, J.A., "The Variation of Minimum Igniting Currents with Pressure, Temperature and Oxygen Enrichment." Electrical Research Association Report. (March 1971)

[37] Tanaka, T., and Ichikawa, K., "Ignition of Flammable Solid Materials by Electrical Discharges Under Artificial Atmospheres." 2nd International Conference on Electrical Safety in Hazardous Environments. (Dec. 1975)

[38] Brennan, J.F.M., "Ignition of Materials Under Conditions of Hyperbaric High Oxygen Concentration." PhD Thesis, Liverpool University. (1987)

CHAPTER 3. THE IGNITION OF MATERIALS: THEORY

When considering the ignition of materials, it is convenient to distinguish two main types of ignition, namely, pilot ignition in which flaming is initiated by an external heat flux called a pilot, and spontaneous ignition, in which flaming develops spontaneously within the material under test.

The aim of this chapter will be to develop an understanding of the processes in volved in ignition and, as the present research is concerned with the ignition of thermally thin - low Biot number - cellulosic samples, the main thrust of the discussion will be centred on the ignition of solids.

As seen in the previous chapter, a considerable amount of research has been performed on combustible solids, producing a variety of ideas as to their ignition behaviour. There is broad agreement, however, that the processes governing the ignition of a cellulosic solid in a fixed atmosphere are transient thermal conduction in the solid, resultant pyrolysis and outflow of gaseous volatile pyrolysates, and, finally, the combustion of gaseous volatiles mixed with oxygen.

In order to gain an insight into the above processes, it will be necessary to consider the ignition of gaseous vapour - oxygen mixtures; developing our ideas through the ignition of vapour - liquid mixtures; finally reaching an understanding of the processes involved in the ignition of solid materials.

3.1 THE IGNITION OF FLAMMABLE VAPOUR - OXYGEN MIXTURES.

In order for a reaction in the gas phase to be self sustaining and to propagate as a flame, it is not the amount of energy formed by the reaction, but the rate of energy release that is important. If, according to Semenov[1], we assume a first order Arrhenius temperature dependence for the oxidation process, we may express the rate of heat release within a small volume, V, as;

$$\dot{Q}_C = QV\rho A \exp\left(\frac{-E_A}{RT}\right) \tag{3.1}$$

where Q is the exothermicity of the reaction; ρ is the density; A is a pre-exponential factor (whose units depend on the order of the reaction); and E_A is the Activation energy.

If we now consider heat losses in the reacting system, we may be able to deduce a critical point which we can define as the onset of ignition of the system. Assuming convective losses;

$$\dot{Q}_L = h.S\Delta T \tag{3.2}$$

where ΔT is a temperature difference between the reaction volume and the surroundings; S is the area of the reaction volume through which heat is lost; and h is the Newtonian heat transfer coefficient.

Clearly, if $\dot{Q}_C = \dot{Q}_L$, then we have a point of equilibrium, and any perturbations will lead to instability. Thus for $\dot{Q}_C < \dot{Q}_L$, the temperature is reduced and the system will cool; for $\dot{Q}_C > \dot{Q}_L$, the system will rapidly

increase in temperature to give a stable high temperature combustion reaction which can propagate as a flame. So, in order to ignite a vapour - oxygen system at an ambient temperature, say T_a, enough energy must be available to change the system from its stable state at a low temperature to an unstable state at a temperature greater than some critical temperature. This is consistent with the concept of a minimum ignition energy[2,3] which has allowed the design of electrical equipment for use in flammable atmospheres.

The existence of a critical ignition temperature for flammable mixtures led Semenov to develop his thermal explosion theory based on equations (3.1) and (3.2). It is assumed that the system can be treated with a "lumped thermal capacity" approach (this will be discussed further in relation to solids); that reactant consumption is negligible and that all heat losses are described by equation (3.2). Values of $\dot{Q}_C$ and $\dot{Q}_L$ are plotted against temperature for different values of T_a.

The critical temperature for ignition ($T_a = T_{cr}$) is defined as that point at which the plot of $\dot{Q}_C$ intersects that for $\dot{Q}_L$. At this point;

$$\dot{Q}_C = \dot{Q}_L \tag{3.3}$$

and, since the two curves are tangential at this point,

$$\frac{d\dot{Q}_C}{dT} = \frac{d\dot{Q}_L}{dT} \tag{3.4}$$

Substituting equations (3.1) and (3.2);

$$QV\rho A \exp\left(-\frac{E_A}{RT}\right) = h.S(T - T_{cr}) \tag{3.3a}$$

and,

$$\frac{E_A}{RT^2}.QV\rho A \exp\left(\frac{-E_A}{RT}\right) = h.S \qquad (3.4a)$$

dividing,

$$\frac{RT^2}{E_A} = T - T_{cr} \qquad (3.5)$$

where T is the equilibrium gas temperature, and T_{cr} is the critical ambient temperature. Thus the right hand side of equation (3.5) is the maximum temperature rise that can occur within the system without ignition taking place.

This an over-simplified view, as temperature gradients do exist in the reacting gas system. A model taking these gradients into account was developed by Frank- kamenetskii[4], and makes use of the three-dimensional heat conduction equation;

$$\nabla^2 T = \frac{1}{\alpha}\frac{\partial T}{\partial t} - \frac{\dot{Q}}{K} \qquad (3.6)$$

where α is the thermal diffusivity, and K is the thermal conductivity. (Equation (3.6) will be discussed in more detail in relation to the ignition of solids).

When this is reduced to the one-dimensional case and assuming an Arrhenius reaction rate; no reactant consumption; high Biot number giving conduction as the process controlling heat loss; and constant thermal properties of the system, an expression for the dimensionless rate of heat production in the system, δ, is obtained[5] thus;

$$\delta = \frac{r_0^2 E_A Q \rho A}{KRT_a^2} \exp\left(\frac{-E_A}{RT_a}\right) \tag{3.7}$$

We can then define a critical rate of heat production, δ_{cr}, such that ignition occurs when $\delta > \delta_{cr}$. Rearranging equation (3.7) and taking logarithms;

$$\log\left(\frac{\delta_{cr} T_{cr}^2}{r_0^2}\right) = \log\left(\frac{E_A Q \rho A}{KR}\right) - \frac{E_A}{RT_{cr}} \tag{3.8}$$

thus, providing our assumptions are valid and that the first term of the right hand side is constant,

$$\log\left(\frac{\delta_{cr} T_{cr}^2}{r_0^2}\right) \propto \frac{1}{T_{cr}} \tag{3.8a}$$

which is a statement on the relationship between r_0 (the characteristic dimension of the system) and the critical ambient temperature.

For a simple physical view of gaseous combustion, equation (3.5) is interesting. However, equation (3.8) takes into account the size of the reacting vessel. It can be seen[6] that the minimum auto ignition temperature of the mixture decreases with increase in the reacting volume. If we consider the boundary layer close to a heated surface of limited area, the temperature necessary for ignition increases with decrease in surface area[7].

3.2 THE IGNITION OF LIQUIDS.

As in the case of combustible gas mixtures, the ignition behaviour of liquids is determined by the attainment of some minimum critical temperature, the flash point, which is the lowest temperature of the liquid at which a flammable vapour - oxygen mixture is formed at its surface[8] and is ignited. This is usually measured in a closed cup apparatus[9]. However, measurements have also been carried out in an open cup arrangement[10]. Generally, open cup flash points are higher than those found using closed cup tests, and vary with height above the liquid due to the change in vapour concentration, which decreases with increase in height from the surface of the liquid.

If the ignition of the vapour is to lead to sustained burning, as opposed to transient burning at the flash point, the temperature of the liquid must be greater than the so-called "fire point". The fire point of a liquid is defined as "the lowest temperature at which ignition of the vapours in an open cup is followed by sustained burning."[11].

We may analyse those factors which determine the fire point of a liquid (and similarly of a solid) by first considering the rate of evaporation from the surface under steady-state conditions, which, according to Drysdale[11], is given by;

$$\dot{m}_e = \frac{\dot{Q}_E - \dot{Q}_L}{L_v} \tag{3.9}$$

Thus the amount of material being evaporated depends on the difference between the energy supplied and the heat losses, divided by a constant

which depends on that particular material (in this case the latent heat of vaporisation).

If a flame is established at the surface, then the rate of evaporation, or rate of burning, is increased due to heat being transfered back to the surface, thus;

$$\dot{m}_b = \frac{f\Delta H_c \dot{m}_b + \dot{Q}_E - \dot{Q}_L}{L_v}. \tag{3.10}$$

where ΔH_c is the heat of combustion, and f is a fraction which represents the proportion of the heat of combustion transfered back to the surface; it has radiative and convective components, f_r and f_c respectively, hence;

$$\{(f_r + f_c)\Delta H_c - L_v\}\dot{m}_b + \dot{Q}_E - \dot{Q}_L = U \tag{3.11}$$

where $U = 0$ for steady burning.

Let us consider equation (3.11) at the fire point. At this point the flame is non-luminous and so f_r is small (it increases under conditions of steady burning); we shall assume zero. Conversely, f_c is large and approaches a maximum at the fire point (decreasing as steady burning develops). At the fire point let $f_r = 0$, $f_c = \psi$, and $\dot{m}_b = \dot{m}_{cr}$, the critical volatile flow rate, then;

$$(\psi\Delta H_c - L_v)\dot{m}_{cr} + \dot{Q}_E - \dot{Q}_L = U \tag{3.12}$$

This gives us the conditions under which the ignition of volatiles leads to sustained burning. Equation (3.12) was first proposed by Rasbash[12], and will be considered in relation to the ignition of solids later in the chapter. Refering to equation (3.12), steady burning will de-

velop after ignition if there is enough heat available to cause an increase in surface temperature and overcome heat losses, i.e. only if $U > 0$. The conditions of flash point and fire point can be observed, under surface heating, for solids[13]. However, unlike for the case of liquids, they cannot be specified merely in terms of a bulk temperature. In the case of a liquid there is an equilibrium vapour pressure, whose existence determines the flashpoint, but does not require chemical decomposition of the liquid state. In the case of a solid, however, the generation of gaseous volatiles normally involves chemical decomposition of the solid, which is an irreversible process.

In order to understand the ignition of a solid material, then, it is not sufficient to define a critical bulk temperature for ignition; it is also necessary to obtain a heat balance at the surface of the solid based on equation (3.6).

3.3 THE IGNITION OF SOLIDS.

As has been shown above, it is desirable to consider the transfer of heat within the surface of a solid, in order to understand the ignition process. Let us refer again to equation (3.6);

$$\nabla^2 T = \frac{1}{\alpha}\frac{\partial T}{\partial t} - \frac{\dot{Q}}{K} \qquad (3.6)$$

This equation is derived[11] by considering transient heat conduction through an element of volume $dx.dy.dz$. Taking the flow of heat in the x-direction, the rate of heat transfer through an area ds is;

$$\dot{q}_x.ds = -K\frac{\partial T}{\partial x}.dy.dz. \tag{3.13a}$$

Similarly, the flow of heat out of the volume element is;

$$\dot{q}_{x+dx}.ds = -K\left(\frac{\partial T}{\partial x} + \frac{\partial^2 T}{\partial x^2}.dx\right).dy.dz. \tag{3.13b}$$

The difference in the two equations gives us the net change of energy content of the small volume, thus;

$$(\dot{q}_x - \dot{q}_{x+dx}) = K\frac{\partial^2 T}{\partial x^2}.dx.dy.dz. \tag{3.14}$$

This can be described in terms of two quantities, namely heat storage and heat generation, thus;

$$K\frac{\partial^2 T}{\partial x^2}.dx.dy.dz = \rho c\frac{\partial T}{\partial t}.dx.dy.dz - \dot{Q}.dx.dy.dz. \tag{3.15a}$$

or,

$$\frac{\partial^2 T}{\partial x^2} = \frac{1}{\alpha}\frac{\partial T}{\partial t} - \frac{\dot{Q}}{K} \tag{3.15b}$$

In three-dimensions;

$$\nabla^2 T = \frac{1}{\alpha}\frac{\partial T}{\partial t} - \frac{\dot{Q}}{K} \tag{3.6}$$

where α is the thermal diffusivity of the material, ρ is the density, and c is the specific heat capacity. $\dot{Q}$ is a heat generation term which takes

into account exothermic or endothermic change due to change of phase and thermal decomposition.

Chemical decomposition and the associated energy changes are neglected in the following discussion, although this is clearly questionable. However, the effect of decomposition can be considered as having second order status in order to allow us to study the basic principles which control the ignition of solids.

We will now write equation (3.6) as;

$$\nabla^2 T = \frac{1}{\alpha}\frac{\partial T}{\partial t} \tag{3.16}$$

or in the x-direction;

$$\frac{\partial^2 T}{\partial x^2} = \frac{1}{\alpha}\frac{\partial T}{\partial t} \tag{3.16a}$$

3.3.1 Ignition Due to Convective and Radiant Heat Fluxes

Equation (3.16) can be applied directly to conduction through materials which may be treated as "infinite slabs" or "semi-infinite solids".

In order to see how the mode of heating (convective or radiative) influences the ignition of a solid, we will consider two cases; firstly, that of a slab exposed to convective heating on both faces; secondly, that of a slab exposed to radiant heating on one face and convective cooling on both faces. Clearly, the latter case is that which is most applicable to

the present research, however there may be some contribution from convective heat transfer, and a comparison between the two cases will be useful.

3.3.1.1 The Convective Case.

The solution to the problem of an infinite slab of thickness $2L$ ($x = 0$ at the mid-plane) and temperature $T = T_0$, suddenly exposed to air at temperature $T = T_\infty$, is non-trivial, but can be found in standard heat transfer texts[14]. Welty at al.[15] state;

$$\frac{\theta}{\theta_0} = \frac{T - T_\infty}{T - T_0} = 2 \sum_{n=1}^{\infty} \frac{\sin \delta_n \cos(\delta_n \frac{x}{L})}{\delta_n + \sin \delta_n \cos \delta_n} \exp(-\delta_n^2 Fo). \quad (3.17)$$

where the $\delta_n$are roots of the equation;

$$\delta_n \tan \delta_n = \frac{hL}{K}. \quad (3.17a)$$

For our purposes this comprehensive solution reveals that the ratio $\frac{\theta}{\theta_0}$, is a function of three dimensionless quantities; the Biot number; the Fourier number; and $\frac{x}{L}$.

The Biot number,

$$Bi = \frac{hL}{K} \quad (3.18)$$

is a measure of the efficiencies with which heat is transfered to the surface, from the gas, by convection, and from the surface into the bulk of the material by conduction.

The Fourier number,

$$Fo = \frac{\alpha t}{L^2} \tag{3.19}$$

is a dimensionless time variable taking into account the thermal properties and characteristic thickness of the body.

The solutions to equation (3.17) are usually displayed graphically[15] to give an idea of the temperature gradients within a slab. As the slab becomes thin the gradients decrease until the "thermally thin" limit is reached, at which point $Bi < 0.1$, and the material may be regarded as having a lumped thermal capacity.

As will be shown later, the samples used in the present research can be regarded as thermally thin, and can be treated using such an approach. The energy balance is then much simpler[16];

$$hA(T_\infty - T) = \rho V c \frac{\partial T}{\partial t} \tag{3.20}$$

where A is the area through which heat is transfered, and V is the corresponding volume.

Integrating, and remembering that $T = T_0$ when $t = 0$;

$$\frac{T_\infty - T}{T_\infty - T_0} = \exp\left(\frac{-2ht}{\tau \rho c}\right) \tag{3.21}$$

where τ is the slab thickness; T, T_0 are the initial and final temperatures, respectively.

3.3.1.2 The Radiative Case.

Let us now consider the case of radiant heating at one face, and convective cooling on both faces. Again, a full analytical solution can be obtained[14]. However, Simms[17] developed a lumped thermal capacity approach, and obtained the equation;

$$a\dot{Q}_R = \tau\rho c\frac{d\theta}{dt} + 2h\theta \tag{3.22}$$

for a thermally thin material; where a is the absorptivity of the material, and $\dot{Q}_R$ is the radiative heat flux per unit area.

As θ is now independent of x (the essence of the lumped thermal capacity approach) we can integrate to obtain;

$$\theta = T - T_0 = \frac{a\dot{Q}_R}{2h}\left\{1 - \exp\left(\frac{-2ht}{\tau\rho c}\right)\right\} \tag{3.23}$$

Having now obtained expressions for both the convective heating and the radiative heating case, it is interesting to define a "fire point" for the thermally thin material[11] - which can be identified as a temperature T_i . Then, assuming ignition of the volatiles, the time to ignition, t_i, can be defined for:

convective heating, from equation (3.21);

$$t_i = \frac{\tau\rho c}{2h} \log\left(\frac{T_\infty - T_0}{T_\infty - T_i} \right) \tag{3.24}$$

and for,

radiative heating, from equation (3.23);

$$t_i = \frac{\tau\rho c}{2h} \log\left(\frac{a\dot{Q}_R}{a\dot{Q}_R - 2h(T_i - T_0)} \right) \tag{3.25}$$

Thus we find that equations (3.24) and (3.25) are of similar form, implying that, when we consider both extremes of heat transfer, the time to ignition is directly proportional to the thermal capacity per unit area ($\tau\rho c$). These equations clearly define minimum thresholds for ignition; for convective heating $T_\infty > T_i$, and for radiative heating $a\dot{Q}_R > 2h(T_i - T_0)$ However it must be remembered that for materials that cannot be regarded as thermally thin, the solutions are more complex.

3.4 TRANSIENT IGNITION BEHAVIOUR.

In the above discussion, we have assumed that the heat flux incident at the surface of the material is continuous, until we reach the point at which the material ignites. It is worthwhile discussing, however the case of ignition during a discontinuous heat flux.

Bamford et al.[18] subjected both sides of a slab of wood to flames from a pair of "batswing" burners, and determined how long it took for

the material to reach a point where flaming would persist when the heat flux was removed. It was concluded that a critical flow rate of volatiles from the surface, $\dot{m}_{cr} \geq 2.5 g/m^2.s$, was necessary for sustained ignition to occur.

Although this condition is necessary, it is not enough for a full description of the ignition criteria[11]. A knowledge of the heating history and temperature gradient within the solid at the moment of ignition, is also required as can be illustrated by considering equation (3.12);

$$(\psi \Delta H_c - L_v)\dot{m}_{cr} + \dot{Q}_E - \dot{Q}_L = U \qquad (3.12)$$

We have ignition if $U \geq 0$, but extinction if $U < 0$. It is possible for self-extinction to occur after ignition, if the heat flux $\dot{Q}_E$, initially responsible for the surface reaching the fire point temperature, is reduced or removed completely. Drysdale[11] has shown that, taking values of the above parameters for P.M.M.A., allowing the sample to reach the fire point condition, and then allowing $\dot{Q}_E \rightarrow 0$, leads to $U < 0$, and the flame will be extinguished. If, however, we consider polyurethane foam, and allow it to reach the fire point temperature, then allow $\dot{Q}_E \rightarrow 0$, we obtain $U > 0$, and flaming will persist. However, we must remember that the above conclusions are valid for a certain set of parameter values only. If, for example, conditions were such that heat loss was less significant than assumed above, the P.M.M.A. sample may well have exhibited persistent flaming after the heat flux was removed.

The reason for including the above discussion here, is to identify several material properties which influence the ease of ignition. A mate-

rial is hard to ignite if L_v is large, and ψ and / or ΔH_c are small - or if $\dot{Q}_L$ is large.

3.5 CONCLUSIONS.

In the discussion concerning the ignition of materials, we have identified some physical mechanisms and properties that influence ignition behaviour.

We have seen that, for ignition to occur, it is necessary to heat the surface of a solid material in order to produce gaseous volatiles, and to ignite these volatiles in order to produce a flame which, at the fire point, will consume the remaining material.

We have also seen that, using a lumped thermal capacity approach, the ignition behaviour of a thermally thin material is dependent on the thermal capacity per unit area ($\tau\rho c$), for radiative and convective heat transfer.

Finally, we have seen that, if the heat flux is discontinuous, a material may exhibit extinction even if the initial flux was sufficient for the material to reach the fire point temperature. This behaviour is dependent on several factors, including the amount of energy feedback from the flame, the heat of combustion of the material, and the rate of energy loss from the surface.

The above theoretical discussion is useful in identifying the principal factors which influence the ignition behaviour of a solid material; treating the solid as inert and ignoring chemical decomposition.

The experimental study which follows, through the investigation of the variation of flammability with pressure, oxygen concentration, input power, input energy, flame spread and critical pulse delay, will attempt to develop a qualitative physical model which builds upon previous ideas of regarding the material as being inert and discusses the influence of solid to volatile decomposition and gaseous diffusion on the combustion process. The conclusions drawn from this model will then be applied to the wider concept of safety engineering in hazardous environments.

3.6 REFERENCES.

[1] Semenov, N.N., "Theories of Combustion Processes." Z, Phys. Chem., 48, pp.571-582 (1928)

[2] Kanury, A.M., "Introduction to Combustion Phenomena." Gordon and Breach, London. (1975)

[3] Lees, F.P., "Loss Prevention in The Process Industries." Volume 2, Butterworths, London. (1980)

[4] Frank-Kamenetskii, D.A., "temperature Distribution in Reaction Vessel and Stationary Theory of Thermal Explosion." Journal of Phys. Chem. (USSR), 13, pp.738-755. (1939)

[5] Gray, P., and Lee, P.R., "Thermal Explosion Theory." Oxidation and Combustion Reviews, Volume 2. (1967)

[6] Setchkin, N.P., "Self Ignition Temperatures of Combustible Liquids." J. Research, National Bureau of Standards, 53, pp.49-66. (1954)

[7] Powell, F., "Ignition of Gases and Vapours: A Review of the Ignition of Flammable Gases and Vapours by Friction and Impact." Industrial and Engineering Chemistry, 61, pp.29-37. (1969)

[8] Burgoyne, J.H., and Williams-Leir, G., "Inflammability of Liquids." Fuel, 28, pp.145-149. (1949)

[9] ASTM., "Standard Test Method For Flash Point by the Pensky-Martens Closed Tester." ASTM. D93-80. (1980)

[10] ASTM., "Standard Test Method for Flash Point and Fire Point by the Cleveland Open Cup." ASTM., D92- 78. (1978)

[11] Drysdale, D., "Introduction to Fire Dynamics." Wiley Press. (1985)

[12] Rasbash, D.J., "Relevance of Fire Point Theory to the Assessment of Fire Behaviour of Combustible Materials." International Symposium on Fire Safety of Combustible Materials, Edinburgh University, pp.169-178. (1975)

[13] Deepak, D., and Drysdale, D.D., "Flammability of Solids: An Apparatus to Measure the Critical Mass Flux at the Fire Point." Fire Safety Journal, 5, pp.167-169. (1983)

[14] Carslaw, H.S., and Jaeger, J.C., "Conduction of Heat in Solids." 2nd Edition, Oxford University Press. (1959)

[15] Welty, J.R., Wicks, C.E., and Wilson, R.E., "Fundamentals of Momentum, Heat, and Mass Transfer." 3rd Edition, John Wiley and Sons, New York. (1976)

[16] Myers, G.E., "Analytical Methods in Conduction Heat Transfer." McGraw-Hill, New York. (1971)

[17] Simms, D.L., "On the Pilot Ignition of Wood by Radiation." Combustion and Flame, 7, pp.253-261. (1963)

[18] Bamford, C.H., Crank, J., and Malan, D.H., "The Burning of Wood." Proceedings of the Cambridge Philosophical Society, 42, pp.166-182. (1946)

CHAPTER 4. EXPERIMENTAL APPARATUS.

During the period of research encompassed by this thesis, two sources of heat energy have been employed: an arc generated between two carbon electrodes, and a carbon dioxide laser producing infra-red radiation. Consequently, the discussion concerning the experimental apparatus will be divided into two parts; the first part will describe the arc apparatus; the second part will describe the laser system.

4.1 THE ARC APPARATUS.

The main body of results contained in the thesis, and associated conclusions, have been obtained using the arc apparatus. The arc apparatus is a development of that which was initially designed by Lai[1], and developed by Brennan[2]; a schematic outline of the system can be seen in Fig. 4.1.

The principal component of the system is a pressure chamber within which are contained the carbon electrodes used to provide a source of energy for the ignition tests. External to the chamber are a variety of stages concerned with both controlling the energy source and environmental parameters, and recording the data associated with the experimental programme. Each stage will be discussed in turn, starting with a description of the pressure chamber.

4.1.1 The Pressure Chamber.

The pressure chamber and pressure gauge can be seen in Plate 1. The chamber is constructed of stainless steel and is cylindrical, with an internal diameter of 19.6 ± 0.1cm and length 20.9 ± 0.1cm; a viewing port made of re-inforced glass is incorporated into the design to allow visual study of the ignition process.

Access to the chamber is from above, via a lid which can be secured by bolts and a clamp. An emergency pressure release valve is attached to the lid, which operates when the pressure within the chamber

Plate 1. The Pressure Chamber.

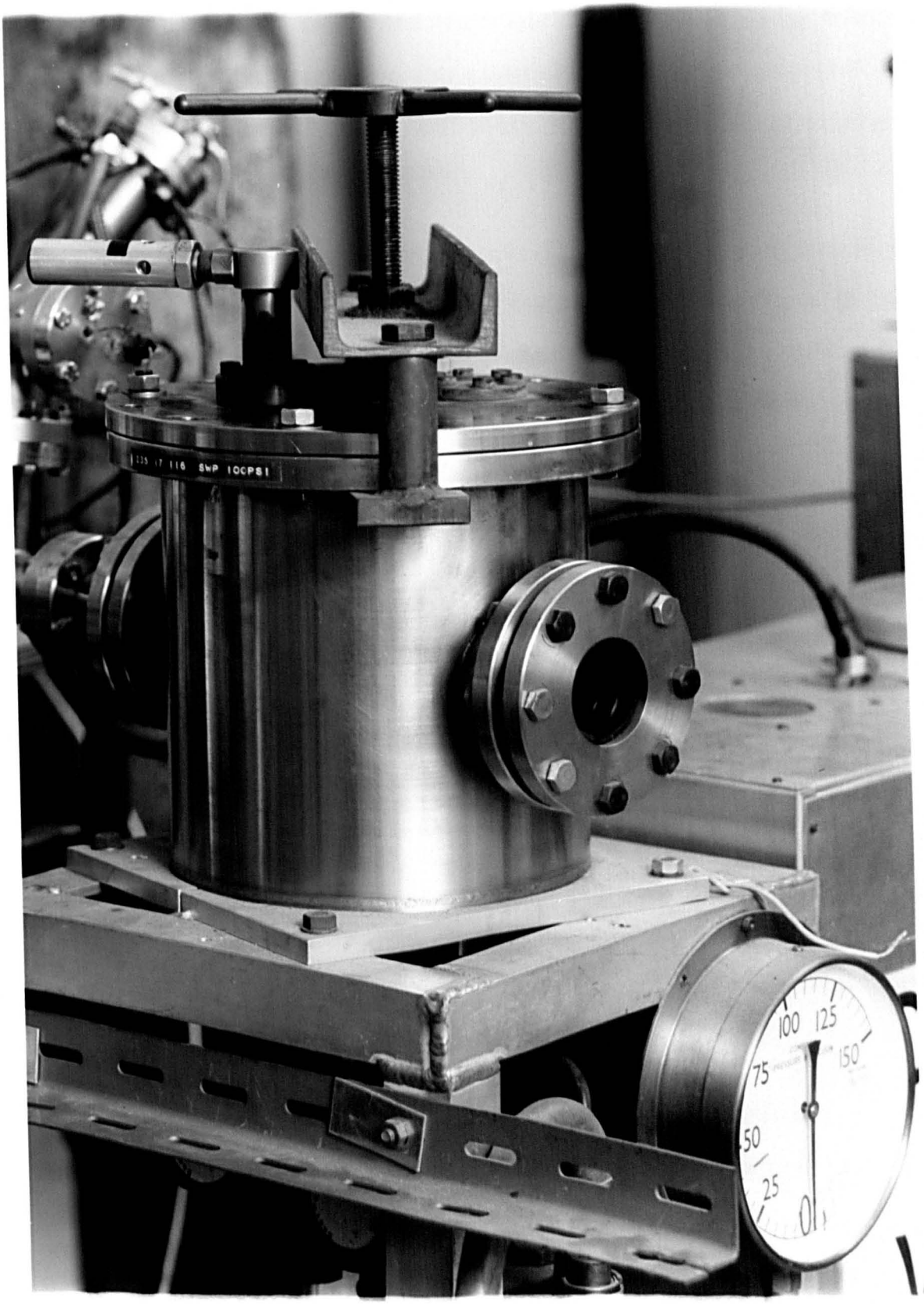
SWP 100PSI
100
125
75
150
50
25
0

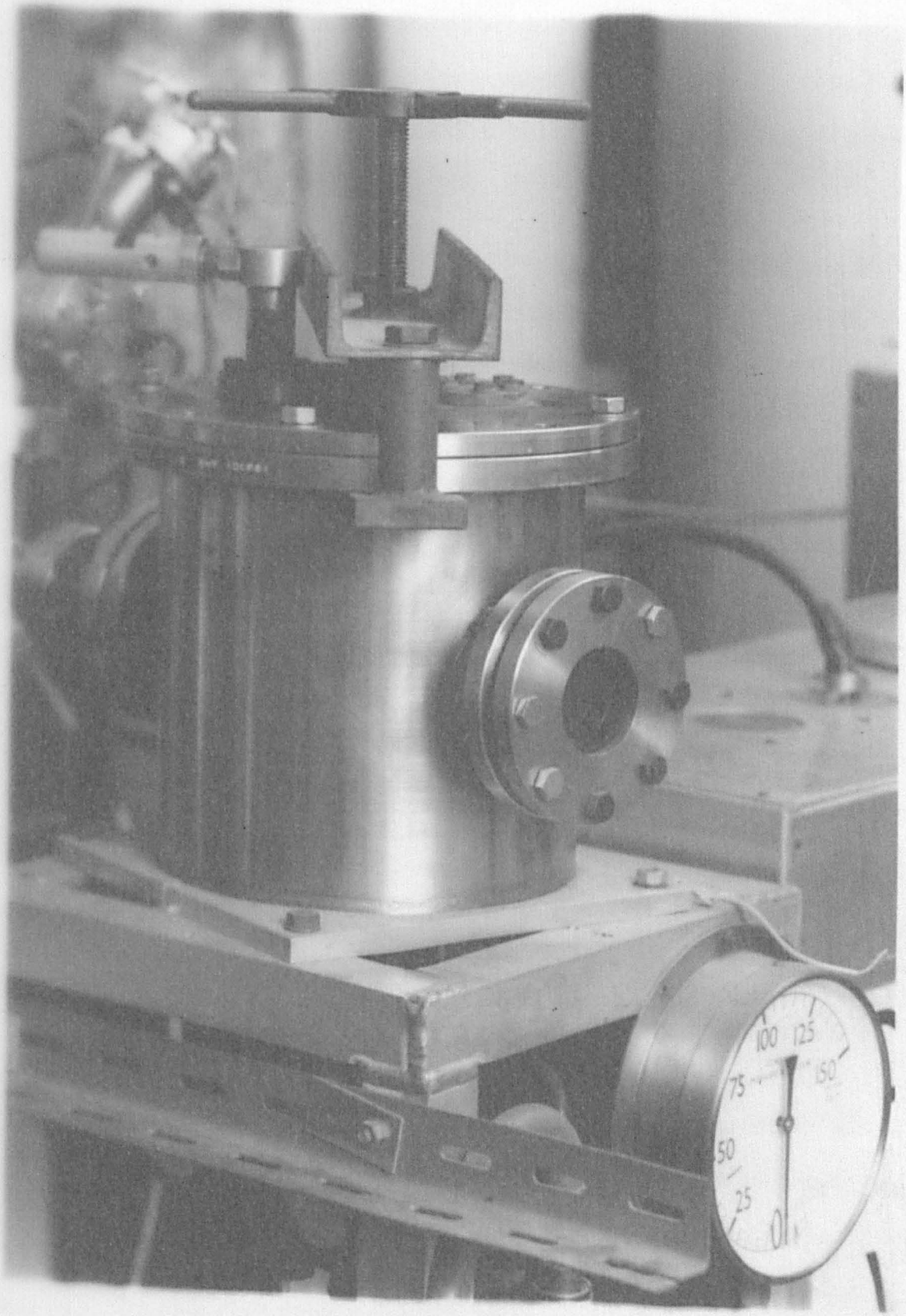

Plate 1. The Pressure Chamber.

exceeds 90 p.s.i. - giving a working pressure range of 0-90 p.s.i. The pressure gauge is attached to the underside of the chamber along with a metrovac rotary vacuum pump; the external gas supply is connected to the underside of the chamber, also, using a flange/copper tube arrangement.

In a position diametrically opposite to the viewing port is a high vacuum port which provides access for the electrical connections to the chamber. These connections are; the leads to the anode and cathode; the output leads from a phototransistor; the connections from a stepper motor to a driver unit.

Plate 2 shows two views of the internal arrangement of the chamber: a) clearly shows the position of the phototransistor with respect to the electrodes, permitting accurate determination of the arc duration and ignition delay time of the sample; b) clearly shows the stepper motor and samples, allowing multiple sample testing during experiments that require high pressure and varying oxygen concentration. The role of the stepper motor for multiple sample testing will be discussed later.

4.1.2 The Arc Generation Stage.

The electrical circuit used to generate the arc discharge can be seen in Fig. 4.2. The following discussion will be concerned with the action of the discharge circuit in producing an arc; the actual control of the discharge, using the switches at points AA and BB, is facilitated us-

a) Photo-Transistor and Electrodes.

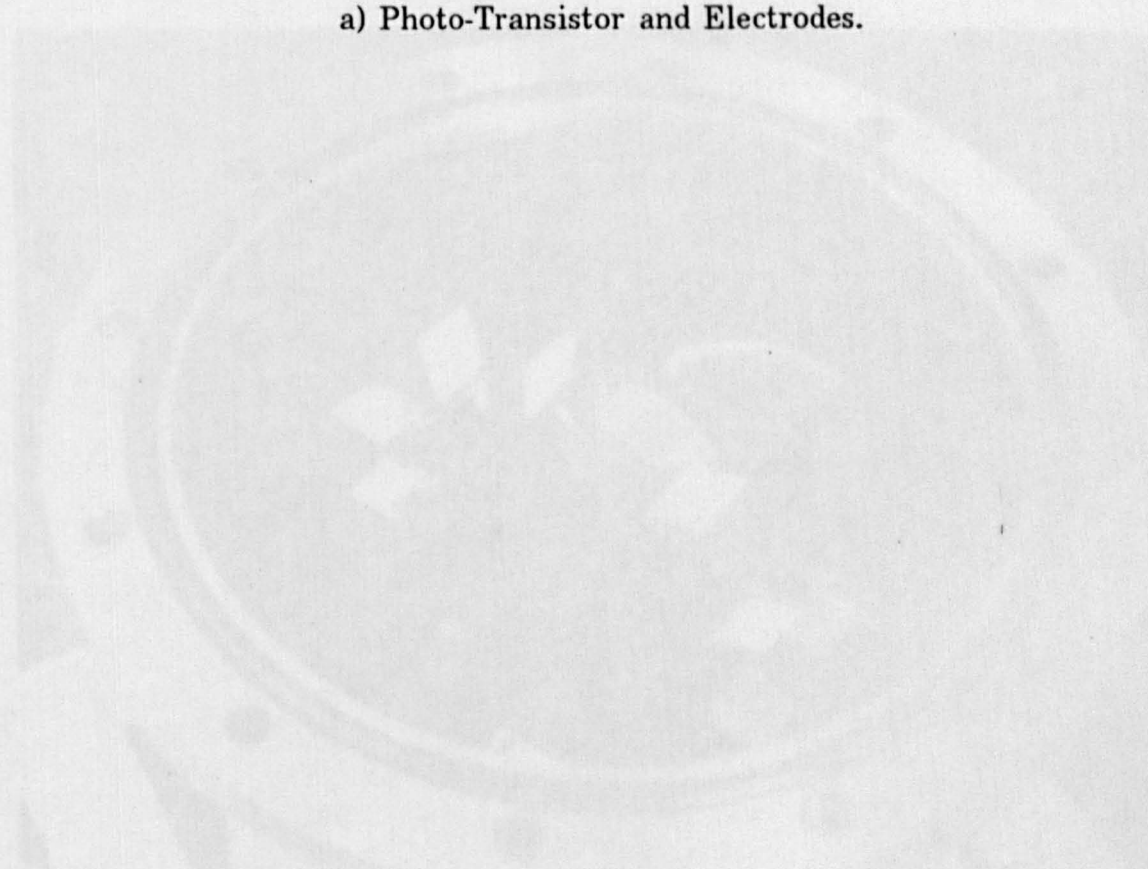

b) Stepper Motor and Samples.

Plate 2. Internal Arrangement of the Chamber.

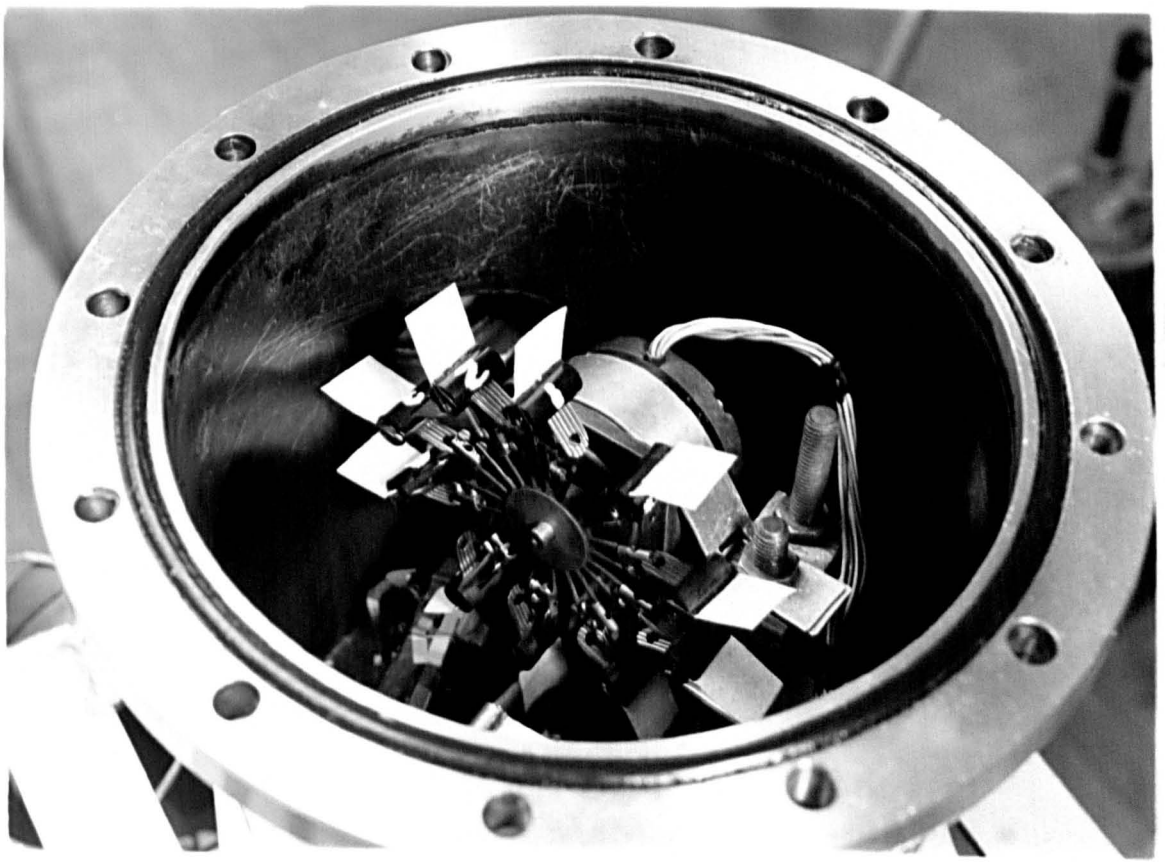

a) Photo-Transistor and Electrodes.

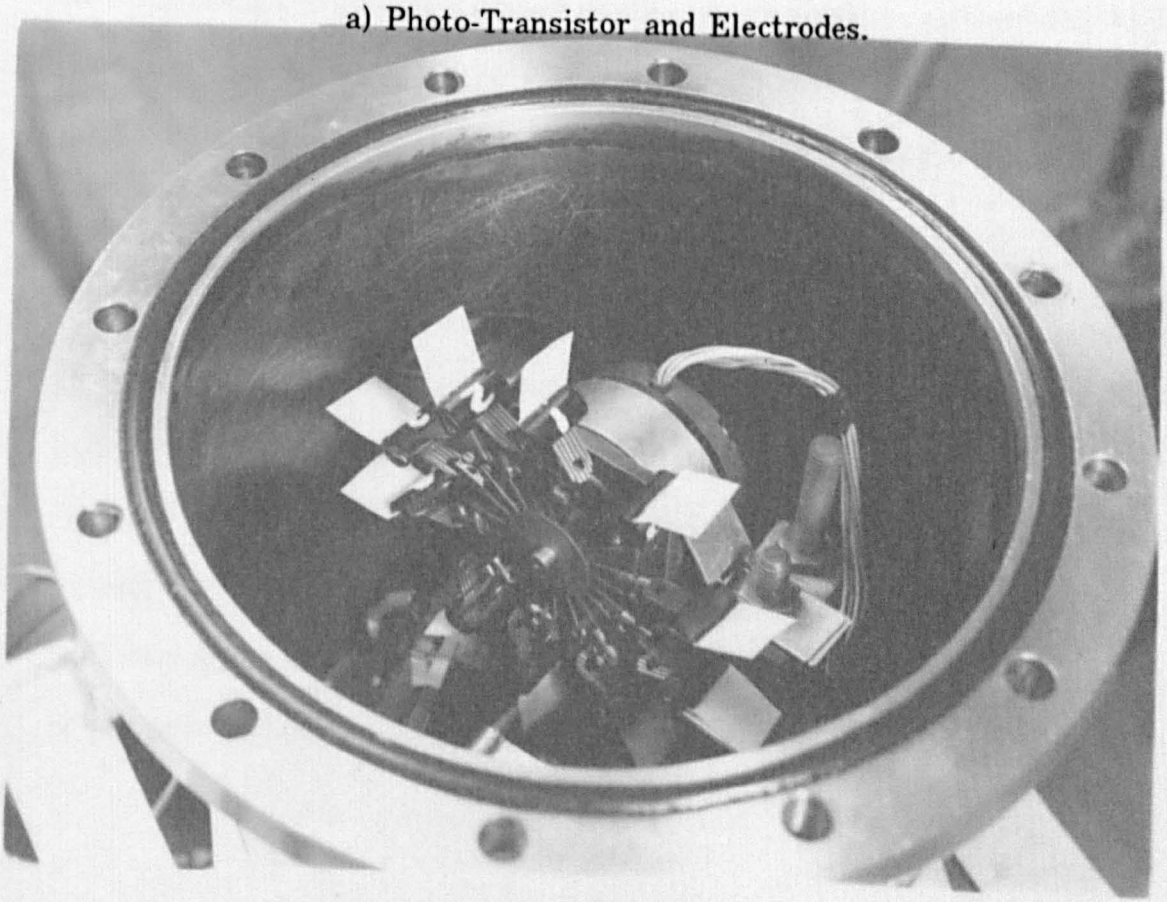

b) Stepper Motor and Samples.

Plate 2. Internal Arrangement of the Chamber.

ing the BBC microcomputer, pulse transmitter, and pulse receiver stages, all of which will be discussed later in the chapter.

The 8 μF capacitor is normally charged to 280V via the 280V D.C. supply. When the switch is connected to AA the charge on this capacitor is transfered, via a Lucas coil, to the two 0.002 μF capacitors. These capacitors charge to give a voltage sufficient to break down the gas at the electrode gap (approximately 20kV), then discharge through it, producing a spark which initiates the discharge.

At this point the 120V, 5A D.C. supply at BB provides a current, the level of which is controlled by a variable resistor, across the electrode gap and through the 200 μH inductor and 2.5 Ω resistor to ground. This has the effect of producing an arc whose voltage can be monitored using an oscilloscope (with appropriate probes for protection against the high voltage spike) to observe the values of anode voltage, V_A , and cathode voltage, V_C, and whose current can be determined using V_C and the resistance from the electrode to ground.

The 0.01 μF capacitor connected across the 120V D.C. supply serves as protection for the supply from the high voltage spike produced by the initiating spark. In previous work by Lai[1], and Brennan[2], the 200 μH inductor and the 2.5 Ω resistor formed part of the protection circuit for a thyristor. The thyristor has been removed, however the inductor and resistor have been retained to allow convenient estimation of the arc current, as described above.

4.1.3 The Pulse Transmitter Stage.

The circuit showing the pulse transmitter stage can be seen in Fig. 4.3. The circuit consists of three transistors in common-emmiter arrangement, each with an infra-red transmitter (TX) connected between the the +15 Volt rail and collector. Each transistor is connected, via a base resistor, to a pin on the user output b port of the BBC microcomputer. The pins are 0,1,2 for transistors 1,2,3 respectively. Each pin is initially low and, on going high, the action of applying a pulse to the base of each transistor is to turn the transistor 'on'; current then flows through the transmitter causing it to transmit.

4.1.4 The Pulse Receiver Stage.

This stage is linked to the pulse transmitter stage by an optical fibre link, and can be seen in Fig. 4.4. Three infra-red receivers RX1,RX2, and RX3 are connected to the base of transistors 4,6, and 8 respectively. The transistors 4,6, and 8 are connected in emitter-follower arrangement to transistors 5,7, and 9 respectively, which are, in turn, interfaced via relays to the main discharge circuit, and to the stepper motor driver unit.

Having seen the principal stages of the arc apparatus it is necessary to see how the integration of each stage produces the desired initiation and inhibition of the arc, and operation of the stepper motor.

4.1.5 Initiation of the Arc.

Fig. 4.5 is a representation of the circuit controlling the initiation of the arc; it incorporates several stages and is operated from the BBC microcomputer using a Basic program, 'DualI' (a description of which will appear later in the chapter).

When pin 0 is sent high, transistor 1 is turned on and current flows from the +15 Volt rail, through TX1 to ground. The current flow is limited by the 82 Ω resistor, to the required operating level for the optical transmitter (< 100mA).

Light is sent down the optical fibre link to the pulse receiver, RX1, turning transistor 4 on. Current flows from the emitter of transistor 4 to the base of transistor 5 turning it on and energising relay 1. The switch is then tripped, the 8 μF capacitor is connected to points AA, and the discharge is initiated as described in section 4.1.2.

When pin 0 is sent low transistor 5 is switched off (via the same operation outlined above), relay 1 is again energised and the 8 μF capacitor is reconnected to the 280V D.C. power supply; essentially 're-setting' the system.

4.1.6 Inhibition of the Arc.

The circuit controlling the inhibition of the arc can be seen in Fig 4.6. As in section 4.1.5, it makes use of several of the control stages

outlined earlier in the chapter and is also controlled by the program 'DualI', which will be described later.

The 120V, 5A D.C. power supply is normally turned on and, upon initiation of the discharge (as described in section 4.1.5), allows a current to flow across the gap between the electrodes; thus establishing an arc. In order to inhibit the arc, the following operation is necessary.

When pin 1 is sent high transistor 2 is turned on and current (the value of which is set by the 82 Ω resistor) flows through TX2 causing it to transmit down the optical link to RX2. At this point transistor 6 is turned on allowing current to flow from the emitter of transistor 6 into the base of transistor 7; turning it on. Relay 2 is then energised and the switch is disconnected from point BB, inhibiting the flow of current across the electrode gap (see Fig 4.2) and stopping the arc.

When pin 1 is sent low, transistor 7 is turned off (in the same way as it was turned on earlier), relay 2 is energised and the 120V, 5A D.C. supply is reconnected to point BB in the arc generation circuit. However, it must be remembered that this action does not allow an arc to be re-established between the electrodes - an initiating voltage, as described in section 4.1.5, is necessary to breakdown the gas before current can again flow across the gap.

4.1.7 Operation of the Stepper Motor.

The stages used in the above operations are again incorporated in the circuit controlling the stepper motor, which is also controlled by the

program 'DualI'. The circuit which allows remote operation of the stepper motor can be seen in Fig 4.7.

Pin 2 of the user output b port is interfaced to the base of transistor 3 via a 1 kΩ base resistor. When pin 2 is sent high, transistor 3 is turned on and TX3 transmits down the optical link to RX3. This has the effect of turning on transistor 8 and, since we have an emitter-follower arrangement, transistor 9 is turned on sending the collector of transistor 9 low.

The open collector inverter at the output of transistor 9 ensures that when the collector is sent low, the input to the stepper motor drive unit is sent high and the stepper motor is activated.

An open collector inverter is used as the driver unit requires an open collector arrangement for operation, with the unit itself providing the 'pull up' load needed for switching between digital voltage levels.

When pin 2 is sent low, transistor 9 is turned off, the collector is sent high, and the inverter ensures that the the input to the driver unit is sent low - thus the stepper motor is de-activated. The degree of step experienced by the stepper motor is determined by the program 'DualI'.

There now follows a description of the program "DualI", which controls the arc initiation and inhibition circuits described above, and operates the stepper motor.

4.1.8 The Computer Program 'DualI'.

A listing of the program can be seen in appendix B.

The BBC Basic program makes use of the internal timer of the computer to control the duration of the pulses and delay used in the main body of the arc experiment. The program also allows the user to control the stepper motor located within the chamber.

Lines 10 to 30 designate the user function keys f_1, f_2 , and f_3; operation of these keys result in jumps to various sections of the program. f_1 sends the program to line 130 which runs the arc control program; f_2 sends the program to line 570 which enables coarse adjustment of the sample using the stepper motor; f_3 sends the program to line 770 which allows fine adjustment of the sample.

The consequence of operating each user function key will now be discussed in detail.

4.1.8.1 Control of the Arc.

Lines 130 to 150 are input statements that allow the user to designate particular values of duration for pulse 1, pulse delay, and pulse 2 respectively; these values may be changed with each experimental run.

Line 180 designates all port b pins on the user port of the BBC as outputs and line 190 sends all of these pins low. There is a pre-discharge

delay of 5 seconds, set at line 210, which is implemented via the "PROCDELAY(X)" statement at line 220.

This statement produces a leap to line 530 where the subroutine PROCDELAY(X) is defined between lines 530 and 560.

At line 240 pin 0 is sent high and relay 1 is switched at point AA (see Fig. 4.5) thus generating pulse 1. Again a delay is generated equal to the value of X1 (specified at line 130 and implemented at lines 530 to 560). After the delay X1, line 290 sends pin 1 high which opens the switch at BB and switches off the arc current - extinguishing the arc. The 120V, 5A D.C. supply is then switched back on by sending all the b pins low (essentially resetting the system) after a delay set at line 300.

The delay between pulse 1 and pulse 2 is now implemented at lines 320 to 360. "PULSE DELAY" has the duration X2 set at line 140 by the user at the start of the experimental run.

At line 370 pulse 2 is generated by repeating the procedure involved in obtaining pulse 1, having duration X3 (set at line 150) and beginning, as before, with pin 0 being sent high and initiating the discharge.

When pulse 2 has been obtained, the 120V D.C. supply is switched off for 4 seconds at line 420 and the system is once again reset for another experimental run at line 480. The user is informed that the experimental run has been terminated via a PRINT statement at line 490 resulting in "END OF DUAL PULSE TEST" being displayed on the monitor.

4.1.8.2 Coarse Adjustment of the Sample.

Ten samples are attached to the sample holder on the stepper motor during any one experimental run. Thus, as each pulse rotates a sample through 1.8°, twenty pulses are needed to rotate a sample through 36° in order to bring it close to the electrode gap.

Pressing f_2 sends the program to line 570 where all port b pins are designated as outputs. Line 610 calls for 20 pulses to be generated as required above and a "REPEAT...UNTIL" loop counts through 20 pulses from z=20 until z=0. When this is finished a PRINT statement informs the user: "SAMPLE IN POSITION". The purpose of lines 640 to 690 is to give a mark-space ratio of the pulses equal to 1:10 and to ensure that, for the majority of the pulse train, the input to the stepper motor drive is low. It is worth noting that in the program pin 2 is low for X=1 (0.01 seconds) and high for X=10 (0.10 seconds); in this form the input to the motor drive would be majority high. However, the open collector inverter connection (see Fig 4.7) ensures that the inverse is true, as desired.

4.1.8.3 Fine Adjustment of the Sample.

This section of the program is implemented in precisely the same way as for the coarse adjustment section. However, the number of pulses to the stepper motor is reduced to 2. This allows the sample to be rotated through 3.6° thus giving a facility for fine adjustment of the coarse position of the sample. Again, a PRINT statement at the end of the program

informs the user of the state of the sample via "FINE ADJUSTMENT COMPLETED".

Fig 4.8 is a timing diagram showing the output of the port b pins when producing an experimental run having $t_1 = 1.0s, t_d = 2.0s$, and $t_2 = 1.0s$

4.1.9 Arc Detection.

The arc is monitored by observing the change in voltage across a 1 kΩ resistor (see Fig. 4.9) connected between +15V and the collector of transistor c. Transistor a is a phototransistor located below the electrode gap and can also be seen in plate 2. When light is incident on transistor a, transistor b is turned on and, in turn, transistor c is turned on. There is a voltage drop across the 1 kΩ resistor of +15V (minus the collecter-emitter drop of +0.2V) which is observed as a rise in the trace on the oscilloscope. Similarly, when light is removed from transistor a, all transistors are turned off and the voltage drop across the resistor becomes zero. Thus the voltage change across the resistor follows the change of incident light at transistor a.

The same circuit is used for the measurements of flame spread and time to ignition of the sample, which will be described in detail in chapter 5.

4.2 THE LASER SYSTEM.

The majority of the results contained in chapter 6 have been obtained using the arc system described in section 4.1. A laser system has also been developed for the present programme and for use in future experimental work. This has been tested and used to obtain the measurements presented in chapter 6; an outline of the system can be seen in Fig. 4.10.

The following discussion will be divided into three sections concerned with the laser (and R.F. and D.C. power supplies), the laser modulation control, and the sample and detector stage. A description will then follow concerning the operation of the whole system using the program 'LASERI' (a listing of which can be found in appendix B).

4.2.1 The Laser and Power Supplies.

The laser incorporated in the experimental system is a Ferranti CM3044 waveguide carbon dioxide laser emitting I.R. radiation at a wavelength of 10.6 microns. The beam has a diameter of 1.3mm and a divergence of 10mrad., and propagates as the TEM00 Gaussian mode. The laser head, which can be seen in plate 3, is water cooled (with a flow rate of 0.5 litres/min.)and operates at a maximum power output of 5W at 20 $^{\circ}C$ (the power measurement will be discussed in chapter 5).

The laser is connected to a CM2345 R.F. power supply, which has an output at a frequency within the range 80 to 85 Mhz, via a one metre

Plate 3. Laser Head and Sample Arrangement.

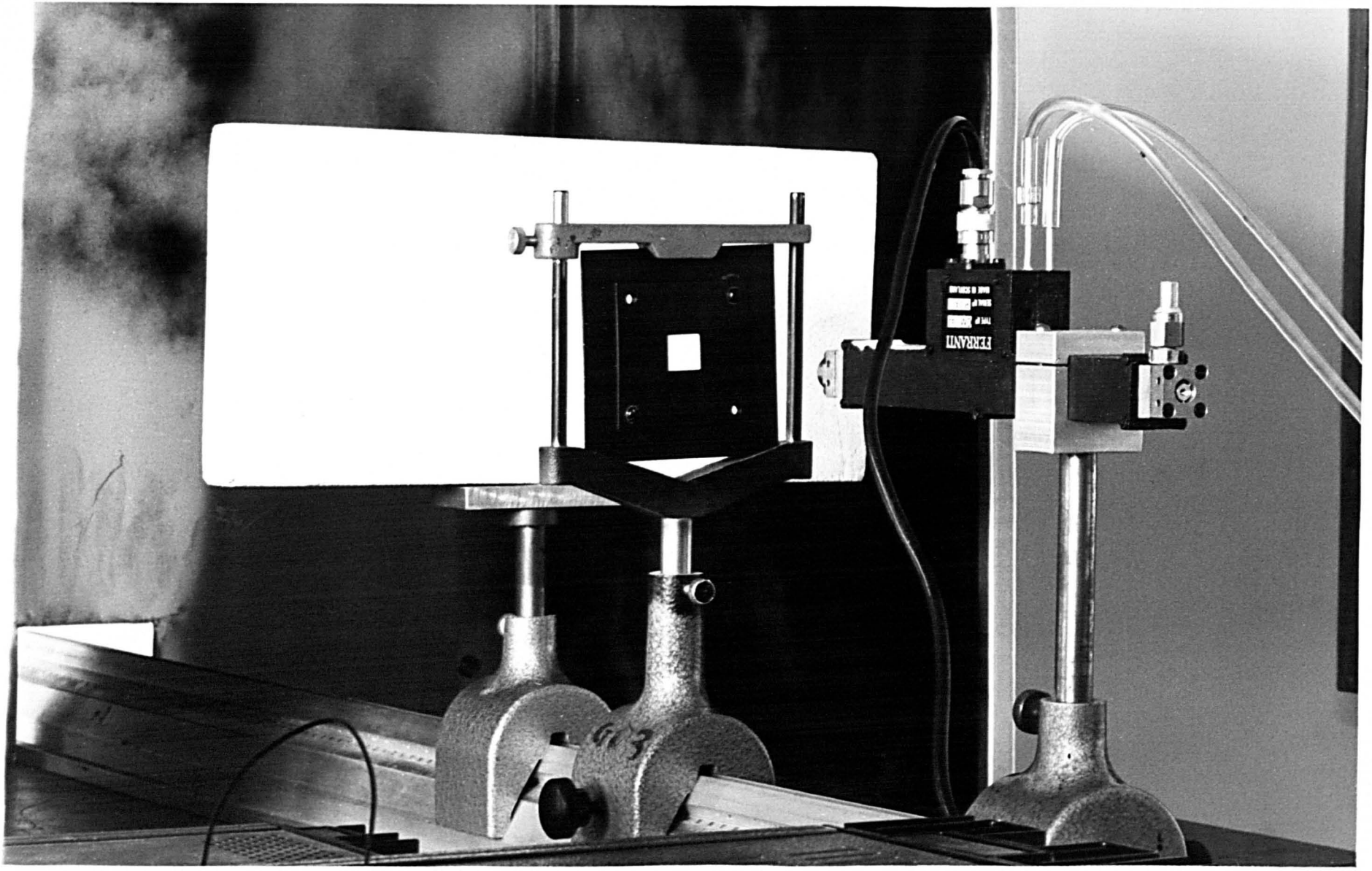
FERRANTI

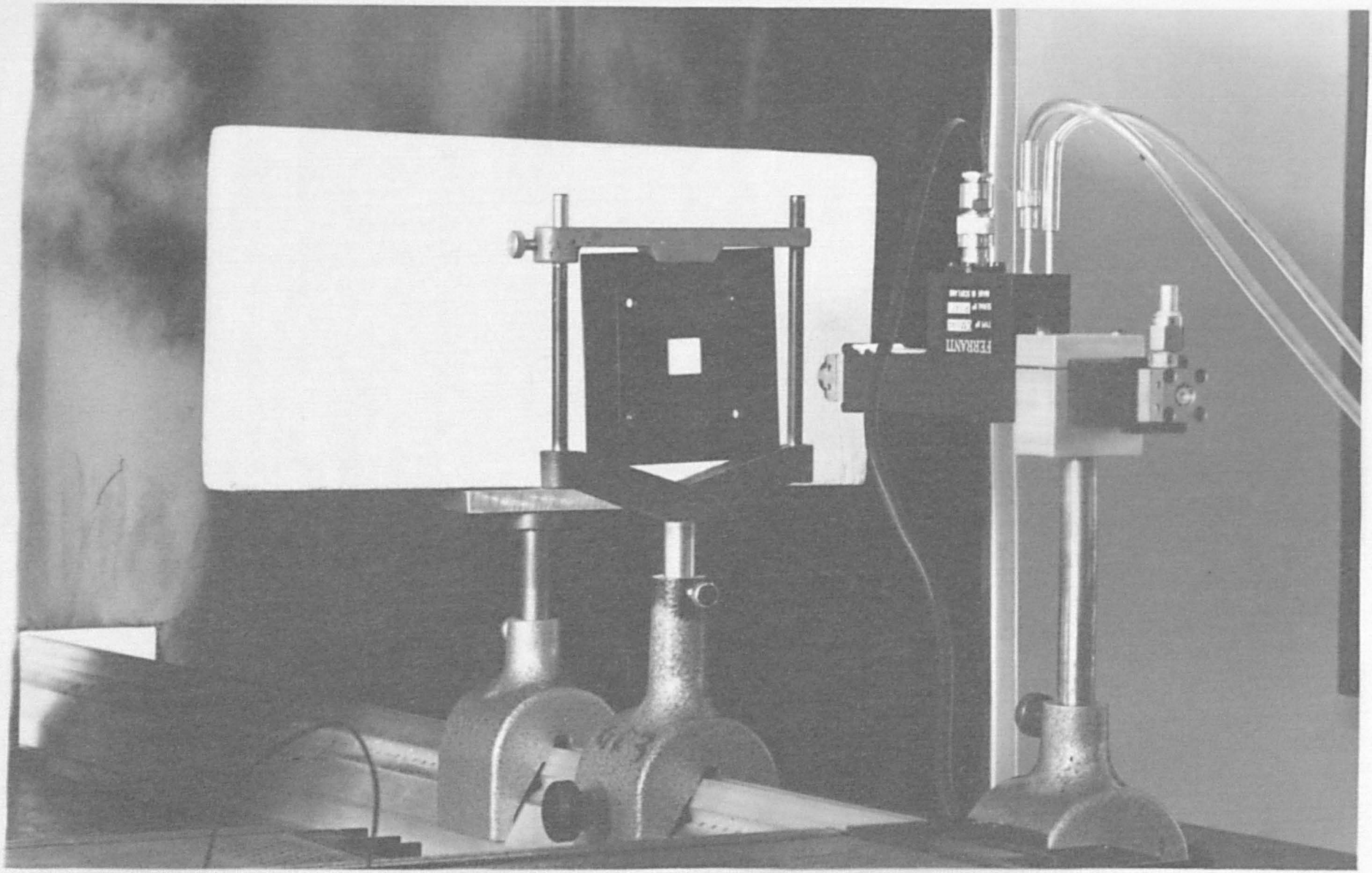

Plate 3. Laser Head and Sample Arrangement.

length of 50 Ω TNC-TNC (male) cable. The R.F. supply is air cooled and has a 'D' connector which enables the laser to be modulated by an external pulse of 12 Volt CMOS logic; this will be discussed further in section 4.2.2.

Power is supplied to the R.F. supply by a Sorenson QRC40-30A D.C. power supply which is voltage limited to supply a stable 12 Volts D.C. supply(± 0.5 Volts) at 15 Amps.

With this arrangement, the laser will strike and operate in continuous wave mode when the D.C. power supply is switched on. For the purposes of the present experimental programme it is necessary to operate the laser with a pulsed output in order to obtain a distinct starting point for the irradiation of the sample; this will be discussed further in section 4.2.3. The method by which a pulsed output is obtained will be discussed in the following section.

4.2.2 Laser Modulation control.

The circuit used to obtain a pulsed output from the laser can be seen in Fig. 4.11. Pin 2 on the 'D' connector to the R.F. supply is the 'mod-in' input: a high of 10V < V(high) < 12V at this pin is Laser 'OFF' and the laser will be inhibited; a low of 0V < V(low) < 1V at this pin is laser 'ON' and the laser will be re-activated. As can be seen from Fig. 4.11 the voltage high of 12V is obtained via an open collector dual input 'and' gate whose inputs are a constant voltage of +5V and pin 0 from the output port of a BBC microcomputer. When pin 0 is sent 'high' the out-

put of the 'and' gate is sent high and, since the output is connected to the +12V voltage rail via a 1 $k\Omega$ 'pull up' resistor, the output high is at +12V; a value sufficient to inhibit the laser. When pin 0 is sent 'low' the output of the 'and' gate, and hence mod-in, is sent low and the laser is re-activated. This sequence of events is controlled by the program 'LASERI' which can be seen in appendix B and will be discussed in section 4.2.4.

Other pin connections on the 'D' connector which are utilised are: 5,6 between which a LED. is connected which indicates that power is available from the D.C. supply for the laser to strike; 7,8 which are connected together in order for the R.F. supply to strike the laser when the D.C. supply is turned on; 9 is connected to ground.

4.2.3 Sample and Detector Arrangement.

The arrangement of the sample and detector can be seen in Fig. 4.12. The sample is mounted in a metal frame which allows a varying thickness of sample to be tested and is coated with high temperature resistant black paint in order to reduce the effect of any reflections of the laser radiation: the laser head and sample holder can be seen in plate 3.

The sample is initially shielded from the beam by a removable metal shutter (which is also coated with temperature resistant black paint). This has two purposes; the first is to shield the user from any radiation due to systems failure which would lead to the laser striking whilst the sample under test is changed; the second is to allow the ob-

whilst the sample under test is changed; the second is to allow the observer to obtain a distinct 'start of sample irradiation'. This is obtained by allowing the laser to strike whilst the shutter is in place and then removing the shutter at a time determined by the program 'LASERI'; this will be discussed in more detail in the next section.

The thermopile seen in Fig. 4.12 is the same as that described in chapter 5 concerning the measurement of the radiation produced by the arc - model 5300 Advanced Photophysics - (and can be seen in plate 4). It is positioned directly behind the sample, in line with the laser beam, and is used in conjunction with the 'start of sample irradiation' in order to obtain a 'sample penetration time' i.e. the time taken for the laser beam to burn through the sample from the start of sample irradiation until first response of the thermopile. This is observed on a dual beam storage oscilloscope and will be discussed further in chapter 5.

The beam is terminated on a monolux block (also seen in plate 3) which absorbs the Infra Red radiation of the beam and re-emits the absorbed radiation as heat - thus destroying the directional properties of the laser beam.

4.2.4 Control of the Laser System Using the Program 'LASERI'.

A listing of the program 'LASERI' can be found in appendix B. The program allows the user to modulate the laser beam by making use of the internal timer of the BBC microcomputer to output a pulse to the mod-in (pin 2) of the R.F. power supply 'D' connector seen in Fig. 4.11.

a) Sample Holder and electrodes.

b) Thermopile and Oscilloscope.

Plate 4. Arc Apparatus.

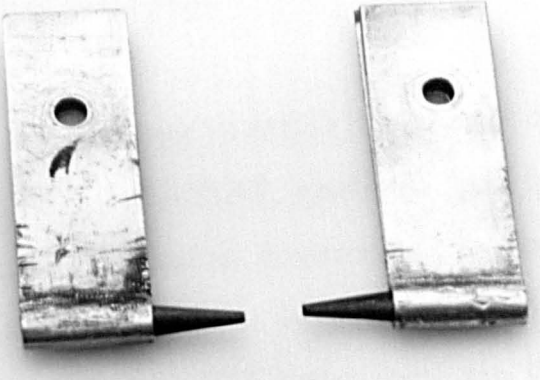

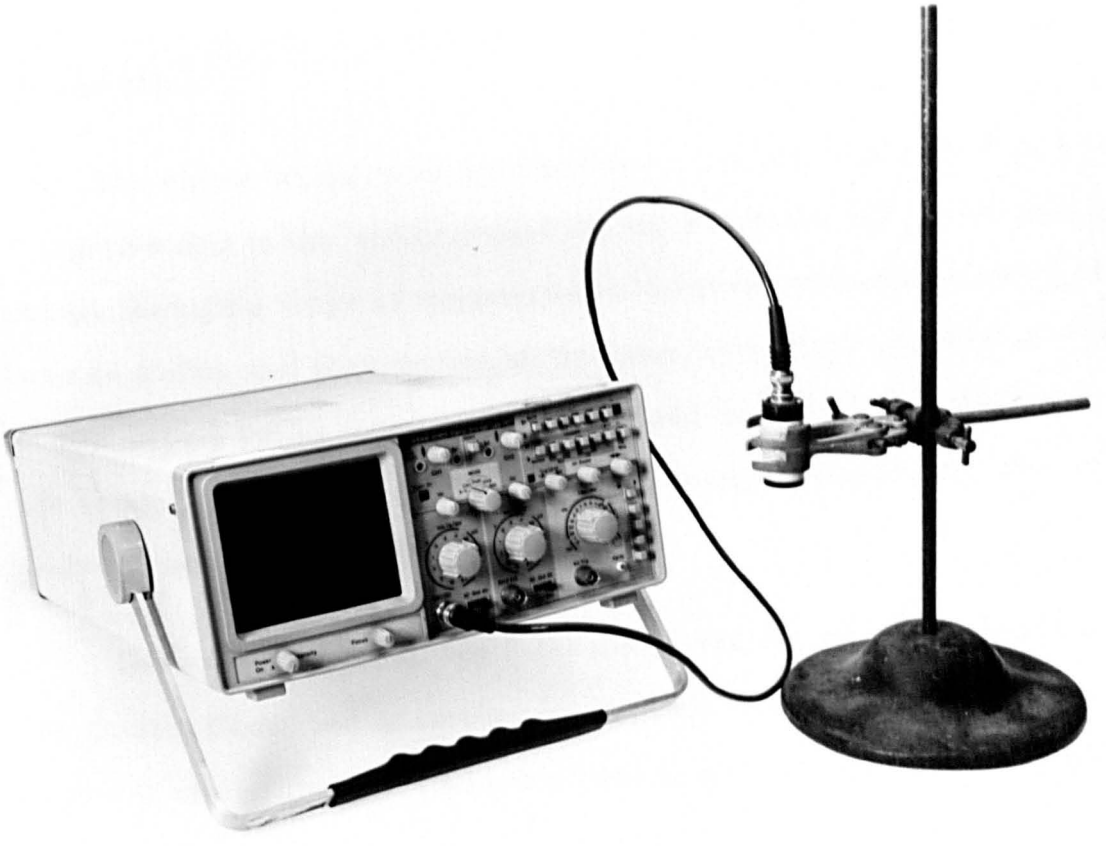

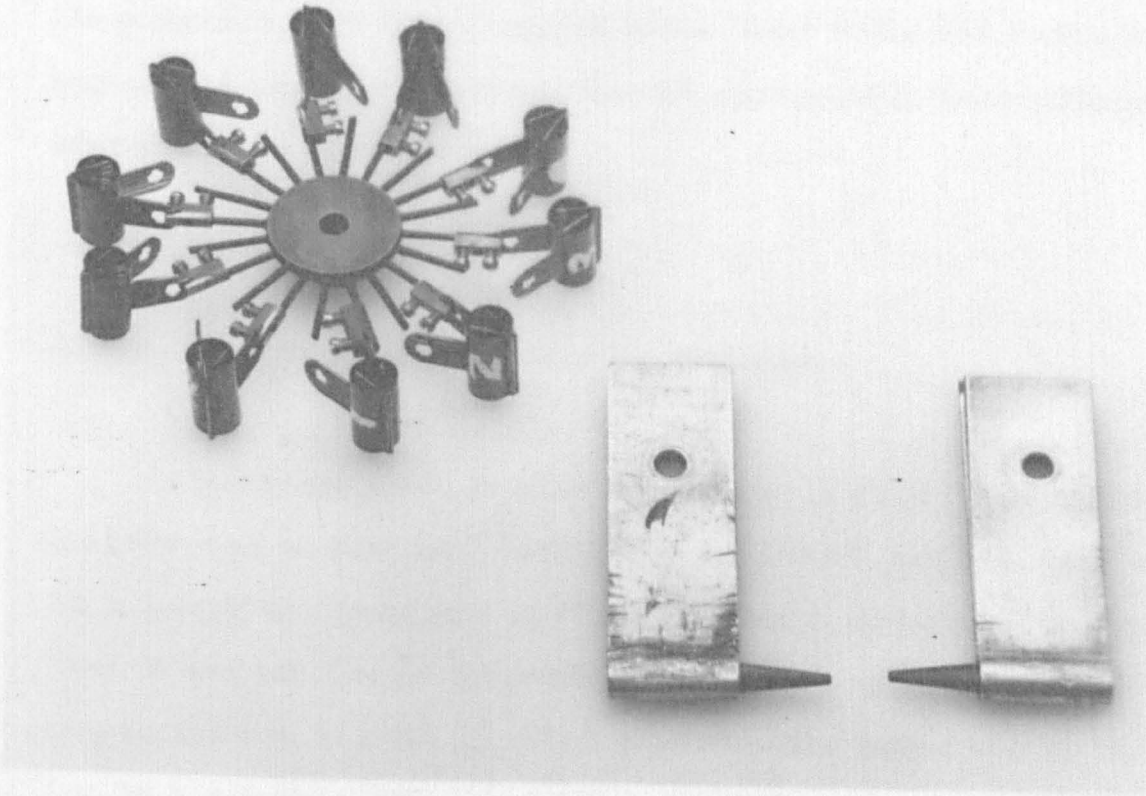

a) Sample Holder and electrodes.

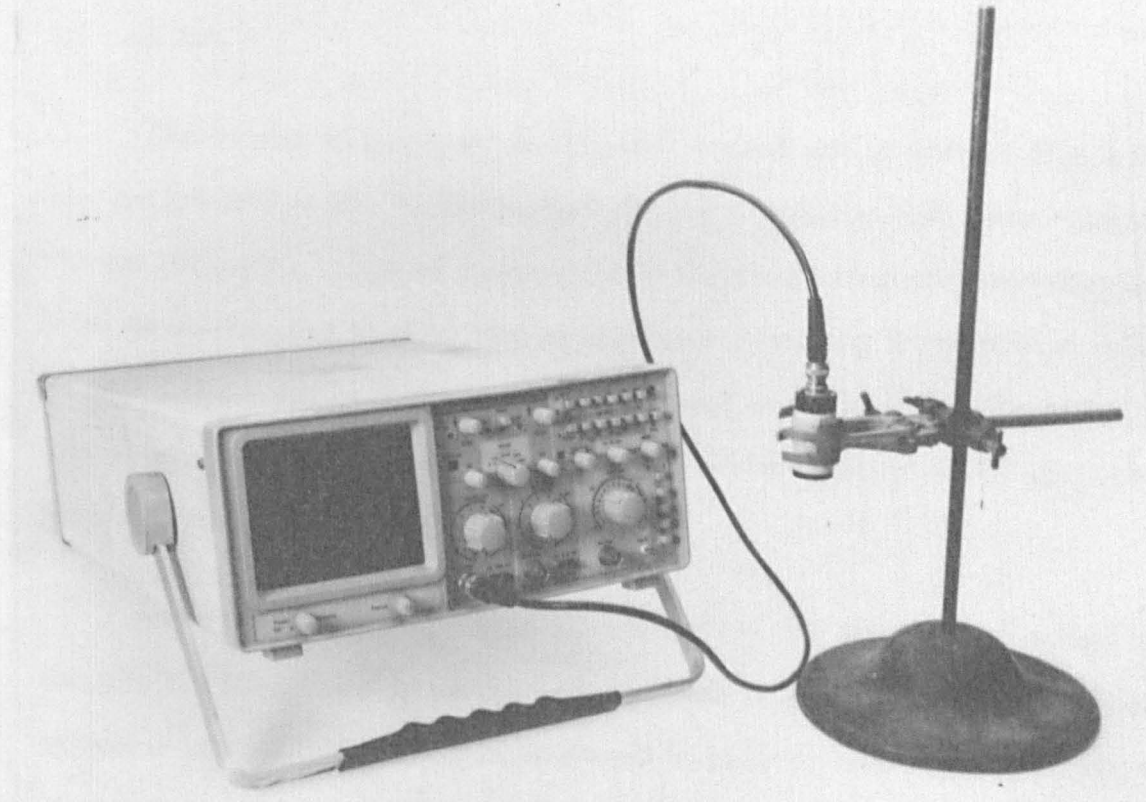

b) Thermopile and Oscilloscope.

Plate 4. Arc Apparatus.

Lines 10 and 20 designate the user function keys f_1 and f_2 ; f_1 sends the program to line 70 and results in the 'laser strike and modulation sequence'; f_2 sends the program to line 270 and results in 'laser inhibition after sample penetration'.

4.2.4.1 Laser Strike and Modulation Sequence.

As mentioned above, in order for the laser to strike, the mod-in for the laser must be held low. In the case of 'LASERI', mod-in is held low for 5 seconds as can be seen in Fig. 4.13. This is implemented between lines 70 and 110: line 80 designates all pins on the BBC user port b as outputs and line 90 sends all output pins low. The output pins are held low for 5 seconds; a period specified at line 100 and implemented at line 110 via the 'PROCDELAY(X)' statement which is located between lines 210 and 240.

The output of the laser during this period can be seen in Fig. 4.13. The period A-B is the 'strike period' during which the R.F. power supply sweeps through a range of frequencies to the strike frequency alowing the laser to strike, and then settles at the laser operating frequency at point B; this period varies from laser to laser and is typically of the order of one second. For the remainder of the 5 second period, A-C, the laser produces an output of 5 Watts.

During the whole of the 5 second period the sample is shielded by the shutter (described in section 4.2.3). This is required since the strike period is unspecified and there is a need to have a distinct point at which

the sample is irradiated. The laser can be inhibited for a two second period during which time the shutter can be removed; the laser can then be re-activated so that irradiation of the sample will occur at a point specified by the user. This point can be measured using an oscilloscope.

Indeed, the program 'LASERI' (see appendix B) inhibits the laser for a 2 second period from C-D as seen in Fig. 4.13. Line 140 sends pin 0 high for a 2 second period specified at line 150 and implemented at line 160. This has the effect of sending the output of the open collector 'and' gate (mod-in) to a high of +12V, thus inhibiting the laser. During this period a buzzer connected between ground an mod-in is sounded, allowing the user to safely remove the shutter from the path of the beam.

The laser is re-activated by sending pin 0 (and hence mod-in) low at line 190 so that irradiation of the sample can begin; this event (point D in Fig. 4.13) is monitored using a storage oscilloscope. Irradiation of the sample continues until the beam is detected by the thermopile (whose response is also monitored using the storage oscilloscope and can be seen in Fig. 4.13). Shortly after, the laser is inhibited by pressing f_2 which sends mod-in high at line 270, represented by point E on Fig. 4.13. The period D-E is variable and depends on the thickness of the sample. This will be discussed further in chapter 5.

4.3 REFERENCES.

[1] Lai, W.K., "Ignition of Materials Under Hyperbaric High Oxygen Content Environment." M.Eng. Thesis, Liverpool University. (1980)

[2] Brennan, J.F.M., "Ignition of Materials Under Conditions of Hyperbaric High Oxygen Concentration." PhD. Thesis, Liverpool University. (1987)

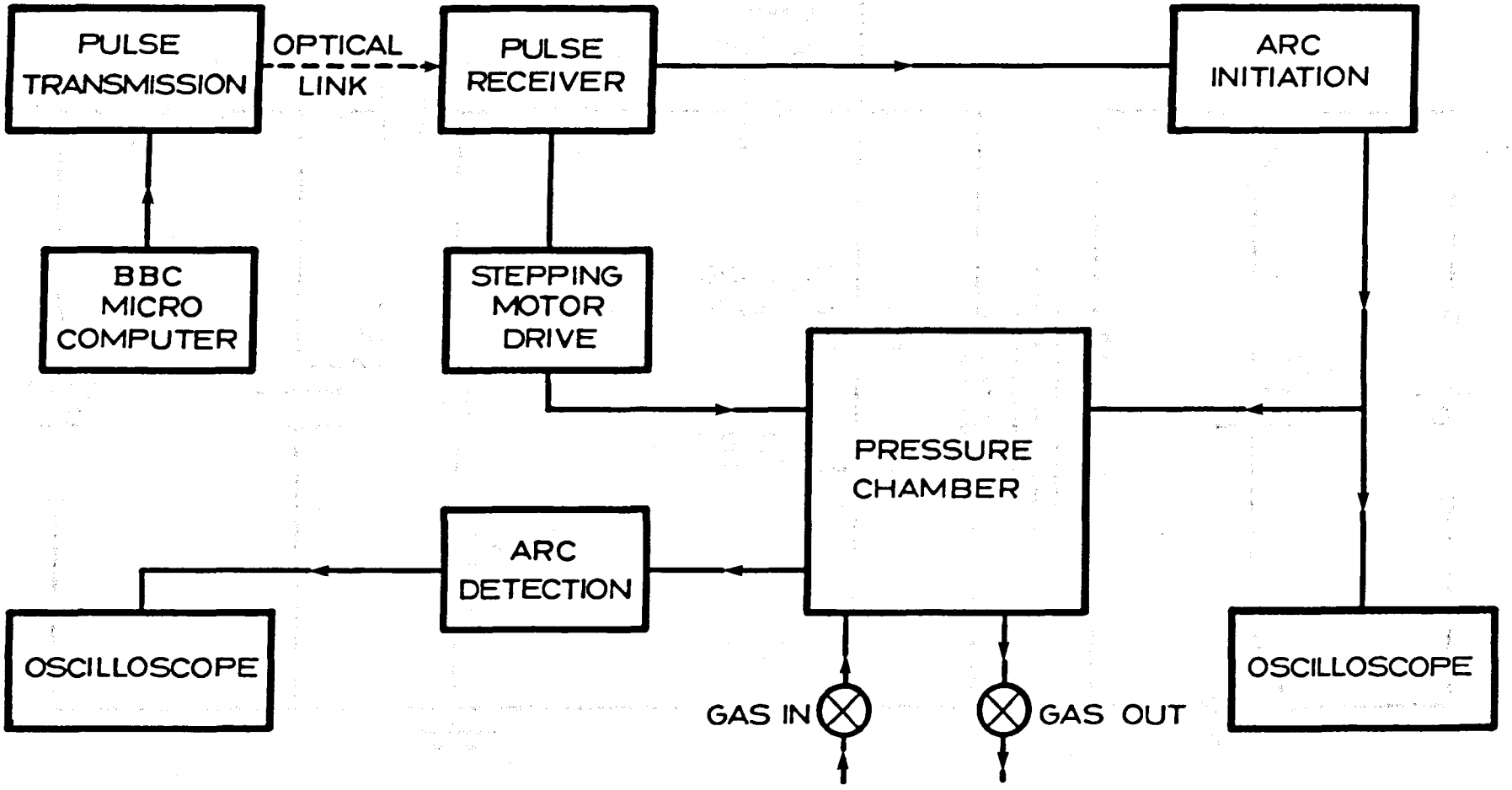

Fig 4.1 Schematic Outline of Arc Apparatus.

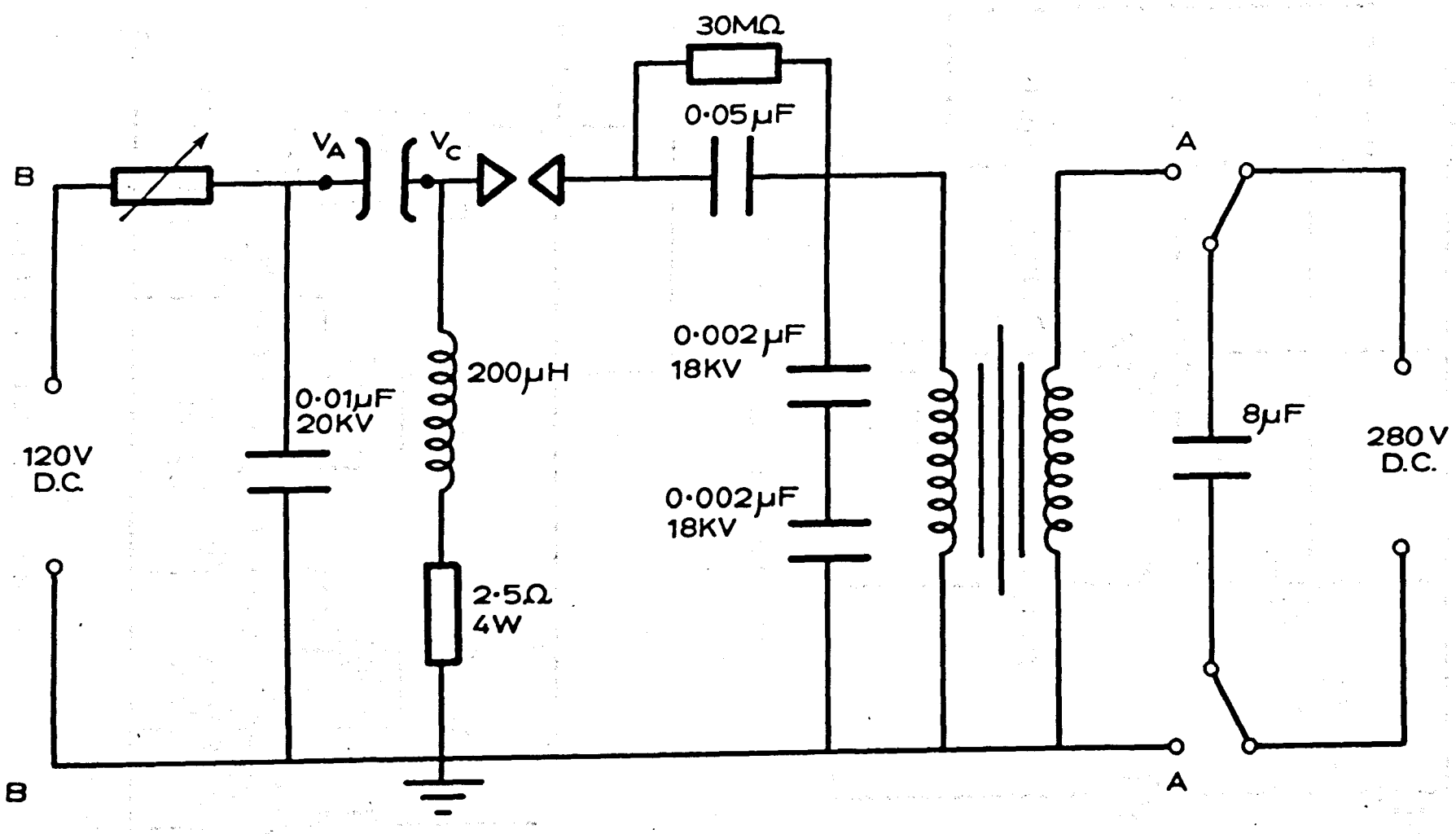

Fig 4.2 The Arc Generation Circuit.

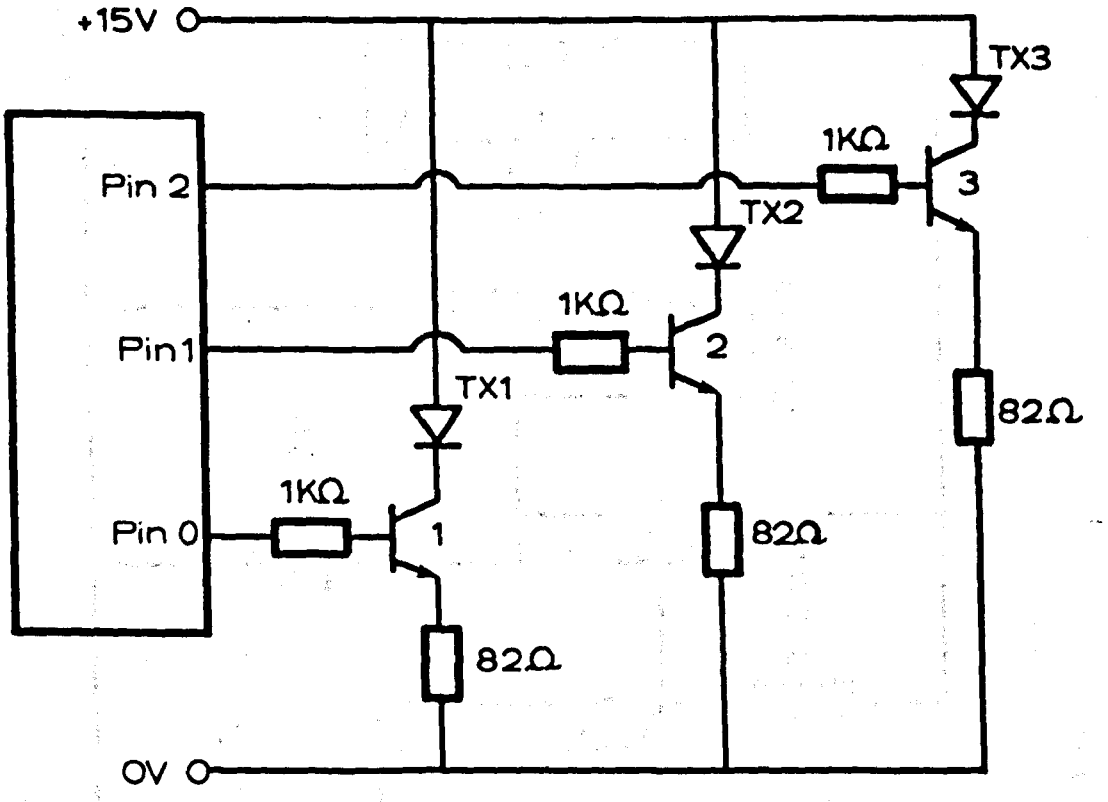

Fig 4.3 The Pulse Transmitter Stage.

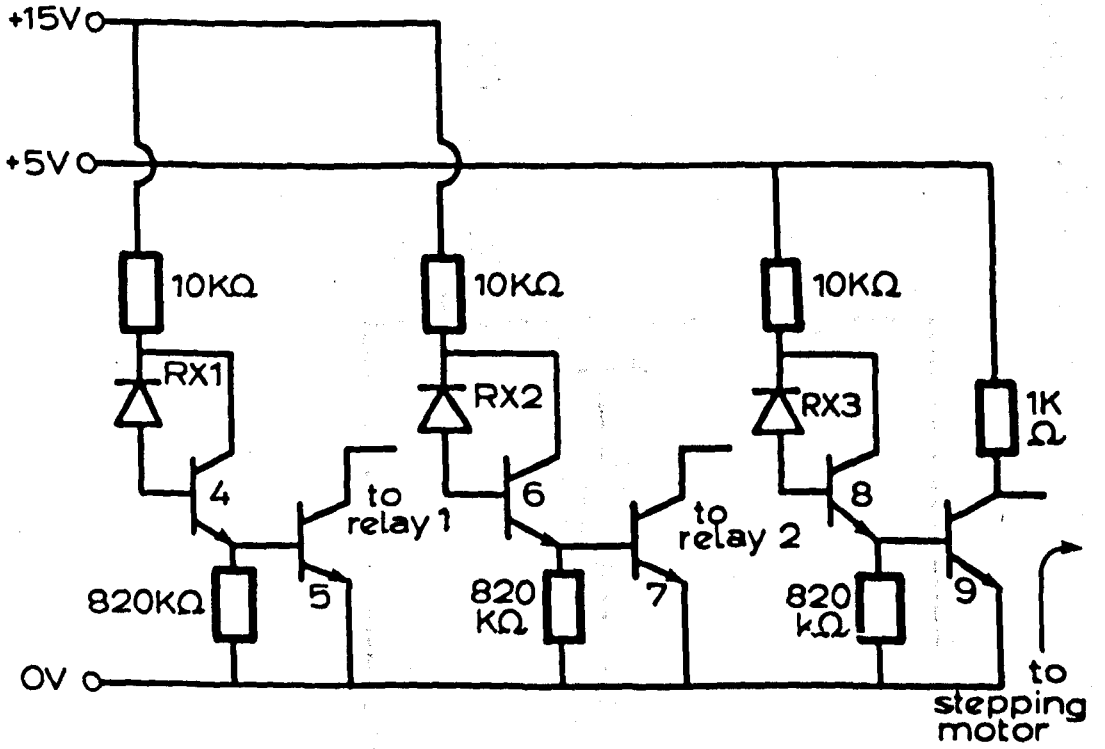

Fig 4.4 The Pulse Receiver Stage.

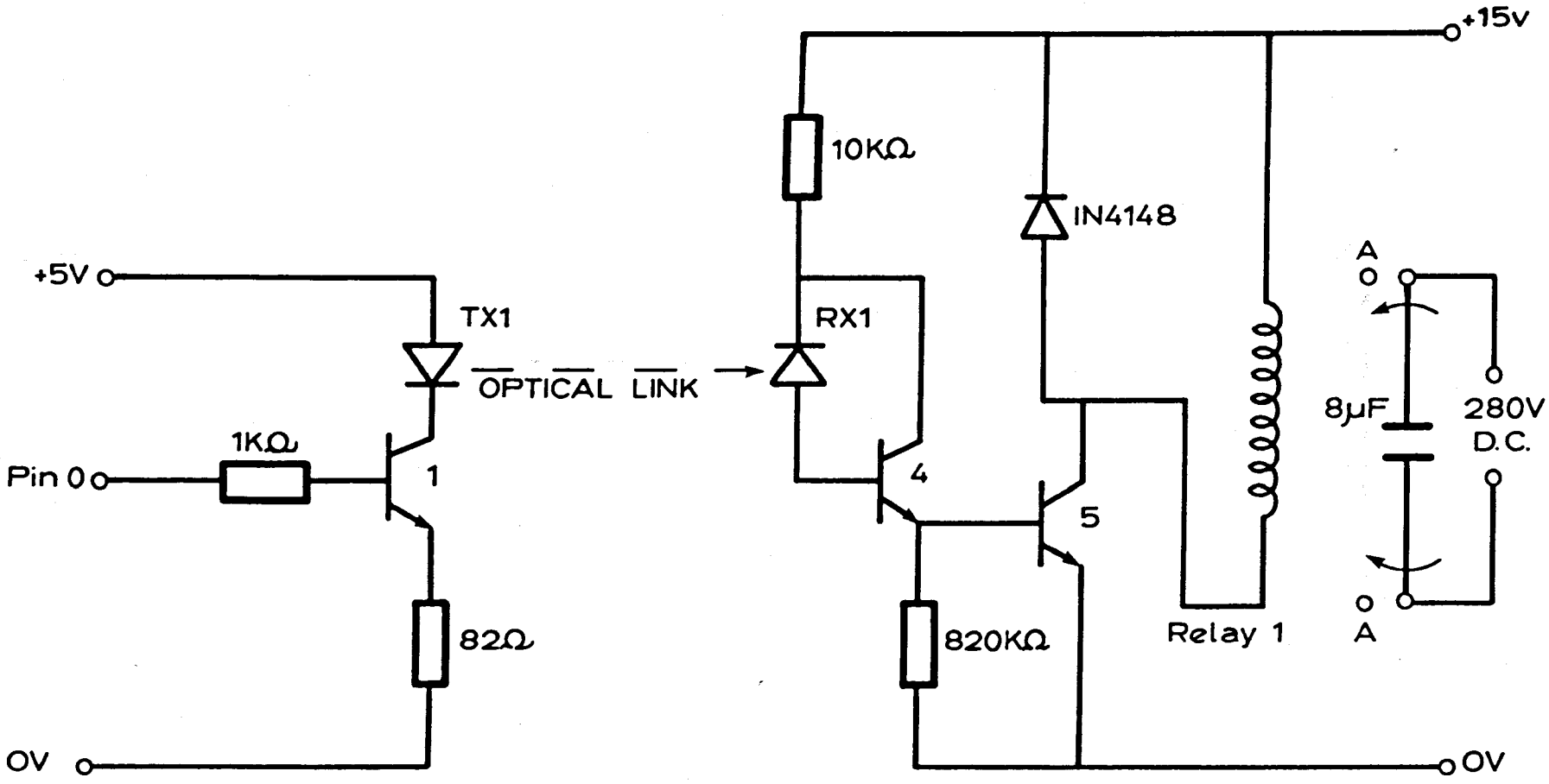

Fig 4.5 Initiation of the Arc.

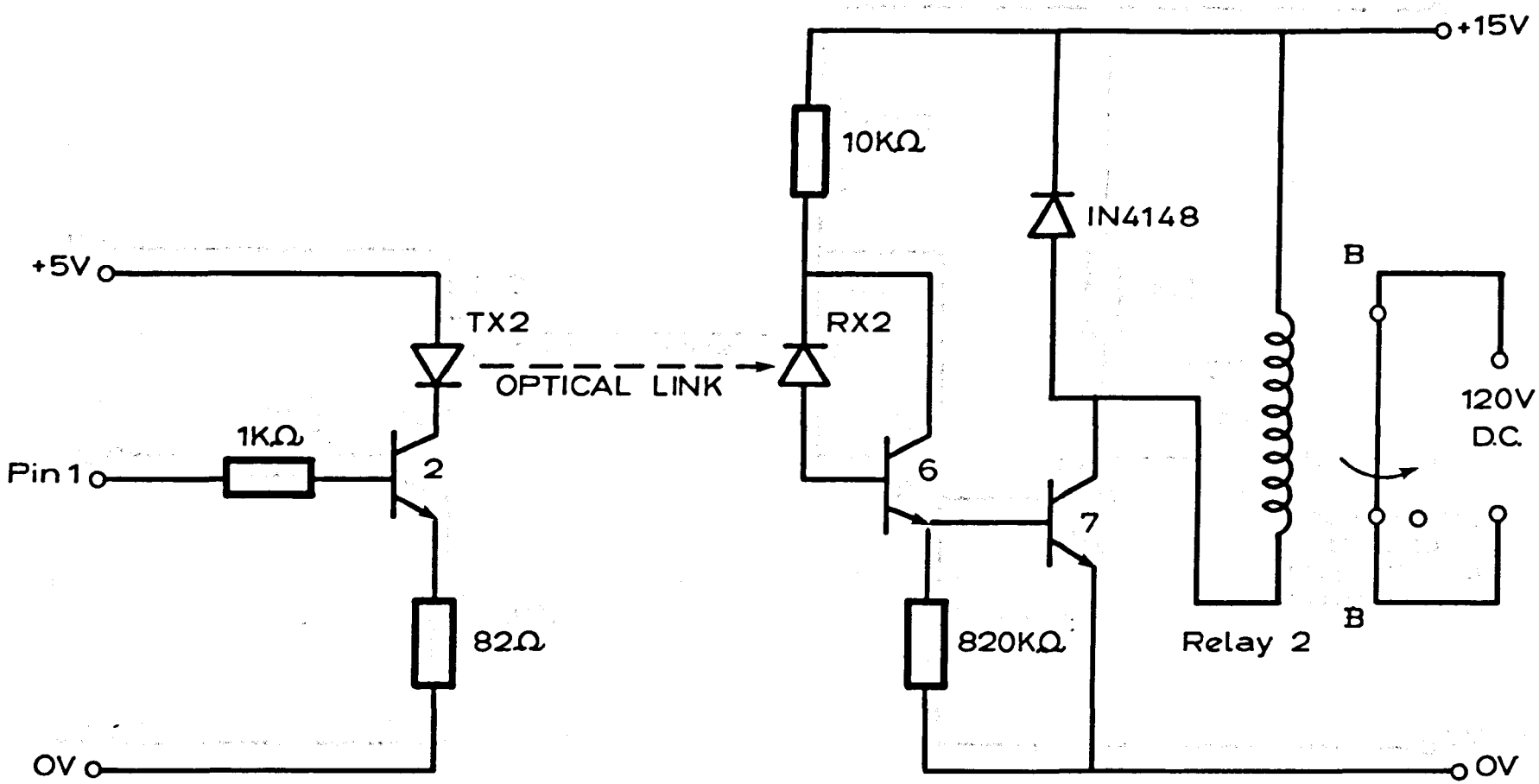

Fig 4.6 Inhibition of the Arc.

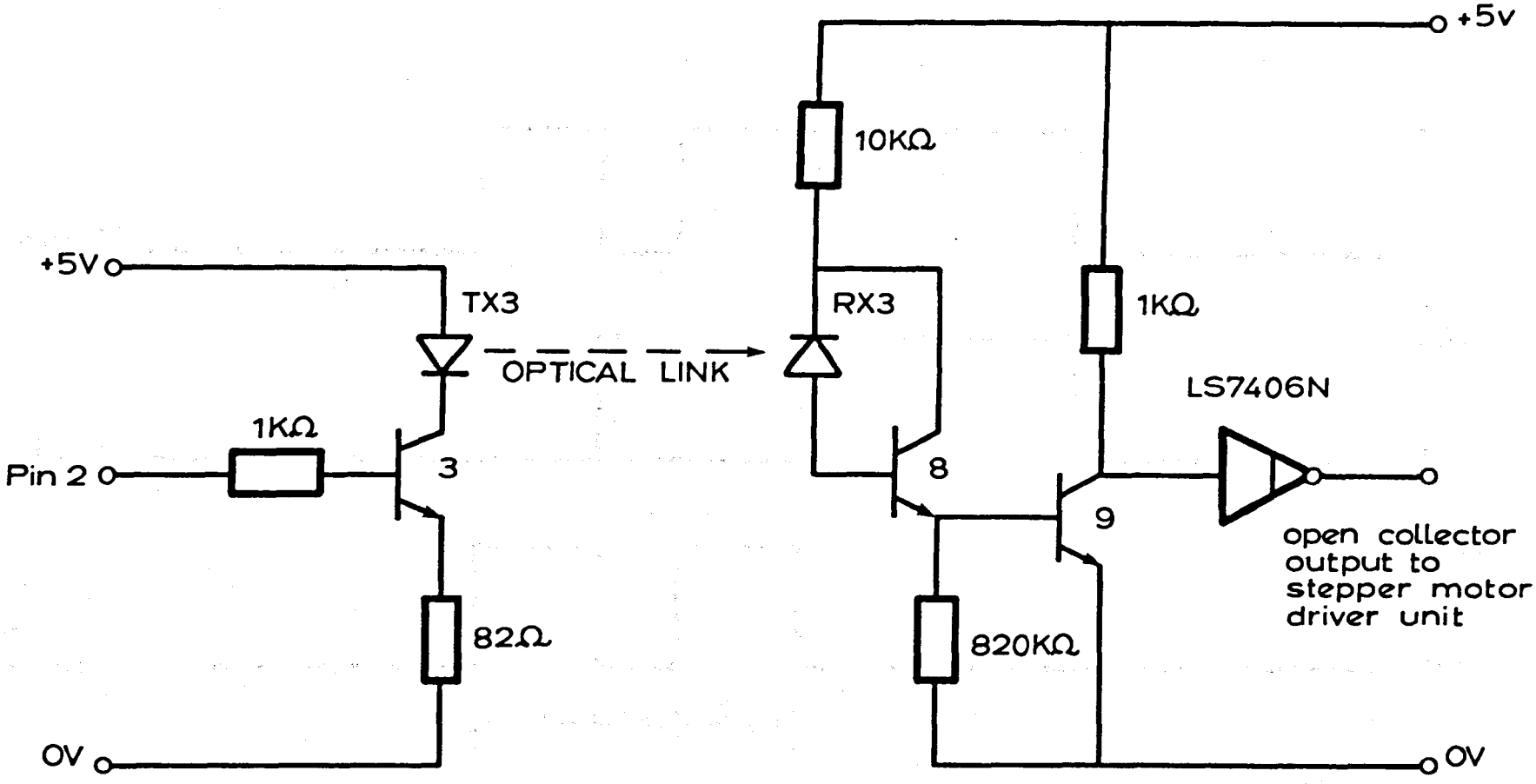

Fig 4.7 Operation of the Stepper Motor.

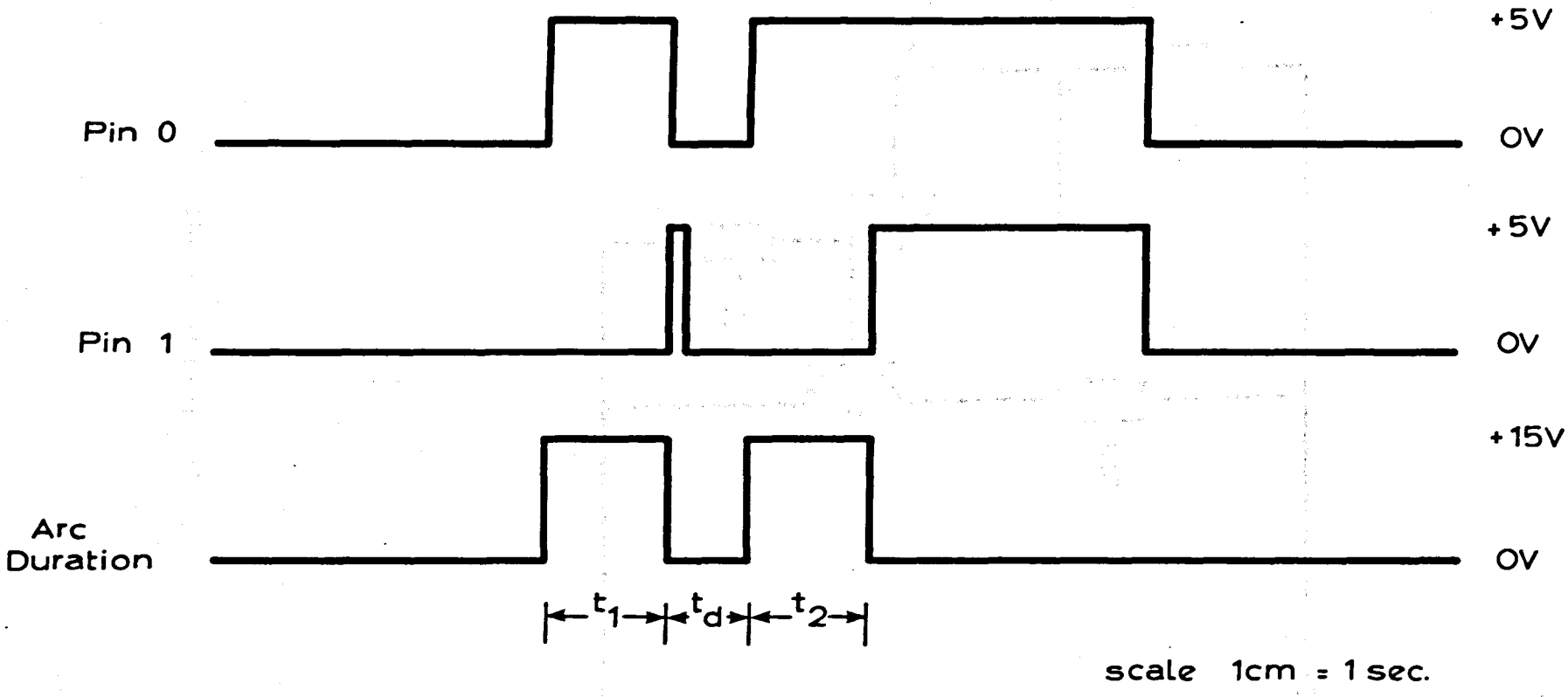

Fig 4.8 Timing Diagram for "DualI".

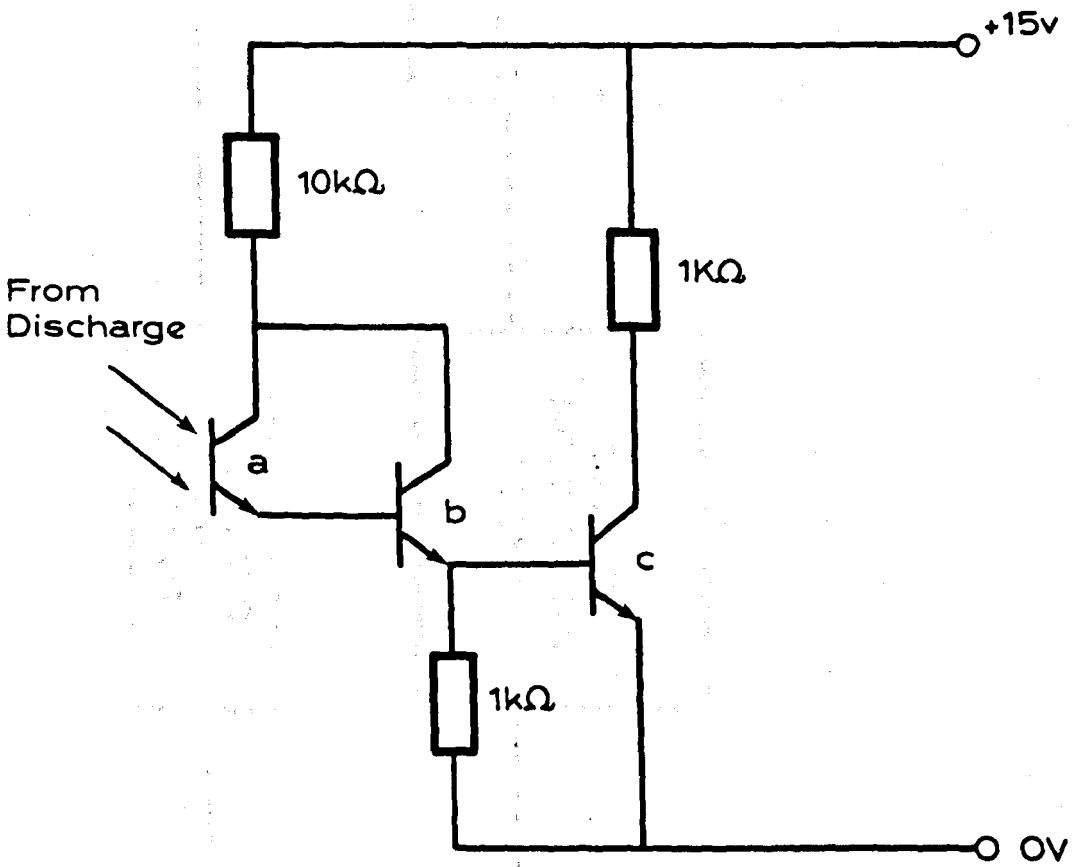

Fig 4.9 The Arc Detection Circuit.

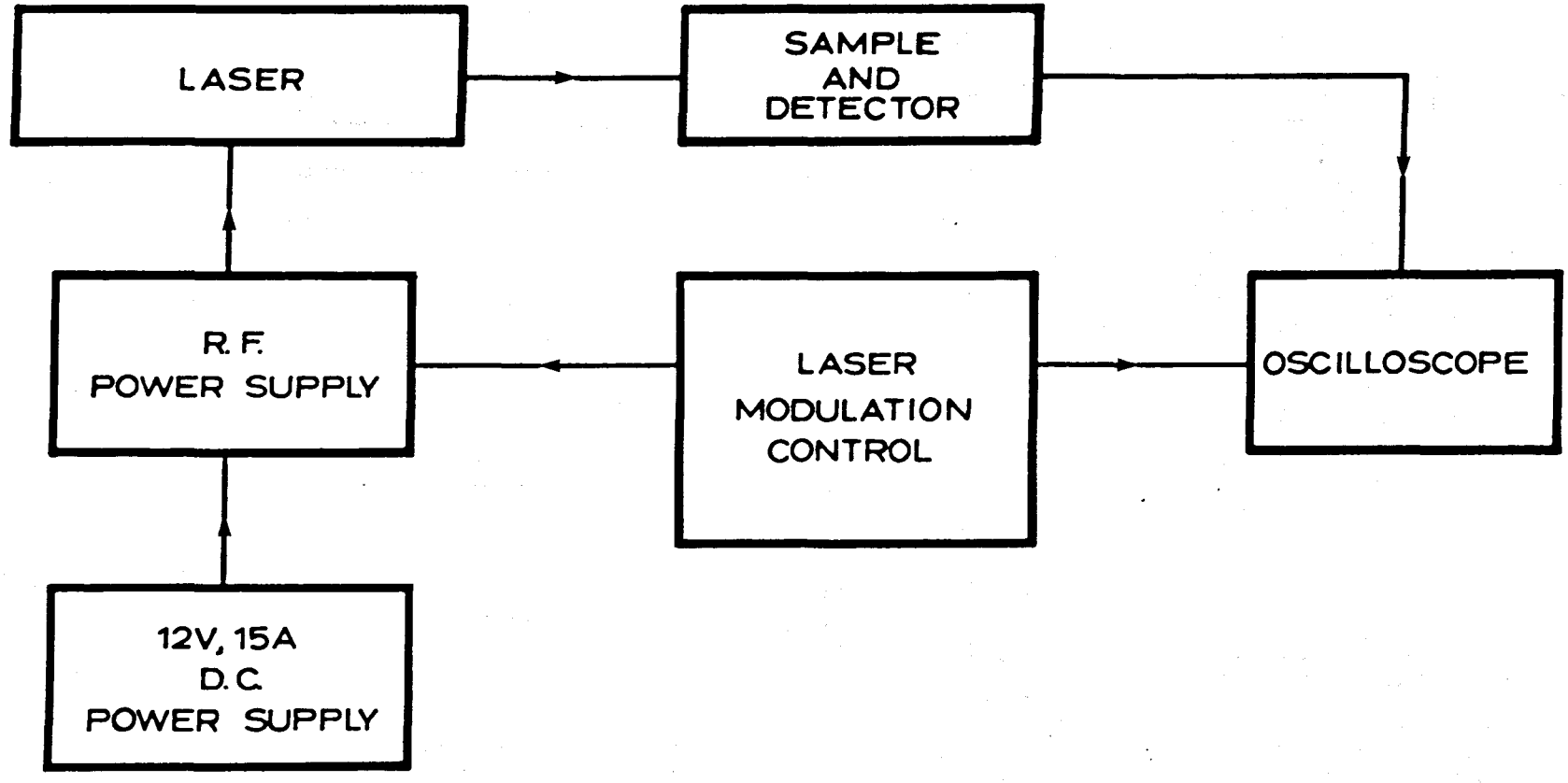

Fig 4.10 The Laser System.

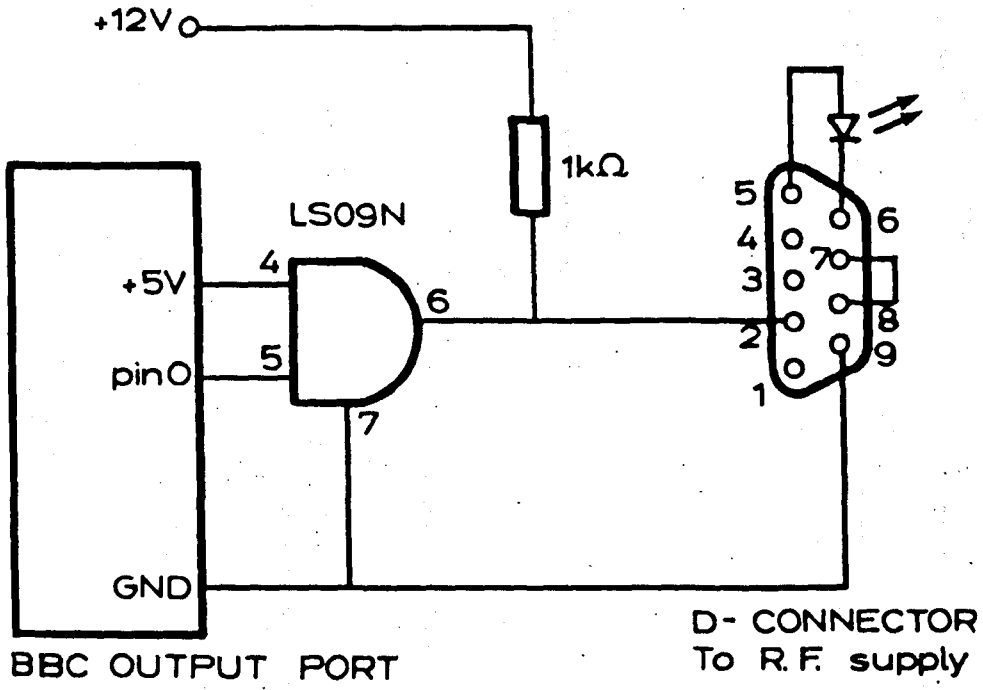

Fig 4.11 Laser Modulation Control.

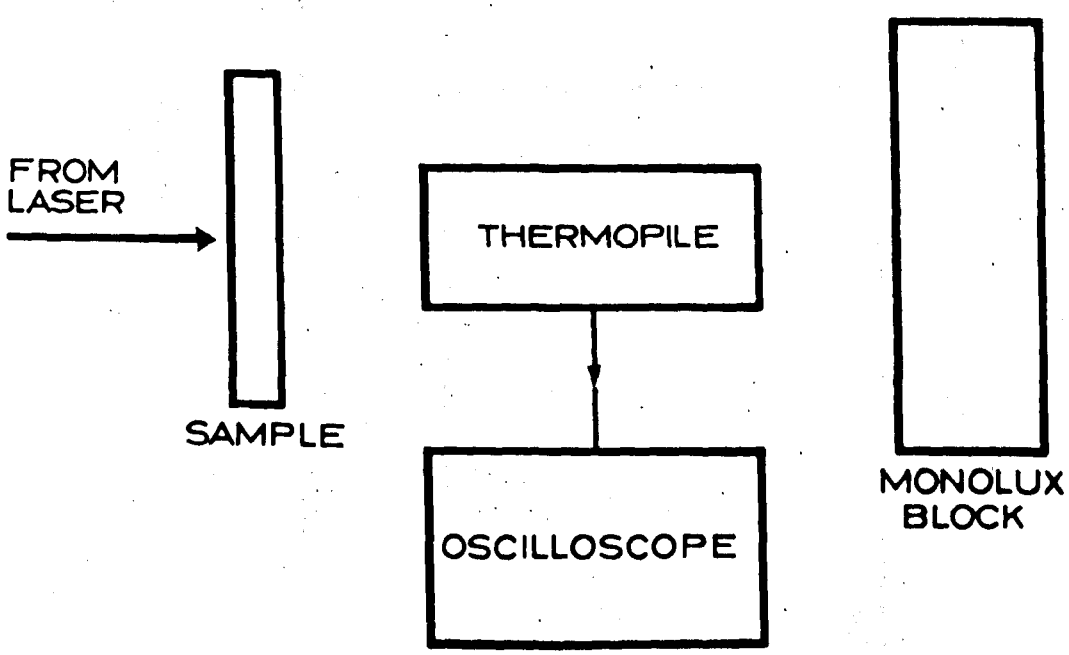

Fig 4.12 Sample and Detector Arrangement.

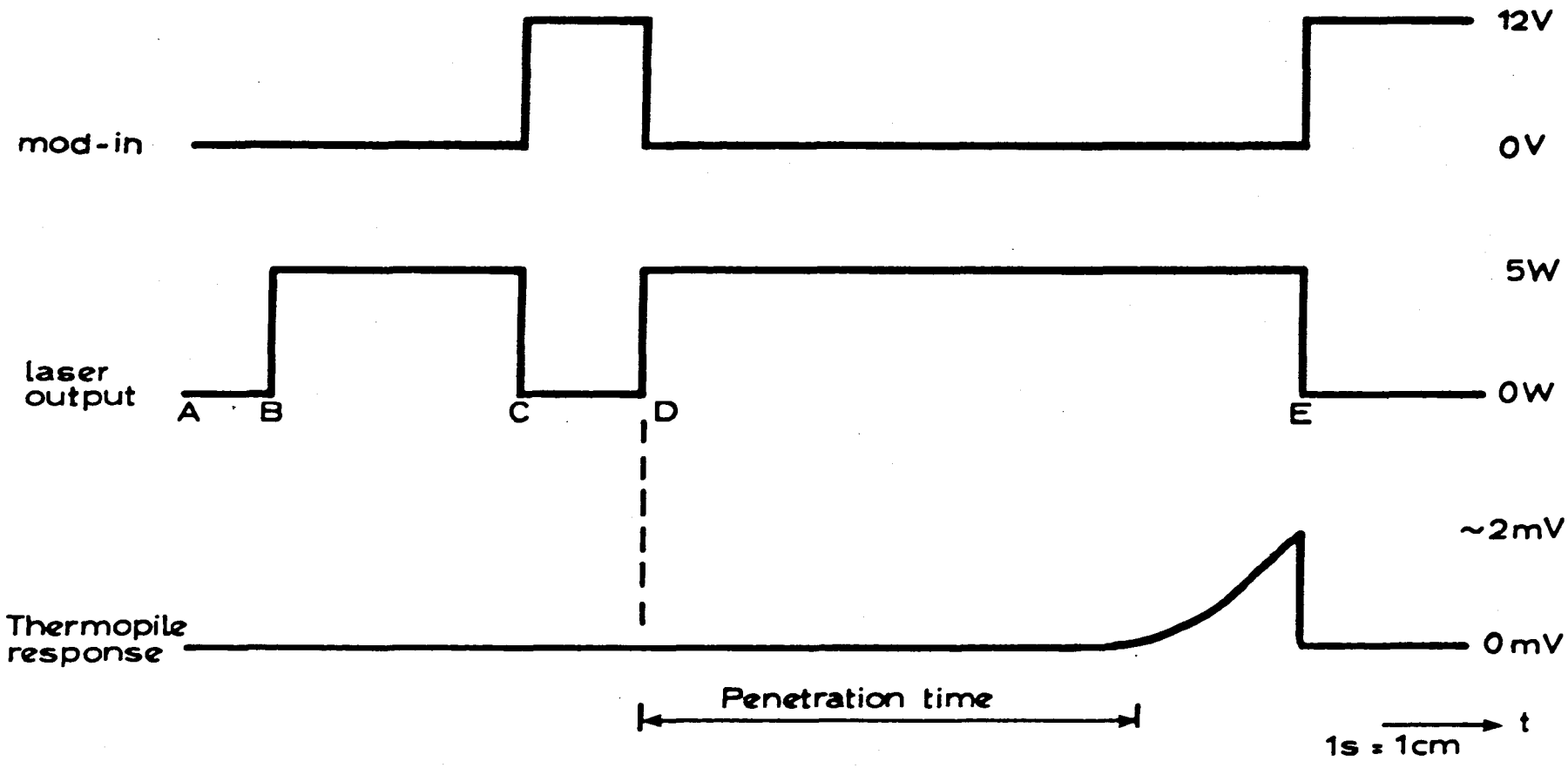

Fig 4.13 Timing Diagram for Laser Strike and Modulation.

CHAPTER 5. EXPERIMENTAL TECHNIQUES.

Having described the apparatus involved in the present experimental programme, it is necessary to include an account of the experimental methods employed and to define the terms used in the subsequent analysis of results contained in chapter 6.

As in chapter 4, this chapter will be concerned with two systems; the arc system and the laser system. The first step will be to discuss the arc system, beginning with a description of the sample and the environmental conditions within the chamber.

5.1 DESCRIPTION OF SAMPLE AND ENVIRONMENTAL CONDITIONS IN CHAMBER.

5.1.1 Characterisation of the Sample.

The samples used in the experimental investigations are consistent with those used by Brennan[1], in order to allow convenient comparison of experimental results.

The samples are thin squares of cellulosic material (tissue paper)[2], having side length 2.00 ± 0.05 cm and weight 0.0130 ± 0.0007 grams. Each sample is checked visually before each test in order to reject any sample that exhibits inconsistencies with a standard specimen.

5.1.2 The Electrodes and Position of Sample.

In order to remain consistent with previous experimental work[1] the electrodes are constructed from sections of "Ultra F" purity carbon rod (spot impurity level of 1PPM) of length 4.00 ± 0.05 cm, tapered at a position midway along the section from 6.00 ± 0.05 mm diameter to 2.00 ± 0.05 mm diameter; the electrodes can be seen in plate 4. The electrodes are replaced regularly during an experimental run due to the tendency of the electrodes to become pitted at the point of the taper. The electrode gap is kept at 0.55 ± 0.05 mm, again in order to be consistent with Brennan.

The position of the sample with respect to the electrodes is vertical, with the electrode gap positioned 1.0 ± 0.5 mm from the centre of the sample; this is consistent with Brennan's "position 6" and also allows convenient visual observation of the spread of flame across the sample (see chapter 6).

5.1.3 The Control of Gas Pressure and Oxygen Concentration in Chamber.

The various gas mixtures used in the research programme are supplied in standard bottles of known concentration of diluents under a pressure of 200 Bar (approximately 200 atm. pressure). When using air at varying pressures, the chamber is closed and the gas is admitted via the underside of the chamber, using the stored pressure of the bottle to pressurise the chamber to the desired level; which is monitored using the gauge which can be seen in plate 1. For gas mixtures other than air the required pressure within the chamber is obtained as above, however the chamber is first evacuated before pressurisation.

The relative concentrations by volume of gases used in the experimental programme are taken from the specifications supplied by B.O.C. Special Gases for each individual gas mixture. We are, however, faced with a problem: if a sample undergoes complete combustion within the chamber, is the concentration of oxygen, by volume percentage, appreciably altered? If it is, the experimental procedure is flawed and the environment is not constant for each sample under test.

An estimate of the change in oxygen concentration experienced within the system upon combustion of one sample can be made:

Consider a gas mixture of 30% O_2 / 70% N_2 at atmospheric pressure, and assume that the sample is totally carbon based having a mass of 0.013g. The chamber is cylindrical having a diameter of 19.6cm and length 20.9cm, and the reaction is 1 : 1, ie.

$$C + O_2 \rightarrow CO_2$$

resulting in complete combustion of the sample. We must first calculate the number of moles of oxygen present in the chamber at standard temperature and pressure (S.T.P.). The volume of the chamber is given by,

$$v = \pi r^2 l = 6306\, cm^3$$

Then as 1 mole of gas at S.T.P. occupies 22.4 litres volume, the number of moles of gas in the chamber is given by,

$$n_G = \frac{6306}{22400} = 0.2815$$

However, we have an oxygen concentration of 30% by volume, so the number of moles of oxygen within the chamber is given by,

$$n_{O_2} = 0.3 \times 0.2815 = 0.0845$$

Assuming the sample is totally carbon based, the number of moles of carbon being consumed in the combustion reaction is given by,

$$n_C = \frac{MASS}{RMM} = \frac{0.013}{12} = 0.0011$$

and, since we have a 1 : 1 reaction, the number of moles of oxygen reacting with the sample during combustion is,

$$n_{O_2} = 0.0011$$

Thus the number of moles of oxygen remaining after the combustion of one sample can be estimated,

$$n_{O_2} = 0.0845 - 0.0011 = 0.0834$$

and the corresponding concentration of oxygen remaining,

$$O_2 = \frac{0.0834}{0.0845} \times 30 = 29.7$$

Thus 0.3% of oxygen by volume is consumed during the combustion of one sample, a value which is considered to be acceptable during the present research.

5.2 DEFINITION AND MEASUREMENT OF EXPERIMENTAL PARAMETERS: THE ARC.

5.2.1 Electrical Input Power for the Production of the Arc.

In any combustion safety investigation it is necessary to quantify the electrical power being supplied to the material under test. As discussed in chapter 4, the electrical input power is obtained using the

anode and cathode voltages (V_A and V_C respectively) and the arc current, I, thus

$$P_A = (V_A - V_C).I \quad Watts \tag{5.1}$$

and the corresponding input energy can be obtained,

$$E = P_A.t \quad Joules \tag{5.2}$$

where T is the duration of the arc.

The absolute values of V_A and V_C are measured using Tektronix X1000 probes and the voltage traces are stored on an oscilloscope. Plate 5 is an example of the voltage trace obtained during a dual pulse test having $V_A = 45.0 \pm 4.0V$, $V_C = 7.5 \pm 0.4V$ and hence $P_A = 70.5 \pm 8.4W$. A discussion of the errors involved in the determination of input power can be found in appendix A.

5.2.2 Radiant Power of the Arc.

In order to estimate the amount of electrical input power being converted to radiant power in the arc it was decided to perform a test using a thermopile, in air at 1 atm. pressure, coupled to a storage oscilloscope with the voltage sensitivity set at a maximum. The thermopile and oscilloscope can be seen in plate 4.

Fig. 5.1 shows the position of the thermopile with respect to the electrodes. The distance from the arc to the thermopile window, r, is

a) Anode Voltage Trace.

b) Cathode Voltage Trace.

Plate 5. Arc Voltage as seen on Oscilloscope.

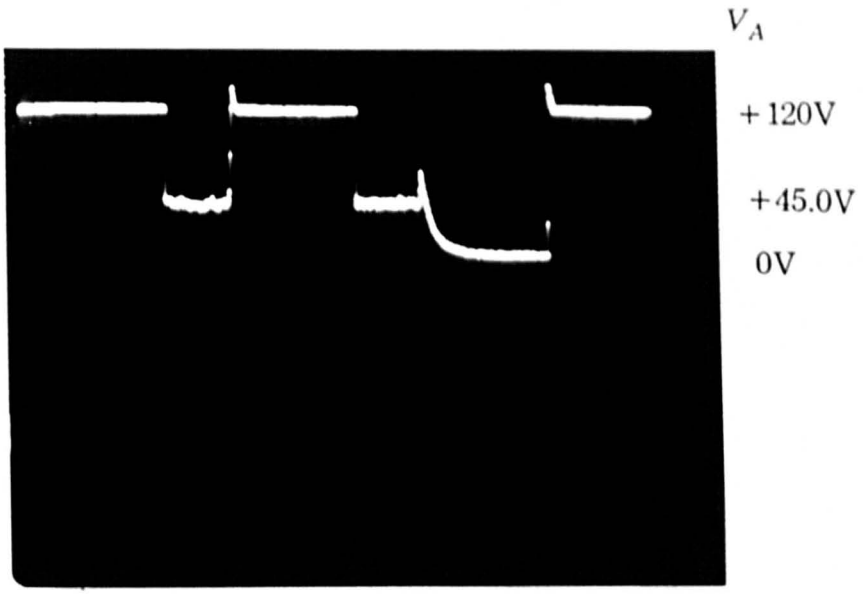

time base: 0.1s/cm

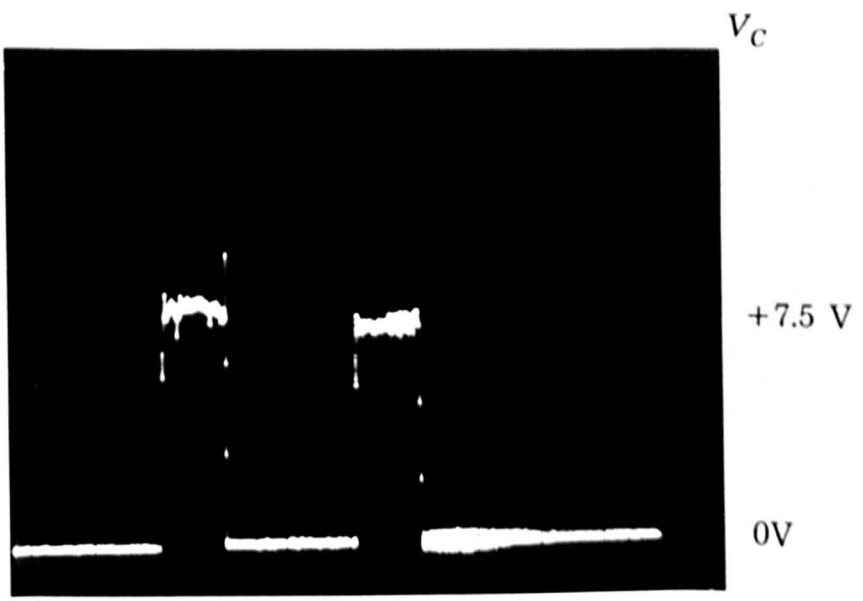

time base: 0.1s/cm

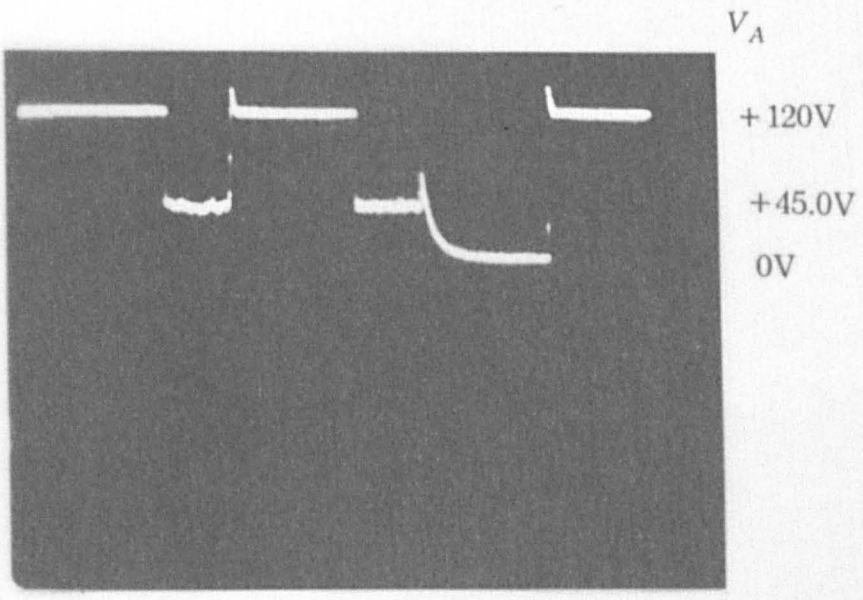

a) Anode Voltage Trace.

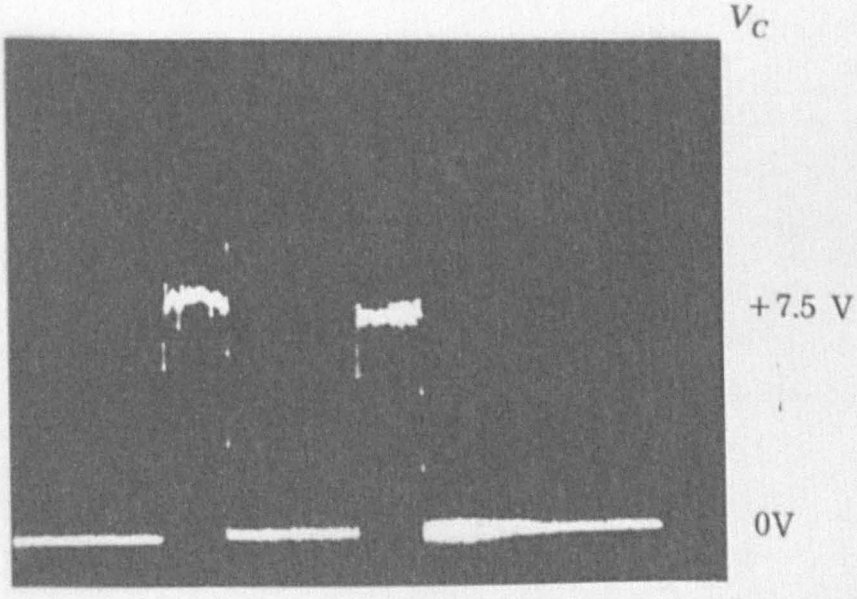

b) Cathode Voltage Trace.

Plate 5. Arc Voltage as seen on Oscilloscope.

$15.0 \pm 0.2cm$, and since $d = 0.55mm$ (the distance between the electrodes), $r \gg d$ and the arc can be approximated to a point source.

By definition[3], the flux per unit solid angle emitted by an entire source in a given direction is the radiant intensity,

$$I_A = \frac{d\phi}{d\Omega} \tag{5.3}$$

If the radiant source is a point source it can be said that the surface of the thermopile of area dA subtends a solid angle,

$$d\Omega = \frac{dA}{r^2} \tag{5.4}$$

If dA is perpendicular to the arc then the flux incident at the thermopile, from equations (5.3) and (5.4), is given by

$$\phi_T = I_S d\Omega = I_A \frac{dA}{r^2}$$

or, the irradiance

$$E_T = \frac{d\phi_T}{dA} = \frac{I_A}{r^2} \tag{5.5}$$

Now I_A is the irradiance of the arc per unit solid angle. However, a point source radiates in a sphere and since the solid angle subtended at the surface of a sphere is

$$\Omega = 4\pi \quad \textit{Steradians}$$

and, from equation (5.5),

$$I_A = E_T r^2 \tag{5.6}$$

the radiant flux produced by the arc is given by,

$$\phi_A = E_T 4\pi r^2 \quad Watts \tag{5.7}$$

The thermopile used in the present investigation has a flat response from U.V. to I.R. and has a responsivity of 27.0 V/W and a sensitive area of 0.04 cm^2. We can define a conversion factor, β, where

$$\beta = \left(\frac{1}{27.0}\right)\left(\frac{1}{0.04}\right) \quad W/Vcm^2$$

thus,

$$\beta = 0.93 \quad W/Vcm^2 \tag{5.8}$$

Thus, for our thermopile, the incident irradiance,

$$E_T = \beta \times \text{voltage output} \quad W/cm^2$$

and the radiant flux at the arc,

$$\phi_A = \beta \times \text{voltage output} \times 4\pi r^2 \quad Watts \tag{5.8}$$

Plate 6a is an example of the response of the thermopile (along with the output of the arc detector used as a timing reference) for the measurement of radiant flux. The output is variable and that shown is typical of those observed for the several values of input power taken in order to produce the graph shown in chapter 6. A discussion of the errors involved in the measurement of radiant flux can be seen in appendix A.

a) Output of Thermopile and Photo-Detector.

b) Output of Photo-detector (Dual Pulse Test).

Plate 6.

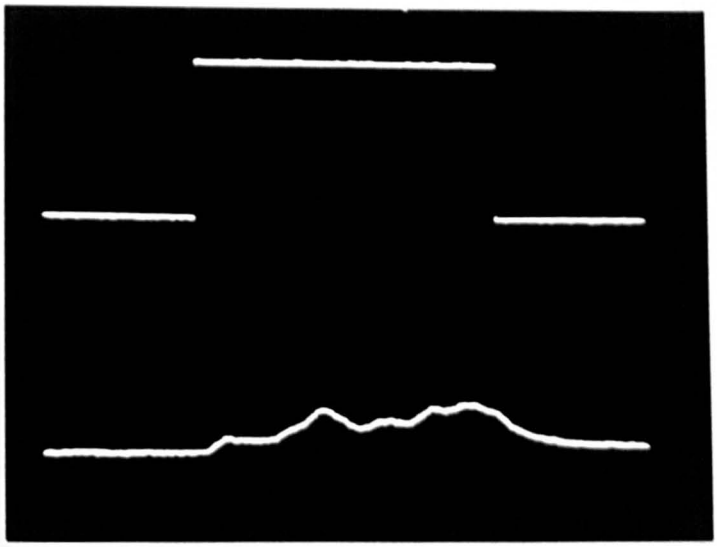

time base: 0.2s/cm

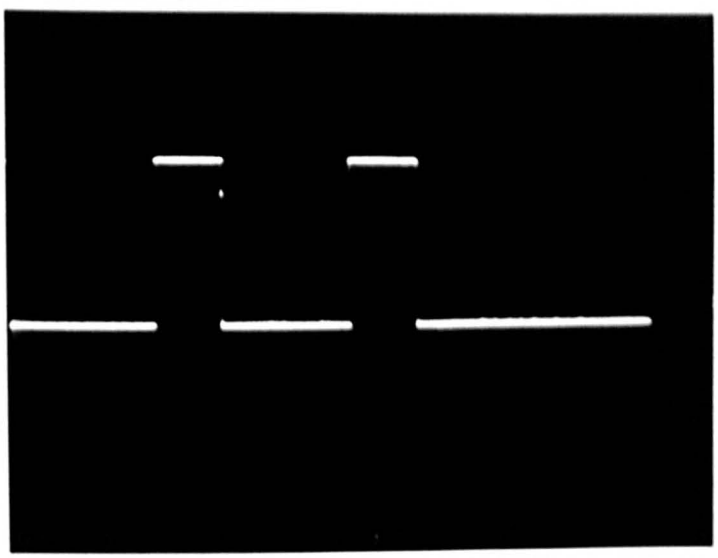

t_1 t_d t_2

time base: 0.1s/cm

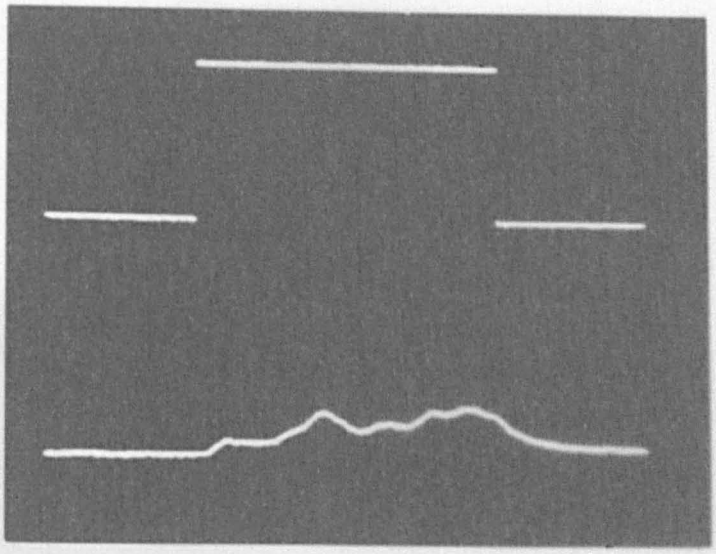

a) Output of Thermopile and Photo-Detector.

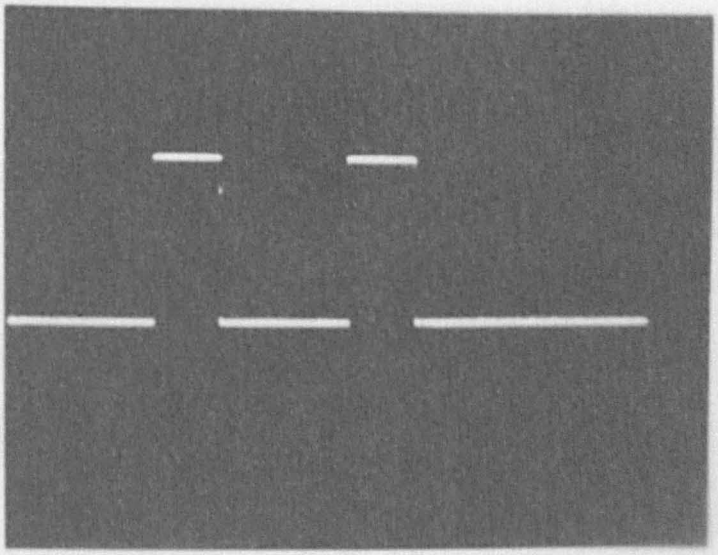

b) Output of Photo-detector (Dual Pulse Test).

Plate 6.

5.2.3 The Probability of Ignition.

The probability of ignition is the parameter that gives us a physical indication of the behaviour of the material under varying conditions of pressure, oxygen concentration and input power, and it is the change in 'zonal ignition' probability (to be discussed later in the chapter) that leads to the measurement of 'critical pulse delay time'. Indeed, Brennan[1] based his measurements of minimum ignition time and time to ignition on some pre-determined level of ignition probability.

The number of samples tested in the present research in order to calculate the probability of ignition is 40 - consistent with Brennan. Thus, since the stepper motor arrangement allows 10 samples to be tested in any one experimental run, four experimental runs are required in order to obtain an estimate of the probability of ignition of a material for a certain set of conditions.

Ignition, in this case, is taken as a sample experiencing persistent flaming ignition and being completely consumed by the flame; this is observed via the viewing port on the side of the pressure chamber. If a sample exhibits charring, or experiences transient flaming ignition followed by extinction, it is not regarded as having undergone complete ignition. The probability of ignition is then calculated as the number of samples experiencing ignition (as defined above) expressed as a percentage of the 40 samples tested. It is worthy of note that once a sample has been tested it is not used again even if, visibly, it seems unaffected by the pulse of radiant energy: it may well have experienced some degree of chemical change, which may effect its subsequent performance. A full

statistical analysis of the probability of ignition can be seen in appendix A.

5.2.4 Dual Pulse Measurement.

The dual pulse measurement procedure forms the basis of the majority of the experimental results contained in chapter 6. Previous experimental work[1] has employed a single pulse of energy from the arc in order to study the combustion behaviour of a sample under varying environmental conditions. The main thrust of the present research programme is to study how the distribution of a known pulse of energy with time affects the combustion behaviour. For instance, let a pulse of energy E produce an ignition probability of, say, 5% and a pulse of energy $E' = 2E$ produce a probability of, say, 30%. If we consider the pulse of energy E' divided into two pulses of energy E with a variable delay between the two such the delay is zero initially and is increased in convenient steps: will the delay have any effect on the combustion behaviour of the sample and will there be a particular delay after which the sample will behave as if it is subject to a single pulse of energy E, as opposed to a pulse of energy $E' = 2E$?

The above investigation is implemented using the program "DualI" and the apparatus described in chapter 4. The timing of the two pulses and the pulse delay are checked using a photodetector whose output is recorded on a storage oscilloscope; see plate 6. An analysis of the errors involved in this procedure can be found in appendix A.

5.2.5 Zonal Probability and the Critical Pulse Delay.

As described above, the Dual Pulse procedure involves dividing a pulse of energy into two equal pulses such that the two pulses, when applied together with no intervening delay, give a 'high' probability of ignition whereas one of the pulses alone gives a 'low' ignition probability. The pulses are then separated by a variable pulse delay and an investigation performed to see if a delay exists at which the original high probability of ignition changes to a low probability due to the material behaving as if it experiences the effect of two individual pulses of energy, as opposed to the two pulses combined.

We will define a CRITICAL PULSE DELAY as that delay at which the ignition probability changes from a high value to a low value, and we will define the two probability levels as HIGH and LOW ZONAL PROBABILITIES. The term 'zonal' is used due to the fact that there is a statistical fluctuation associated with a particular value of ignition probability due to a variety of factors which include the variability of environmental parameters, inconsistencies within each sample, and the variability of the energy source - thus the fluctuation produces a band of values within the high zone and the low zone. In chapter 6 each zone will be represented by a line corresponding to the mean ignition probability (or FLAMMABILITY). A comprehensive analysis of the errors involved in the zonal probability analysis can be found in appendix A.

5.2.6 Time to Visible Flame Front and Sample Burn Time.

The Time to Visible Flame Front is defined as the time from the end of pulse 2 in the Dual Pulse Test to the first appearance of a visible flame, provided the sample is completely consumed by the flame.

The Sample Burn Time is defined as the time from the first appearance of a flame to the extinction of that flame, provided the sample is completely consumed by that flame.

Both of the above parameters are measured using the photodetector whose output is monitored using an oscilloscope as described in chapter 4. An example of the output for a Dual Pulse Test with sample ignition can be seen in plate 7.

5.3 DEFINITION AND MEASUREMENT OF EXPERIMENTAL PARAMETERS: THE LASER.

5.3.1 The Output Power of the Laser.

The maximum output power of the laser beam is measured using a Scientech 374 power meter. The power meter is positioned on the optical bench such that it replaces the sample seen in plate 3 and absorbs the beam at a distance of 20cm from the laser.

The maximum beam power is measured as,

$$P_L = 5.0 \pm 0.5 \quad Watts$$

The error quoted is an estimation of the accuracy of the meter and the fluctuation of the reading whilst the measurement was taken.

As mentioned in section 4.2.1 the laser has a gaussian beam profile with a $\frac{1}{e^2}$ beam diameter of 1.3mm and a divergence of 10mrad. The beam diameter a distance of 20cm away from the laser head can be calculated from[4]:

$$W(z) = z\theta$$

where $W(z)$ is the beam waist a distance z from the laser, and θ is the beam divergence. As,

$$\text{Beam Diameter} = 2W(z)$$

then $W(z)$ is effectively the new $\frac{1}{e^2}$ beam radius,

$$W(z) = 0.01 \times 200 = 2.0mm$$

For a gaussian laser beam the above calculation means that the power at the centre of the beam is at a maximum of 5.0W, but at a distance of 2.0mm away from the centre of the beam the power will drop to 13.5% of its maximum value, which in this case, is 0.7W. This radical drop in power across the beam has far reaching physical implications which will be discussed in more detail in chapter 6.

5.3.2 The Sample Penetration Time.

The sample penetration time is defined as the time taken for the thermopile to detect the laser beam from the moment of first irradiation of the sample.

The sample and sample holder are placed directly in the path of the beam, a distance of 20cm from the laser head, with the thermopile directly behind the sample. The laser is allowed to strike as described in chapter 4 and, between points C and D of Fig. 4.13, the shutter is removed. Irradiation of the sample begins at point D of Fig 4.13 which can be monitored using an oscilloscope at the mod-in of the laser. The response of the thermopile is also monitored using the oscilloscope, and the time between point D and the first response of the thermopile is the sample penetration time.

It is worthy of note that, at all times, the user is screened from the laser beam by a metal canopy which has been coated with temperature resistant paint. Safety goggles are also worn to protect against random scattering of the laser radiation.

The variation of sample penetration time with sample thickness in air at 1 atm. pressure is investigated and the results presented in chapter 6.

5.4 REFERENCES.

[1] Brennan, J.F.M., "Ignition of Materials Under Conditions of Hyperbaric High Oxygen Concentration." PhD. Thesis, Liverpool University. (1987)

[2] Kimberly-Clark Ltd., Larkfield, Maidstone, Kent.

[3] Boyd, R.W., "Radiometry and the Detection of Optical Radiation." Wiley Press. (1983)

[4] Melles-Griot, Optics Guide 3, pp334-343. (1985)

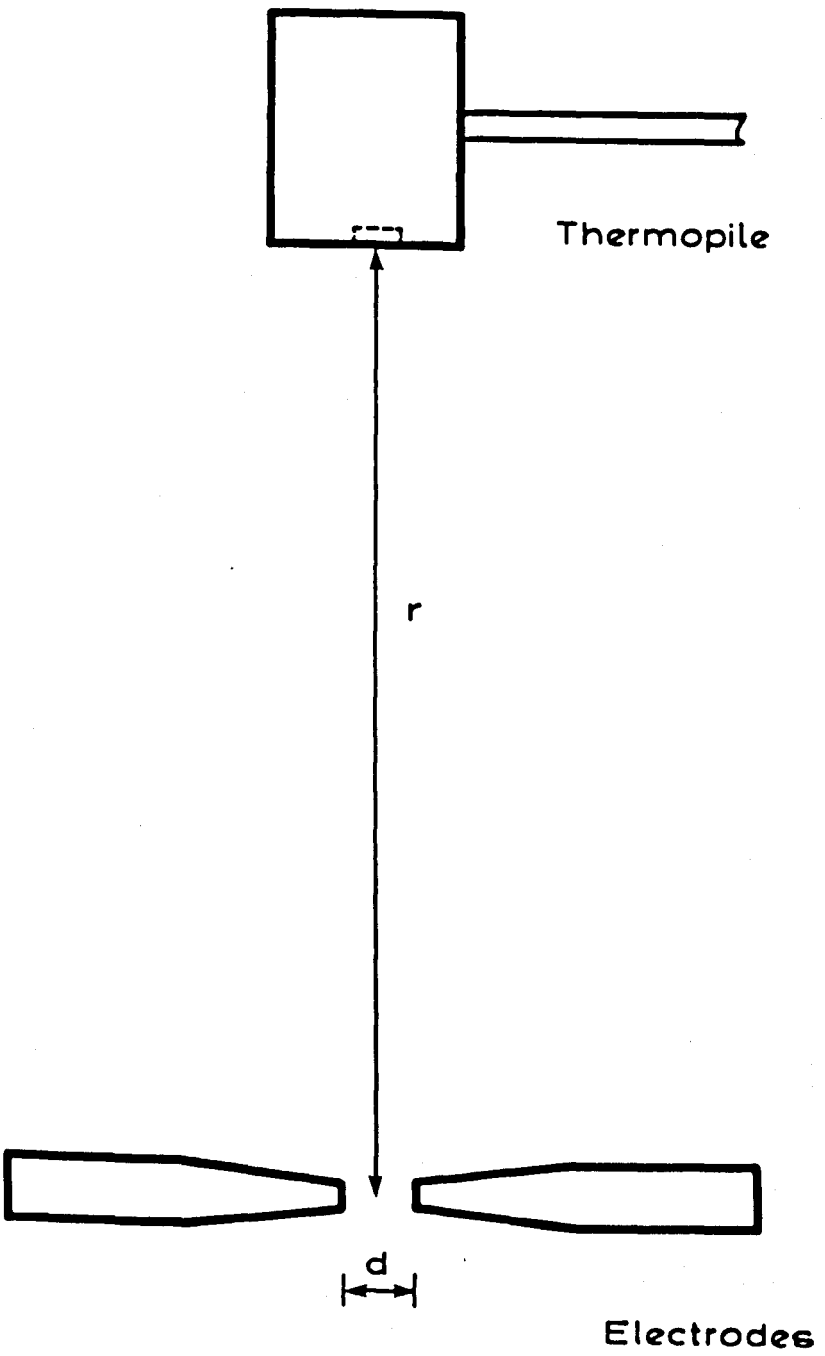

Fig 5.1 Position of Thermopile with respect to Electrodes

CHAPTER 6. DISCUSSION AND ANALYSIS OF RESULTS.

The results presented within this chapter have been obtained mainly using the arc apparatus described in chapter 4 and are concerned principally with obtaining a physical understanding of the combustion process and the effect of the temporal distribution of energy on the ignition safety of a material.

Some measurements have been made using a laser system, however these will be discussed towards the end of the chapter after the discussion of the experimental data obtained using the arc.

6.1 MEASUREMENT OF THE RADIANT FLUX PRODUCED BY THE ARC.

A graph of radiant flux (ϕ_A) versus electrical input power (P_A) corresponding to the results of table 6.1 can be seen in Fig. 6.1. As described in chapter 5, a thermopile having a flat response from U.V. to I.R. was employed, with its responsive area 15cm from the arc kernel and normal to it. The masurements were carried out in air at a pressure of 1 atm. and, although the level of radiant flux incident at the thermopile window will vary with conditions of gas pressure and oxygen concentration, it is useful to gain an insight into the fraction of electrical input power converted to radiant power by the arc.

From Fig. 6.1 it can be seen that for an input power of 54.5W, the conversion to radiant power is of the order of 6%, increasing to 12% for an input power of 99.0W. This percentage of radiant power output seems reasonable when refering to work by Rykalin et al.[1] in which an arc was generated between an iron rod electrode and plate electrode, in air: it was found that 40-45% of the arc power was consumed by the rod electrode and 30-35% by the plate electrode through such processes as electrode heating and the transfer of material by the vapour stream, with the percentage consumed by the rod decreasing with increase of arc current. It is not unreasonable, therefore to assume a power consumption of 80% for a rod - rod electrode system; in the present case graphite is the electrode material having a thermal conductivity of the same order as iron[2]. Power will also be consumed through heating of the bulk gas, leaving 10-15% of the input power as radiant power output.

6.2 THE EFFECT OF INPUT POWER AND ENERGY ON COMBUSTION CHARACTERISTICS.

6.2.1 Flammability and Critical Pulse Delay.

Figures 6.2 to 6.5 are examples of the behaviour of a sample when subjected to a Dual Pulse Test under conditions of varying electrical input power and energy. In each of the tests the gas mixture is air at a pressure of 15 p.s.i. (which approximates to 1 atm. pressure).

In Fig. 6.2 the electrical input power is 54.5W; two curves are seen with the higher probability curve corresponding to a Dual Pulse Test in which each individual pulse has an energy of 7.0J (t = 0.13s) and the lower probability curve corresponding to a Dual Pulse Test with individual pulses of 5.4J of energy (t = 0.10s).

Each curve shows two distinct probability zones with a sharp transition between them at a well defined pulse delay time, which will be refered to as the 'CRITICAL PULSE DELAY'. The higher energy curve has a mean zonal ignition probability (which is essentially a measure of the flammability of the material) initially of 16% which decays to $\approx$ 4% at the Critical Pulse Delay. The lower energy curve is of the same form, with an initial probability of $\approx$ 3.6% decaying to 0% at the Critical Pulse Delay. The Critical Delay Times for the two curves are approximately equal, at a value $\approx$ 0.37s.

In Fig. 6.3 the electrical input power has been increased to 70.5W with the higher energy curve again corresponding to a Dual Pulse Test

with individual pulse energy of 7.0J (t = 0.10s) and the lower energy curve having individual pulses of energy 5.6J (t = 0.08s) ie. again close to the 5.4J used in Fig. 6.2. Both tests shown in Fig. 6.3 behave similarly to those seen in Fig. 6.2 with two distinct high and low ignition probability zones and a sharp transition between them at the Critical Pulse Delay. The mean zonal flammabilities of 16.5% found at short delay times for the higher energy curve, decaying to 4.9% at longer delay times, and the corresponding values of 3.5% and 0% for the lower energy curve, are very close to the values shown in Fig. 6.2. The Critical Delay Times $\approx$ 0.20s are, however, shorter by a factor of two.

Similar behaviour is exhibited with the input power levels increased further to 81.0W and 93.5W, as shown in Figs 6.4 and 6.5 respectively. In Fig. 6.4 the transition for the higher energy curve ($\approx$ 7J) is from a mean high zonal ignition probability of 18% to a mean low zonal ignition probability of 5.6% at the Critical Pulse Delay and the transition for the lower energy curve ($\approx$ 5J) is from a mean high zonal probability of 3.0% to a mean low zonal probability of 0%; the Critical Pulse Delay again decreasing with increase of input power level. In Fig. 6.5 the transition for the higher energy curve (again $\approx$ 7J) is from 16.6% to 5.6% at the Critical Pulse Delay and the transition for the lower energy curve (again $\approx$ 5J) is from 3.5% to 0%; again the Critical Pulse Delay decreasing with increase of input power level.

It is clear from the above that the behaviour of the test samples under different conditions of electrical input power and energy for the Dual Pulse Test is consistent in that in all cases two distinct ignition probability (or flammability) zones are observed with a sharp transition

between the two, at a well - defined critical value of the time delay between the twin pulses. Figs. 6.2 to 6.5 demonstrate some interesting trends concerning the dependency of mean flammability levels and Critical Pulse Delay on input power and energy levels; these are illustrated further in Figs. 6.6 and 6.7.

Fig. 6.6 is a graph of the mean zonal ignition probability for the 'high' zones (corresponding to short delay times) for the two input energy levels used in Figs. 6.2 to 6.5 plotted as a function of the electrical input power. Two straight lines have been plotted and, whilst this is easily justifiable for the 5J energy level, the relationship for the 7J energy level may at first glance seem less justifiable; however the spread of points is regarded by the observer as within experimental limits and the straight line is plotted in order to identify a trend, rather than to express absolute flammability limits. The implications of Fig. 6.6 are that the flammability of the cellulosic samples is dependent on the electrical input energy and reasonably independent of electrical input power, provided the rate at which the energy is supplied is above the flammability limit of the material; i.e. the greater the input energy the higher the mean ignition probability of the sample.

Fig. 6.7 is a graph of critical pulse delay versus electrical input power for the two energy levels plotted in Figs. 6.2 to 6.5. Several interesting conclusions can be drawn from Fig. 6.7:

1. The critical pulse delay is independent of the input energy of each pulse.

2. The critical pulse delay is dependent on the electrical input power (or rate of energy supply), decreasing with increasing power.

The consequences of varying the rate of supply of energy on the combustion behaviour of materials have been discussed by a number of observers.

Lincoln[3] found that slow heating rates (i.e. low power heating) produce volatile products with an average molecular wight which is higher than those formed under conditions of rapid heating. It was also found that higher irradiances yield larger amounts of CO and organic volatiles with many of the products of the flash pyrolysis of cellulose (rapid heating) being short-lived species. Martin[4] found that for short heating exposures the yield of ethylene and hydrogen (which are flammable species) was increased by increasing the rate of heating whilst the yield of water and CO_2 was decreased.

Considering the physical implications of the present Dual Pulse Test and the critical pulse delay, the critical pulse delay may be taken as that point at which the zonal ignition probability of the sample changes due to a change in the concentration of volatile gases at the surface of the test sample. We can then consider the first pulse of the pair as having two principal effects: it supplies energy at a rate which is sufficient to 'boil off' volatile gases from the surface of the sample and causes ignition of those gases, and the solid sample, with a flammability level which is dependent on the energy of the pulse; it also causes 'boil off' of volatile gases which if not ignited by the pulse are available for ignition by the second pulse of the pair.

Initially pulse 1 and pulse 2 are applied together as one continuous pulse of energy having an associated zonal ignition probability as can be seen in Figs. 6.2 to 6.5. The pulse delay is then increased steadily until a point is reached at which the concentration of volatiles at the surface has changed to such an extent that a significant change in zonal ignition probability is observed. It is worthy of note that the lower flammability limit reached long after the critical pulse delay still exhibits an ignition probability greater than that experienced for a single pulse. It may be concluded from this that pulse 1 has altered the surface of the sample to such an extent that the sample will be more susceptible to ignition by pulse 2 than a fresh sample subjected to pulse 2 alone.

Having postulated that the critical pulse delay is dependent on the nature and amount of volatile gas close to the surface of the sample, the effect of input power can be more clearly explained.

Figure 6.7 shows that the critical pulse delay decreases with increase of input power (or rate of supply of energy); this is reasonable when refering back to the findings of Lincoln and Martin that, as the rate of supply of energy is increased, the volatile species 'boiled off' from the surface are lighter in weight and relatively short-lived when compared to those observed for lower heating rates. Thus the volatiles produced by pulse 1 will remain longer near the surface of the sample for a lower value of input power than for a higher value of input power. As the input power is increased the volatile species will be correspondingly lighter and will consist of shorter lived species. These will either decay to less flammable forms or will diffuse away from the surface at a

faster rate than at low input powers and the critical pulse delay will be reduced.

The conclusions drawn from the above observations will be discussed further in chapter 7.

6.3 THE EFFECT OF PRESSURE CHANGE ON THE COMBUSTION CHARACTERISTICS.

6.3.1 Flammability and Critical Pulse Delay.

Figure 6.2 and Figs. 6.8 to 6.11 are examples of the combustion behaviour of the cellulosic samples when the pressure is varied from 1 to 5atm. (here, the unit of 1atm. pressure is taken as an integer multiple of 15 p.s.i. although, strictly, it should be 14.67 p.s.i.). The conditions for each test are that the gas mixture is air, and the input power and energy are held constant at 54.5W and 7.0J per pulse respectively.

Behaviour similar to that seen in section 6.2 can be seen under Dual Pulse Test conditions, with two distinct flammability zones observed and a sharp transition between the two occuring at the critical pulse delay. Taking each figure in turn it is seen that both the mean ignition probability for the high zone and the mean ignition probability for the low zone increase with increase of atmospheric pressure. The critical pulse delay is also seen to increase with increase of pressure.

The effect of pressure on the mean zonal ignition probability (or flammability) for both the high and low zones is summarised in Fig. 6.12. There is close similarity between the upward trends for both the high and the low zones. The increase in flammability is much sharper for an initial increase of pressure from 15 to 45 p.s.i. (1 to 3atm.) with the effect of pressure becoming less marked as higher pressures are reached. This increase in flammability with increase of pressure is consistent with the work of Johnson and Woods[5], Bartels and Howes[6] and Brennan[7] who all found that an increase of pressure increases the flammability of a material under conditions of electrical ignition.

The effect of pressure on the critical pulse delay can be seen in Fig. 6.13. The observed trend is that the critical pulse delay increases with an increase of pressure. This behaviour can be conveniently discussed using the concept of a 'cellulose matrix', introduced by Lewellen et al[8] in which the system under test was divided into two areas, namely the cellulose matrix and the ambient atmosphere, and a 'residence time' was defined as the period spent by a pyrolysis product within the cellulose matrix (i.e. close to the surface) before entering the ambient atmosphere. As discussed in section 6.2, the critical pulse delay is dependent on the rate of supply of volatile products for mixing with air near the surface and on the diffusion rate of these products away from the surface before pulse 2 is incident at the sample. An increase of pressure will act so as to increase the residence time of the volatile products; decreasing the diffusion rate of the volatiles away from the surface of the sample. Thus the effect on the critical pulse delay will be to increase with increase of pressure, and this can be seen in Fig. 6.13.

The above behaviour will be discussed further in chapter 7.

6.3.2 Time to Visible Flame Front and Sample Burn Time.

The effect of an increase of total gas pressure on the time to visible flame front and the sample burn time can be seen in Fig. 6.14. Both parameters are seen to decrease with an increase of total pressure due to the increase of partial pressure of oxygen and improved mixing rate of the volatile products with the oxygen causing acceleration of the combustion reactions. This effect is moderated to some extent by the increase of thermal capacity of the bulk gas with increase of gas pressure, which will adversely affect the transfer of energy between the arc and the sample; however the net effect will be to reduce the time to visible flame front and the sample burn time. The observed decrease of the above parameters with increase of total gas pressure is consistent with the work of previous investigators[5,6,7].

Further discussion of the above observations can be found in chapter 7.

6.4 THE EFFECT OF OXYGEN ENRICHMENT ON THE COMBUSTION CHARACTERISTICS.

6.4.1 Flammability and Critical Pulse Delay.

Figures 6.15 and 6.16 are examples of the combustion behaviour of the cellulosic samples when the oxygen content is increased to 30% and 36% by volume respectively, with balance nitrogen at a pressure of 1atm. The conditions for each test are that the electrical input power and energy are held constant at 54.5W and 7.0J per pulse respectively.

Behaviour similar to that seen in sections 6.2 and 6.3 can be seen under Dual Pulse Test conditions, with two distinct flammability zones observed and a sharp transition between the two occuring at the critical pulse delay. Taking each figure in turn it can be seen that both the mean ignition probability for the high zone and the mean ignition probability for the low zone increase with increase of oxygen concentration at constant pressure. The critical pulse delay is also seen to increase with increase of oxygen concentration at constant pressure.

The effect of oxygen concentration on the mean zonal ignition probability for both the high and low zones is summarised in Fig. 6.17. Both curves exhibit similar behaviour with a concentration of 16% by volume as the limiting oxygen concentration, giving a zero level of flammability for the Dual Pulse Test conditions. This level of oxygen content is insufficient to allow adequate mixing with the volatile gases produced under dual pulse conditions, and no combustion reactions can

proceed. As the oxygen content is increased at constant pressure, the mixing of volatile species with oxygen is improved and a corresponding increase of flammability is observed with both the high and low probability curves having similar slopes, until the slopes of the curves decrease at an oxygen concentration of 36% in balance nitrogen.

The effect of varying the oxygen concentration at constant pressure on the critical pulse delay is summarised in Fig. 6.18. As discussed above , a concentration of 16% oxygen in nitrogen is the flammability limit for ignition as defined in chapter 5, therefore no critical pulse delay can be observed for this level of oxygen concentration. The trend observed in Fig. 6.18 is for the critical pulse delay to increase with increase in the level of oxygen enrichment. As discussed above, there is an increase in flammability associated with an increase of oxygen content; the resulting effect on the critical pulse delay, which will be discussed in more detail in chapter 7, is that diffusion and chemical decay of flammable species to less flammable forms will occur at a higher initial concentration of gaseous fuel species than for lower values of oxygen content, allowing more time for pulse 2 to reinforce pulse 1 and hence increasing the critical pulse delay - as observed in Fig. 6.18.

6.4.2 Time to Visible Flame Front and Sample Burn Time.

The effect of a change of oxygen concentration at constant pressure on the time to visible flame front and sample burn time can be seen in Fig. 6.19. The observed trend for both curves is to decrease with in-

crease of oxygen concentration, the rate of decrease of sample burn time being less than that of the time to visible flame front.

The above behaviour is reasonable for an increase of oxygen concentration at constant pressure; the improved mixing rate of the volatile fuel with oxygen and the accelerated combustion reactions will have the effect of reducing the time from the end of the energy input region to the first signs of sample combustion; the improved mixing rate of the volatile gases produced by the advancing flame front will increase the sample burning rate, hence decreasing the sample burn time. This is consistent with the findings of the present research programme and is in agreement with the work of a variety of investigators[5,6,7].

6.5 THE SPREAD OF FLAME ACROSS THE SAMPLE.

During the present programme of research, three principal types of flame spread were observed through the viewing port of the pressure chamber; these will be classified as 'outward concentric flame front', 'reversing flame front', and 'reversal/extinction behaviour'. For each example of flame spread observed through the viewing port, the photodetector located beneath the sample gave a response dependent on the particular type of flame spread under consideration. Typical examples of the 'signatures' of each of the three different types of flame spread observed and detected by the photodetector can be seen in plate 7.

a) is an example of outward concentric flame spread. With this mode of flame spread an ignition site is first seen at the centre of the

sample, in close proximity to the arc kernel, and combustion proceeds with the flame front spreading outward from the centre in all directions; finally consuming the material. The consistent light output due to the relative uniformity of the flame spread gives rise to the response of the photodetector seen in plate 7 a. The first two 'spikes' correspond to the two pulses of the Dual Pulse Test, separated by the (variable) pulse delay.

b) is an example of flame spread due to reversing flame front. As in a), the two 'spikes' seen at the start of the trace correspond to the Dual Pulse Test. With this mode of flame spread the ignition site is again seen at the centre of the sample with the flame front spreading downwards towards the bottom edge of the sample. The flame front then appears to momentarily extinguish as it reverses and spreads upwards along the edges of the sample, consuming the remaining material. This effect is mirrored by the output trace of the photodetector with an initial output due to the downward flame spread, a short zero output region due to momentary extinction and reversal of the flame front, and another region of positive output due to consumption of the remaining material.

c) is an example of reversal/extinction behaviour and is the least common of the flame spread phenomena discussed here. The ignition site is again at the centre of the sample with the flame front spreading downwards and then experiencing extinction. The trace seen in plate 7c shows a short region of output from the photodetector which represents the initial downward flame spread followed by extinction. The sample shown with the trace shows visible signs of charring above the ignition site as the flame front has attempted reversal. Since a concentration of

a) Outward Concentric Flame Front.

b) Reversing Flame Front.

c) Reversal/Extinction.

Plate 7. Output of Photo-Detector (Flame Spread).

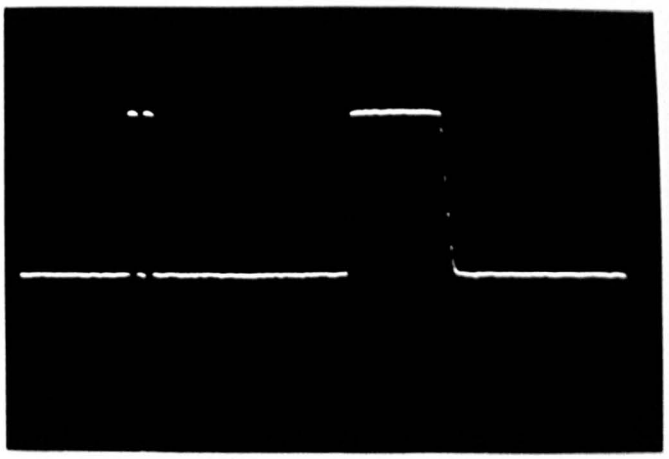

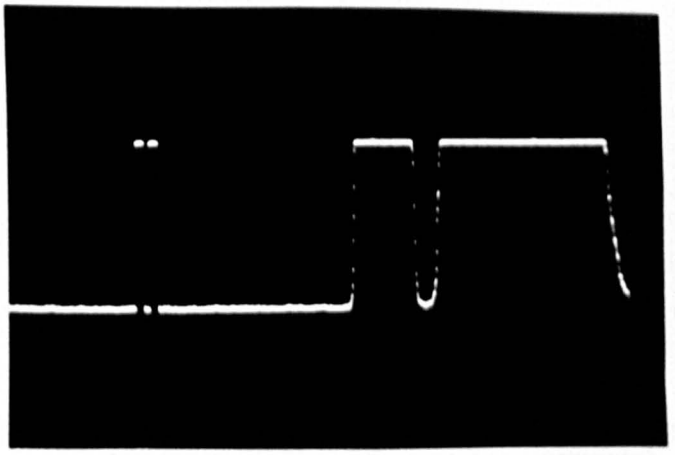

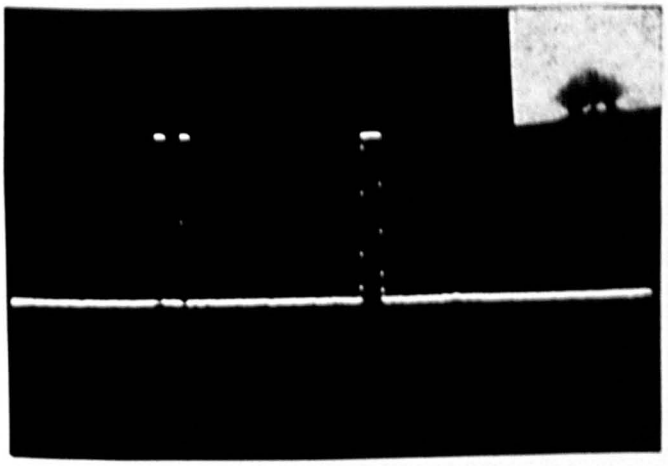

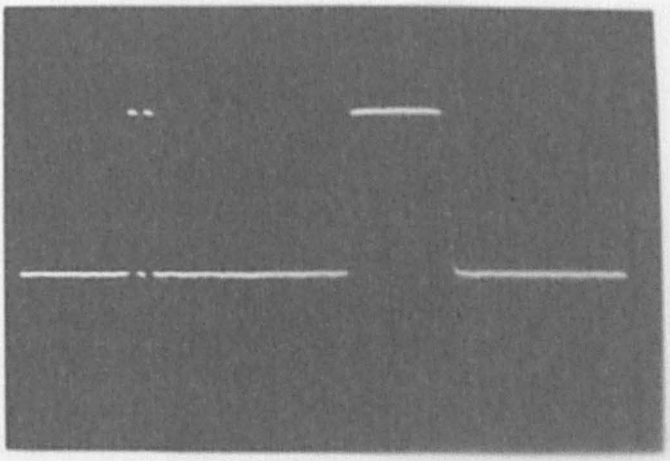

a) Outward Concentric Flame Front.

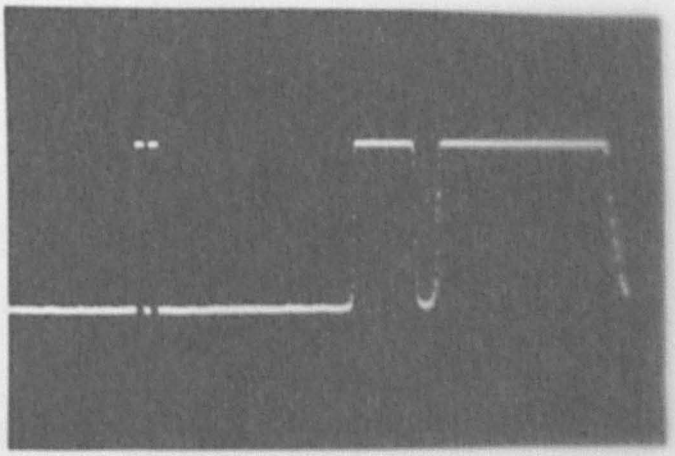

b) Reversing Flame Front.

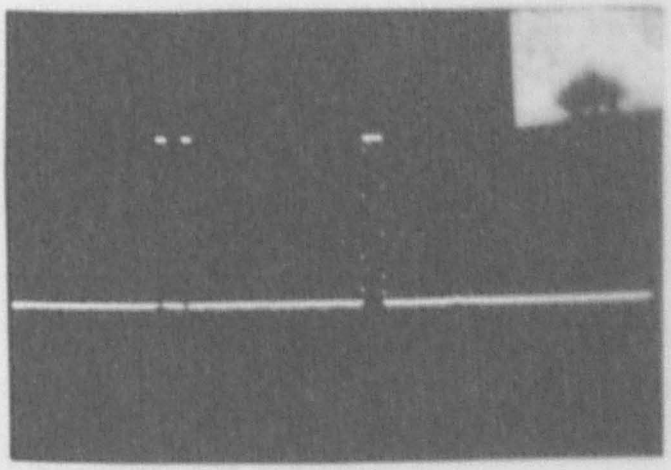

c) Reversal/Extinction.

Plate 7. Output of Photo-Detector (Flame Spread).

volatiles insufficient to allow further combustion of the sample was then produced, the flame was extinguished.

The relative probabilities of occurence of a), b), and c) appear to be independent of input power, energy, gas pressure and oxygen concentration.

6.6 SAMPLE PENETRATION TIME OF THE LASER.

A graph of sample penetration time versus thickness of material can be seen in Fig. 6.20. As described in section 5.3.2. the results are taken using a thermopile positioned directly behind the sample and in line with the laser beam. The thickness of sample is varied by clamping a varying number of 0.01mm thick samples together in the blackened sample holder seen in plate 3. The time between first irradiation of sample and first response of thermopile as seen in Fig 4.13 is plotted against thickness of sample. The results displayed in Fig. 6.20 are obtained by taking the average of ten repeated measurements.

Through visual observation of the samples under test it is observed that the samples do not combust completely with the appearance of a flame. Initially, charring of the material occurs followed by vaporisation of a small area of sample: the beam then 'bores' through the material, penetrating through to the thermopile in a time that depends on the thickness of the material as seen in Fig. 6.20. The relationship of Fig. 6.20 is initially linear, with a sample thickness of 0.10cm having a penetration time of 8.0s, becoming non-linear as the thickness is increased

above 0.15cm. It is postulated that the non-combustion and 'boring' behaviour of the sample is due principally to the properties of the laser radiation.

The gaussian profile of the laser beam, as mentioned in chapter 5, is such that the laser beam has a peak power of 5.0W at the centre of the beam waist. However, the power falls sharply with distance, radially from the centre, until it is at a value of 0.7W at the edge of the beam waist (2mm from the centre of the beam). From section 6.2. the nature of the decomposition products given off from the sample is power dependent, with an increase of power having a tendency towards the production of lighter, more volatile species. Thus the relative concentrations of flammable species produced by the beam will vary along the radius of the beam as the power is reduced (from above). It is proposed that, due to this effect, the volatile cloud produced during the vaporisation of the sample does not have a unique balance of flammable species, as is the case of that produced by the more uniform arc source, but has a varied concentration of flammable species, due to the variable power profile of the beam, which is insufficient to produce the combustion reaction balance necessary for the spread of flame.

Another characteristic of the laser beam is that it produces radiation of a single wavelength of 10.6 microns. It is proposed that in order for the many combustion reactions within the volatile cloud to proceed, a wide range of wavelengths are required from the incident radiation. Thus a single wavelength energy source may be insufficient to produce the flammable species necessary to combine and initiate the complete combustion of the sample.

The influence of the above beam properties on the combustion behaviour of the sample will be discussed further in chapter 7.

6.7 REFERENCES.

[1] Ryalkin, N.N., Kulagin, I.D. and Nikolaev, A.V., "Vaporised Electrode Material and Energy Balance in Welding Arcs." A Symposium, The Institute of Welding. (1962)

[2] Kaye, G.W.C., and Laby, T.H., "Tables of Physical and Chemical Constants." 14th Edition, Longman Press. (1985)

[3] Lincoln, K.A., "Flash Pyrolysis of Solid Fuels by Thermal Radiation." Pyrodynamics, 2, pp.133-143. (1965)

[4] Martin, S., "Ignition of Organic Materials by Radiation." Fire Research Abstracts and Reviews, 14, pp. 24-25. (1972)

[5] Johnson, J.E., and Woods, F.J., "Flammability in Unusual Atmospheres, Part 1. Preliminary Studies of Materials in Hyperbaric Atmospheres Containing Oxygen, Nitrogen, and/or Helium." NRL. Report 6470. (Oct. 1966)

[6] Bartels, A.L. and Howes, J.A., "The Variation of Minimum Igniting Currents with Pressure, Temperature and Oxygen Enrichment." Electrical Research Association Report. (March 1971).

[7] Brennan, J.F.M., "Ignition of Materials Under Conditions of Hyperbaric High Oxygen Concentration." PhD. Thesis, Liverpool University. (1987)

[8] Lewellen, P.C., Peters, W.A., and Howard, J.B., "Cellulose Pyrolysis Kinetics and Char Formation Mechanism." Sixteenth Symposium(International) on Combustion,pp.1470-1480.(1979)

P_A Watts	$\pm \Delta P_A$ Watts	ϕ_A Watts	$\pm \Delta \phi_A$ Watts
21.5	2.9	0.31	0.05
31.5	4.3	0.63	0.08
54.5	6.4	3.20	0.50
70.5	8.4	5.30	0.90
74.0	8.8	6.30	1.10
81.0	10.1	7.90	1.30
87.5	11.4	9.50	1.60
93.5	12.9	10.50	1.90
99.0	13.4	12.10	2.10

Table 6.1 Variation of Radiant Flux with Electrical Input Power.

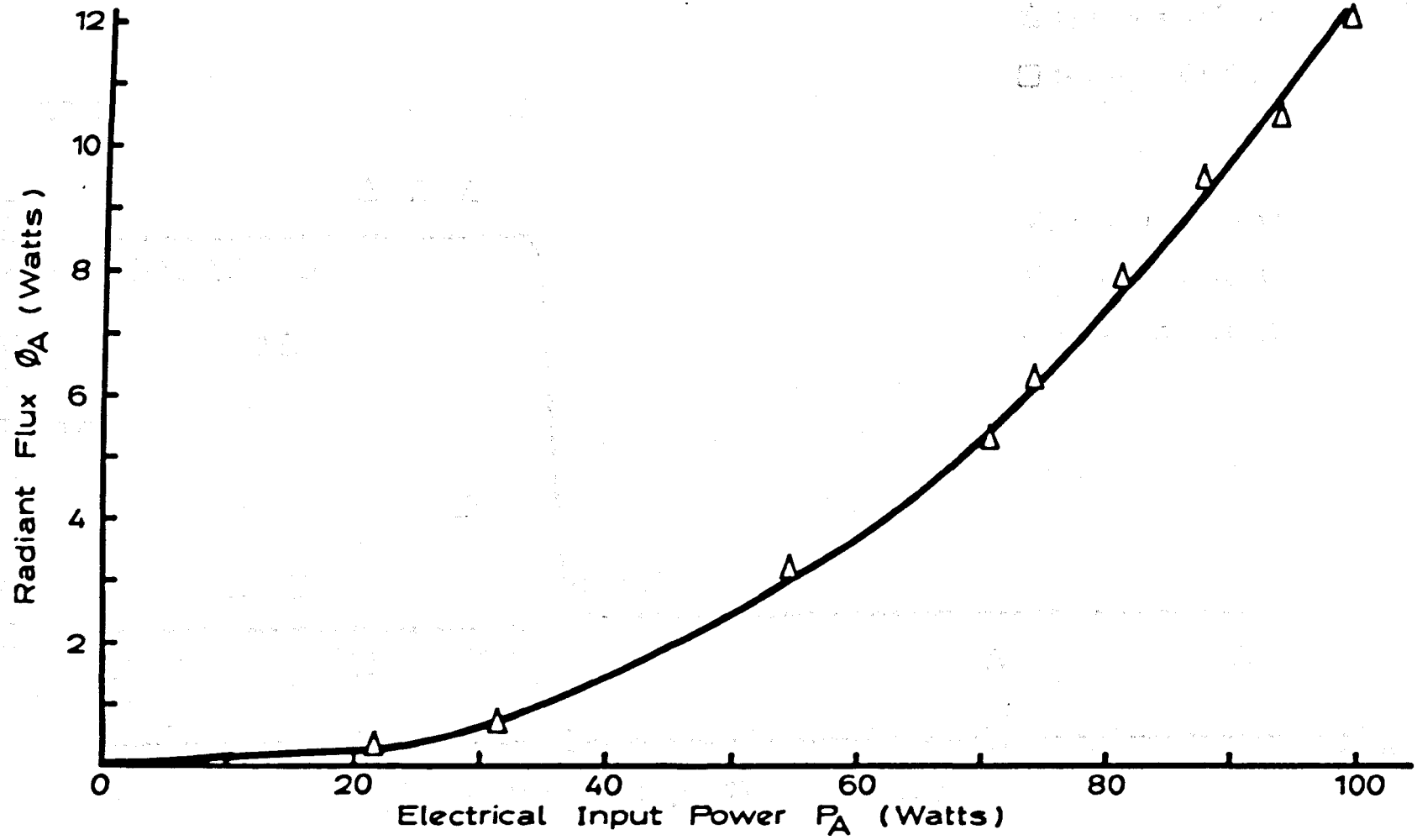

Fig. 6.1. Radiant Flux versus Electrical Input Power for Arc in Air at 1 atm.

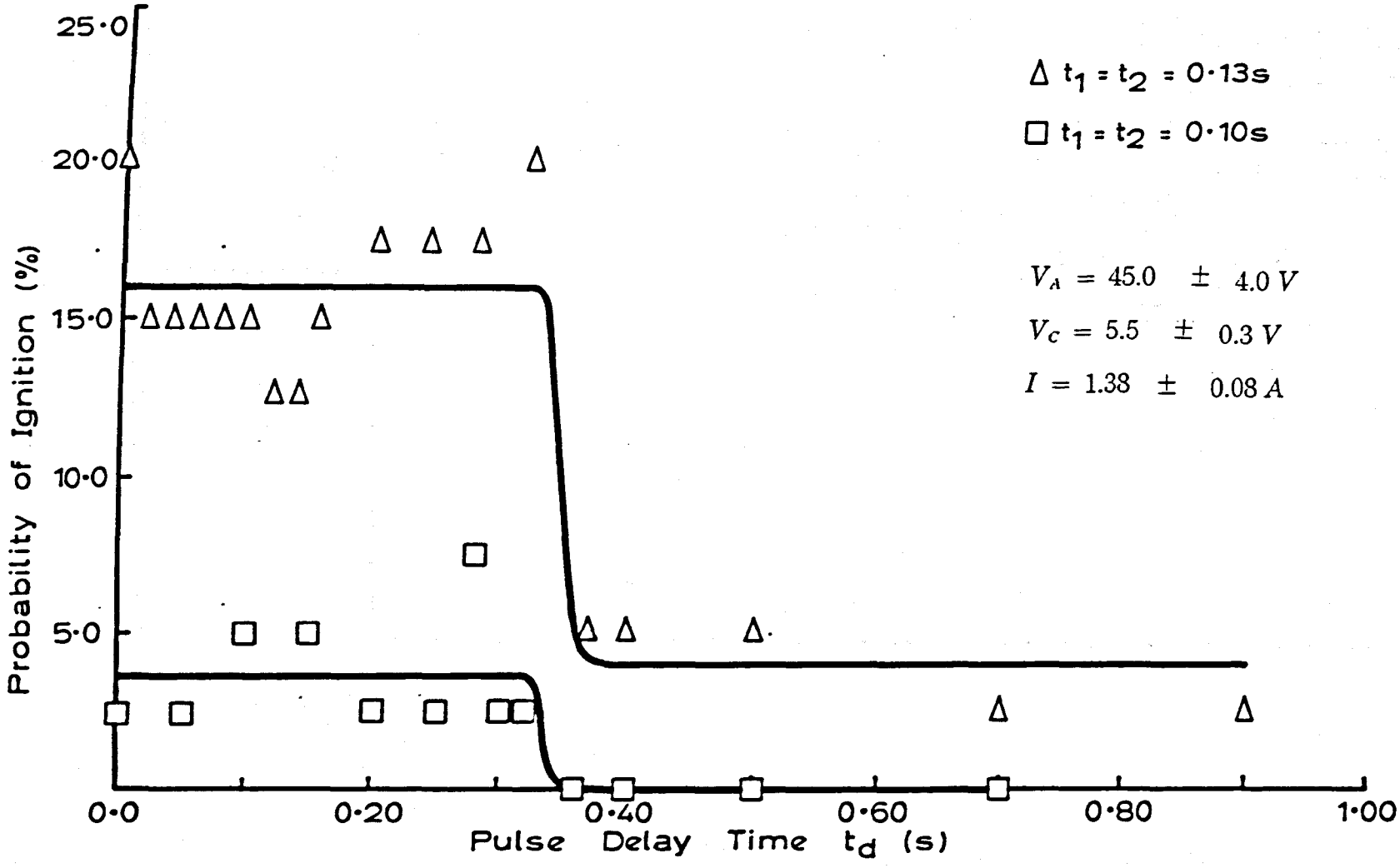

Fig. 6.2. Dual Pulse Test for an Electrical Input Power of 54.5W in Air at 1 atm.

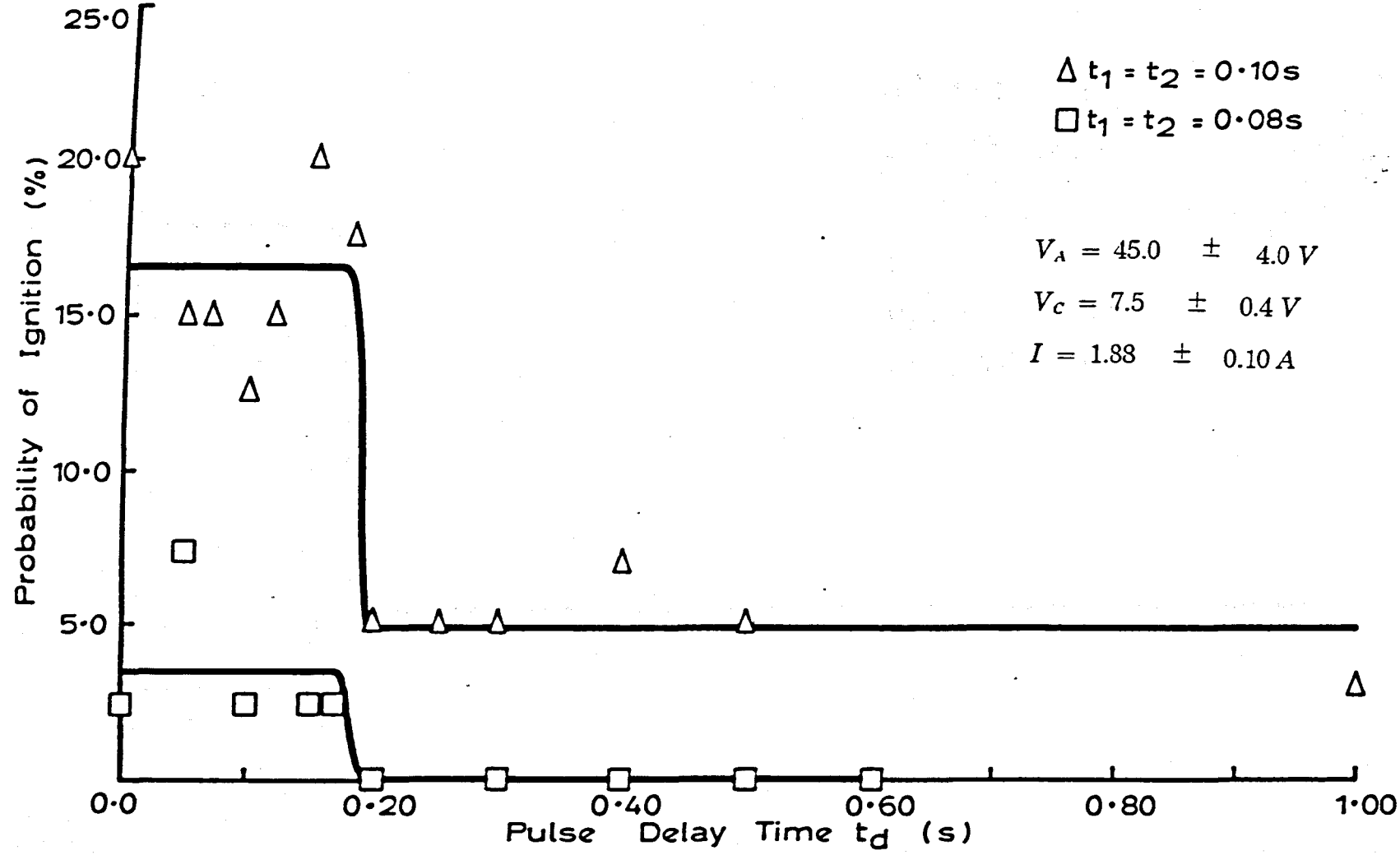

Fig. 6.3. Dual Pulse Test for an Electrical Input Power of 70.5W in Air at 1 atm.

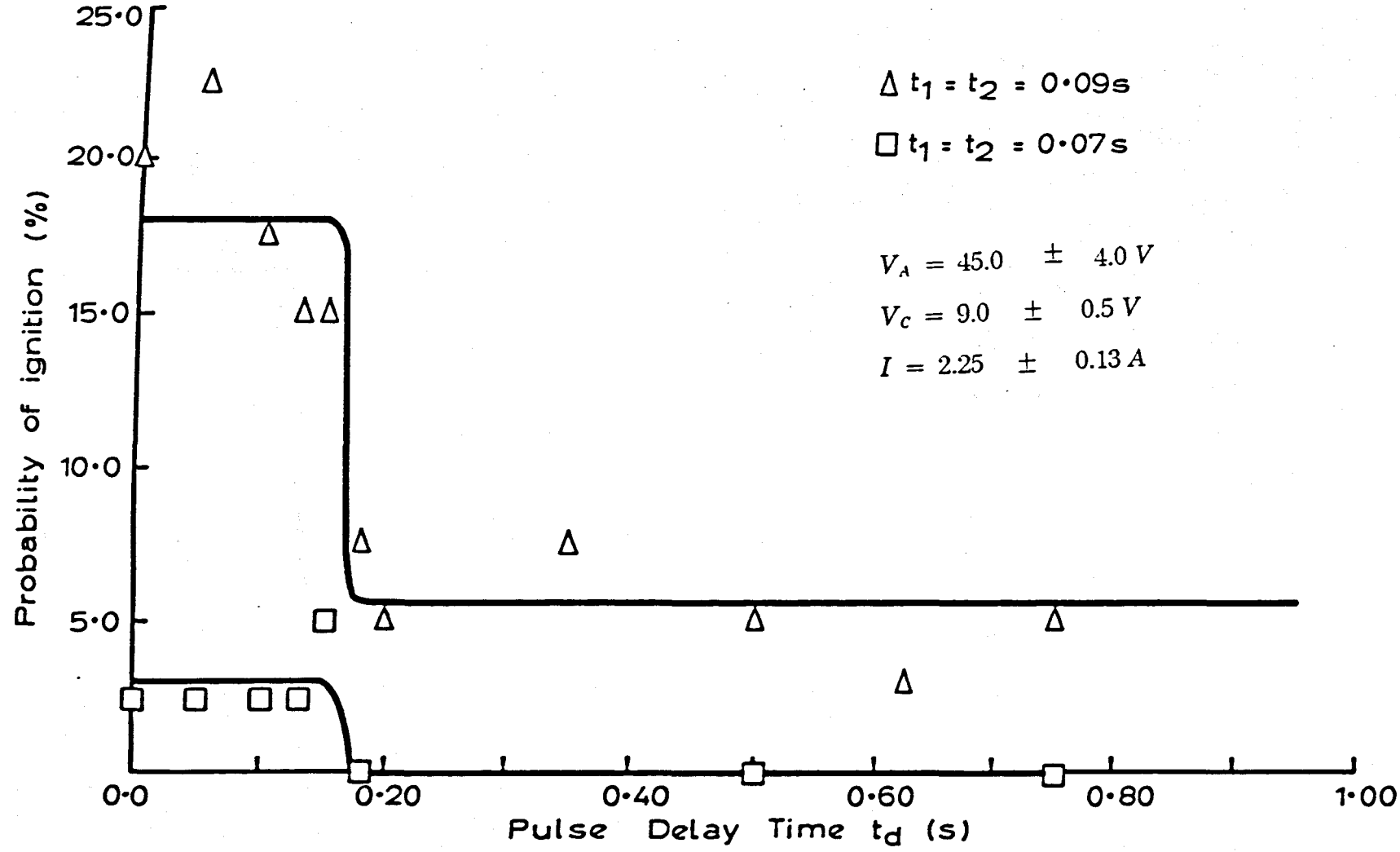

Fig. 6.4. Dual Pulse Test for an Electrical Input Power of 81.0W in Air at 1 atm.

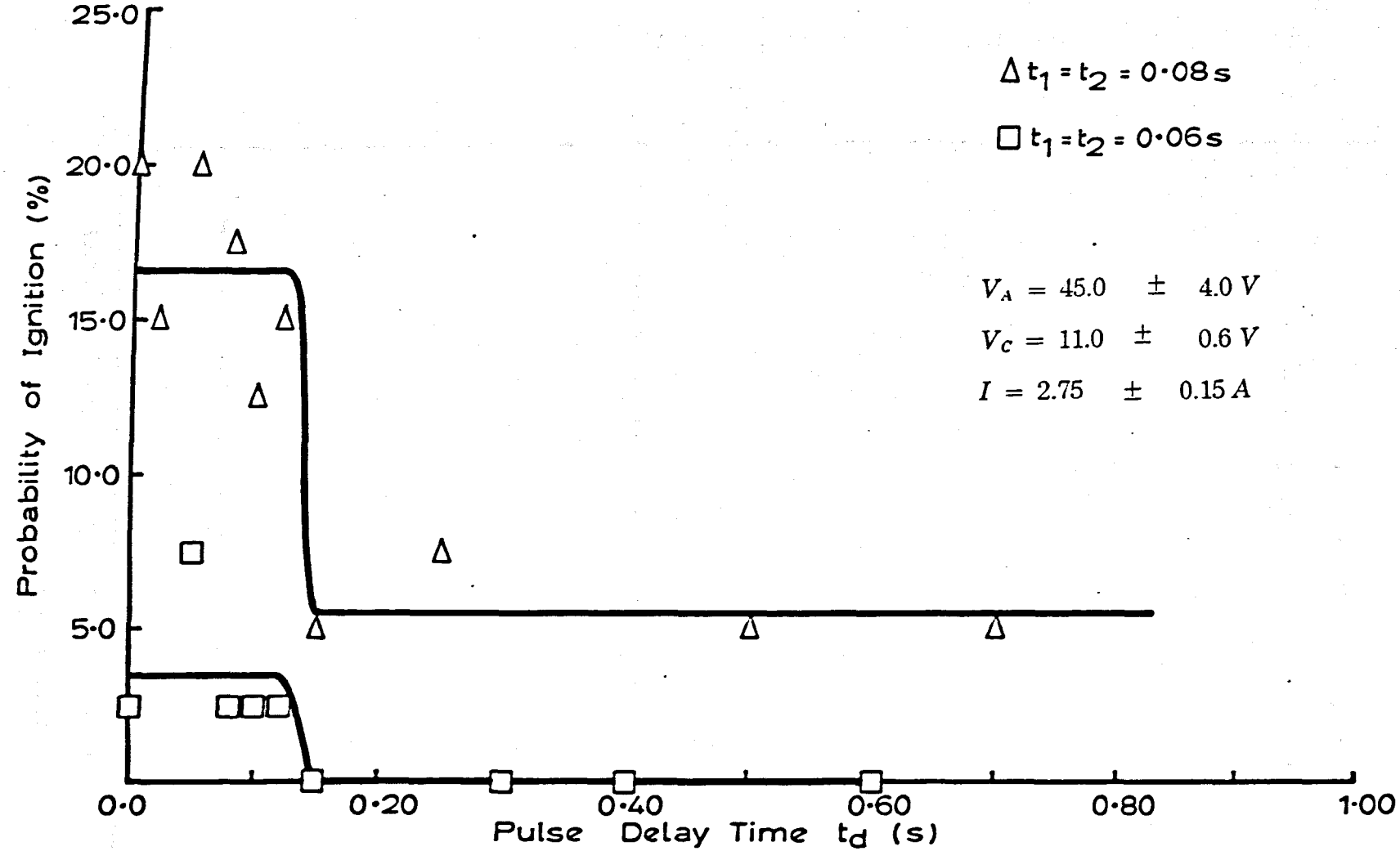

Fig. 6.5. Dual Pulse Test for an Electrical Input Power of 93.5W in Air at 1 atm.

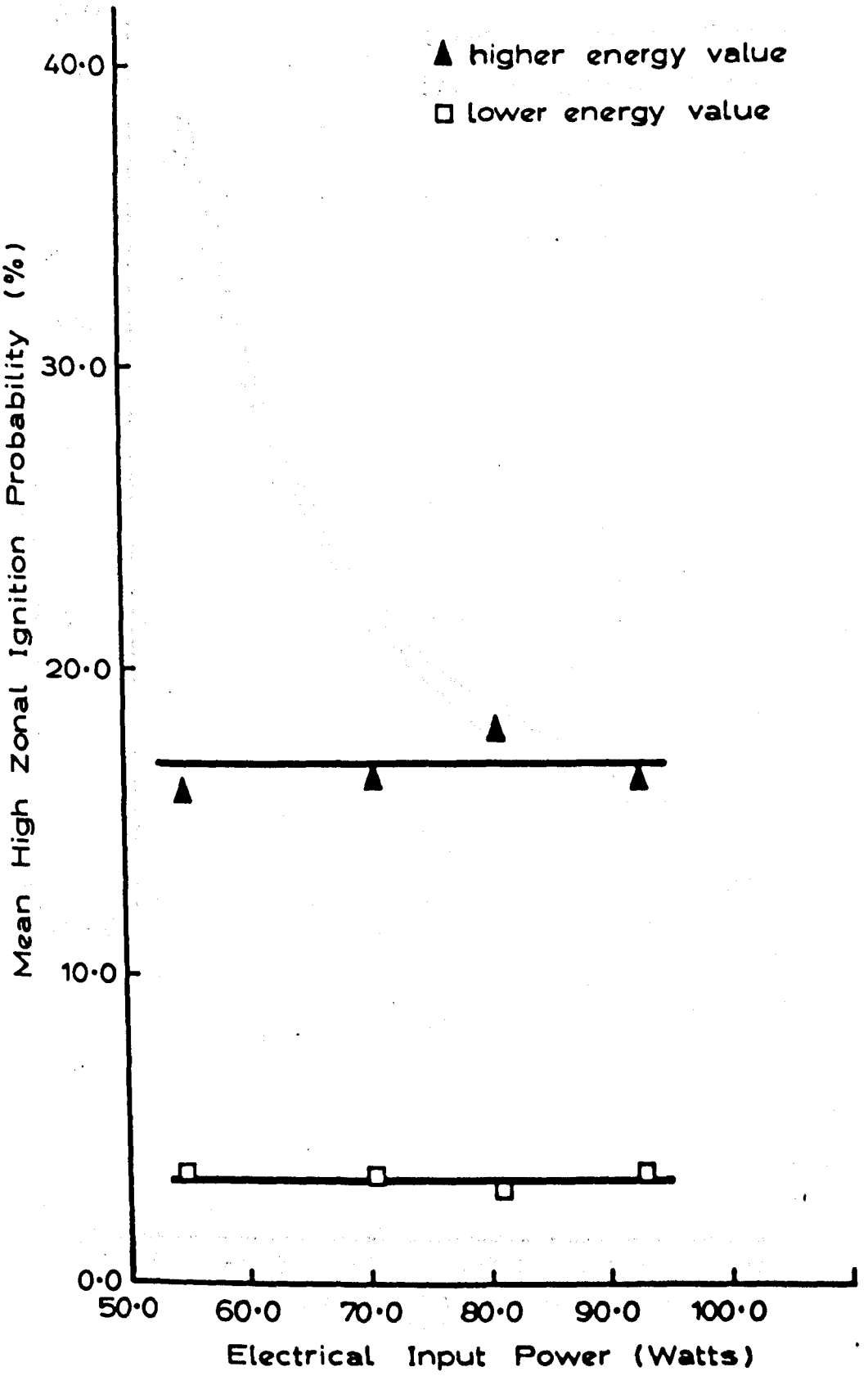

Fig. 6.6. Variation of Mean Zonal Probability for the High Zone with Power and Energy in Air at 1 atm.

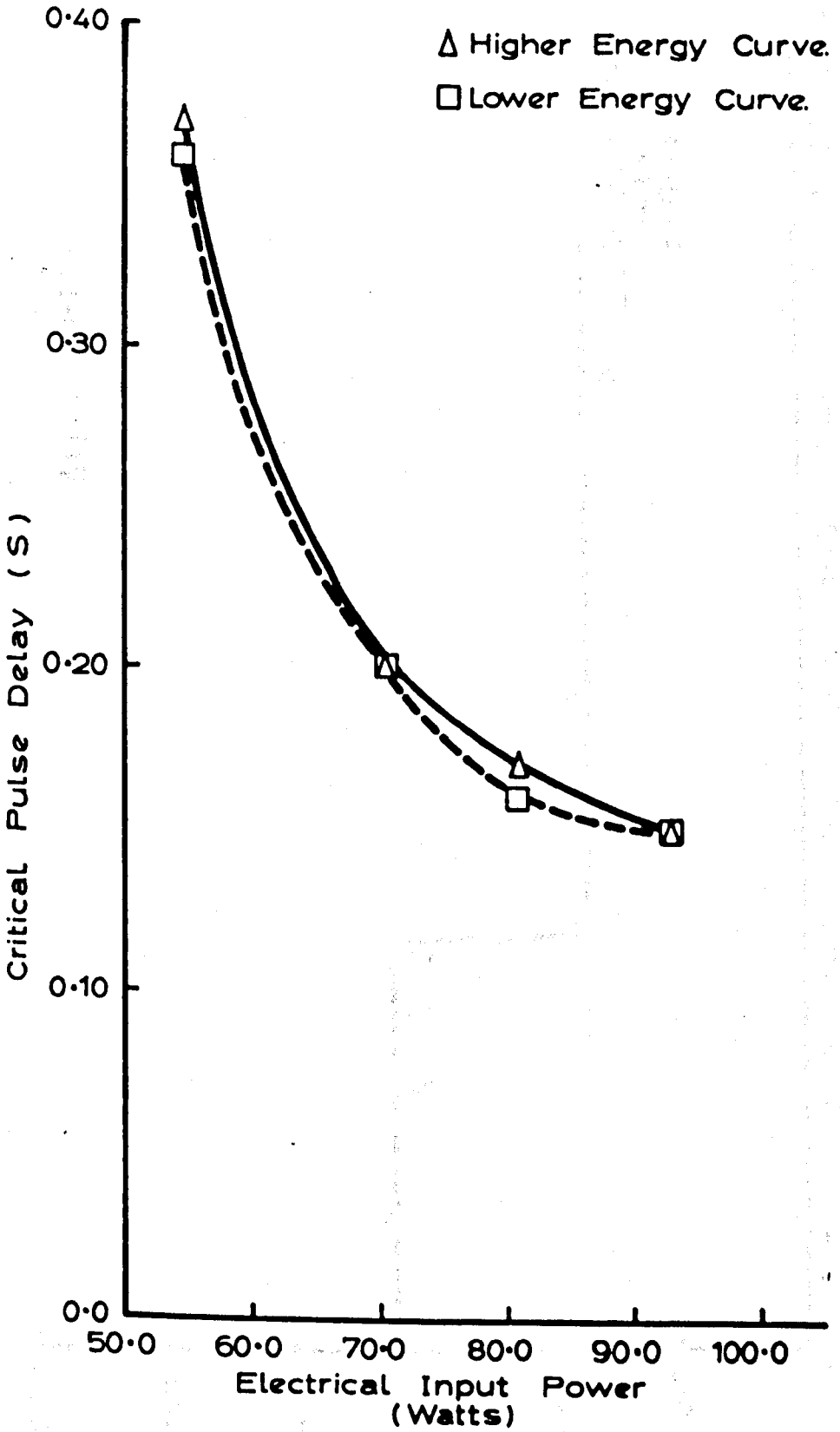

Fig. 6.7. Variation of Critical Pulse Delay with Electrical Input Power and Energy in Air at 1 atm.

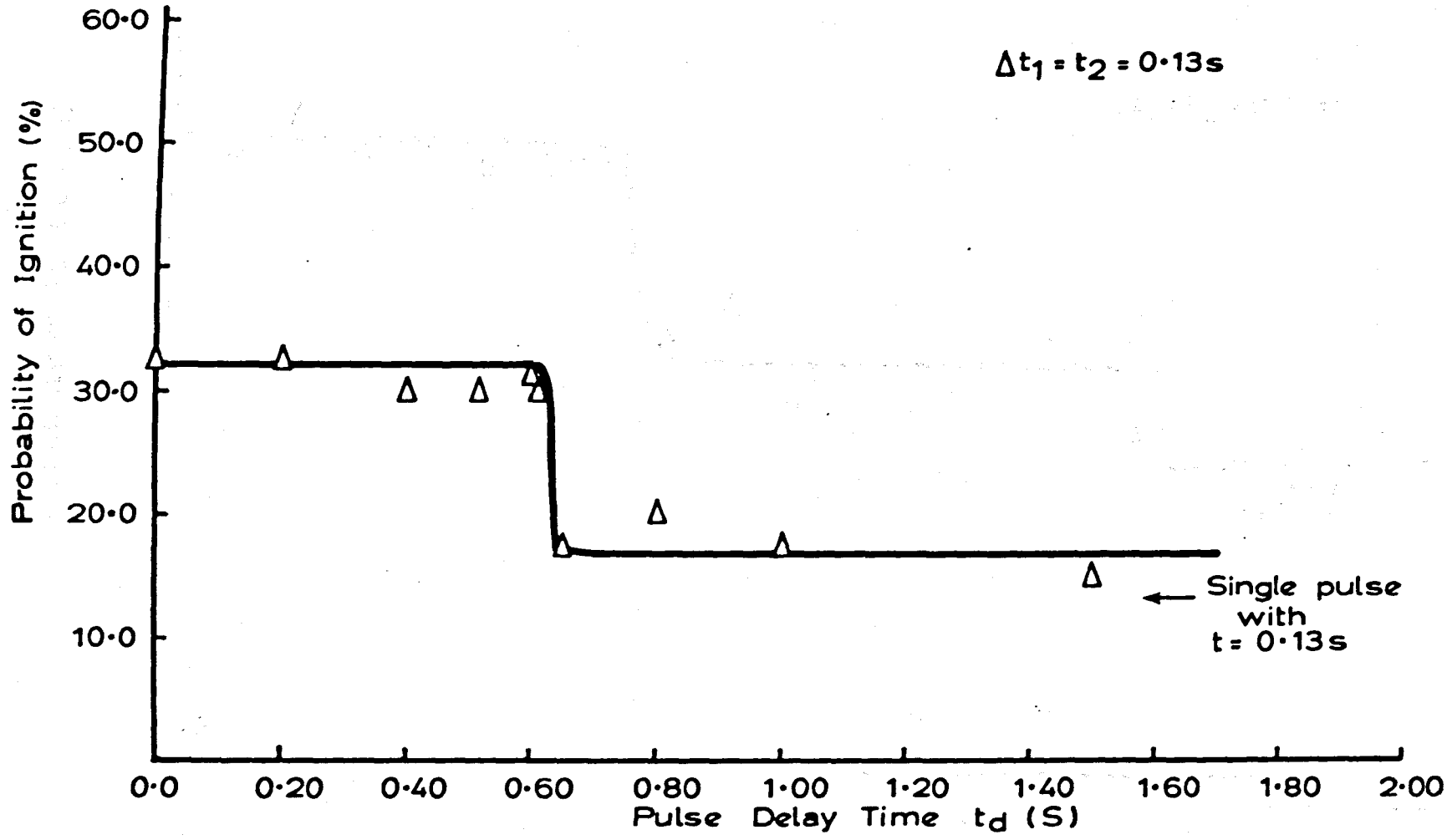

Fig. 6.8. Dual Pulse Test for an Electrical Input Power of 54.5W in Air at 2 atm.

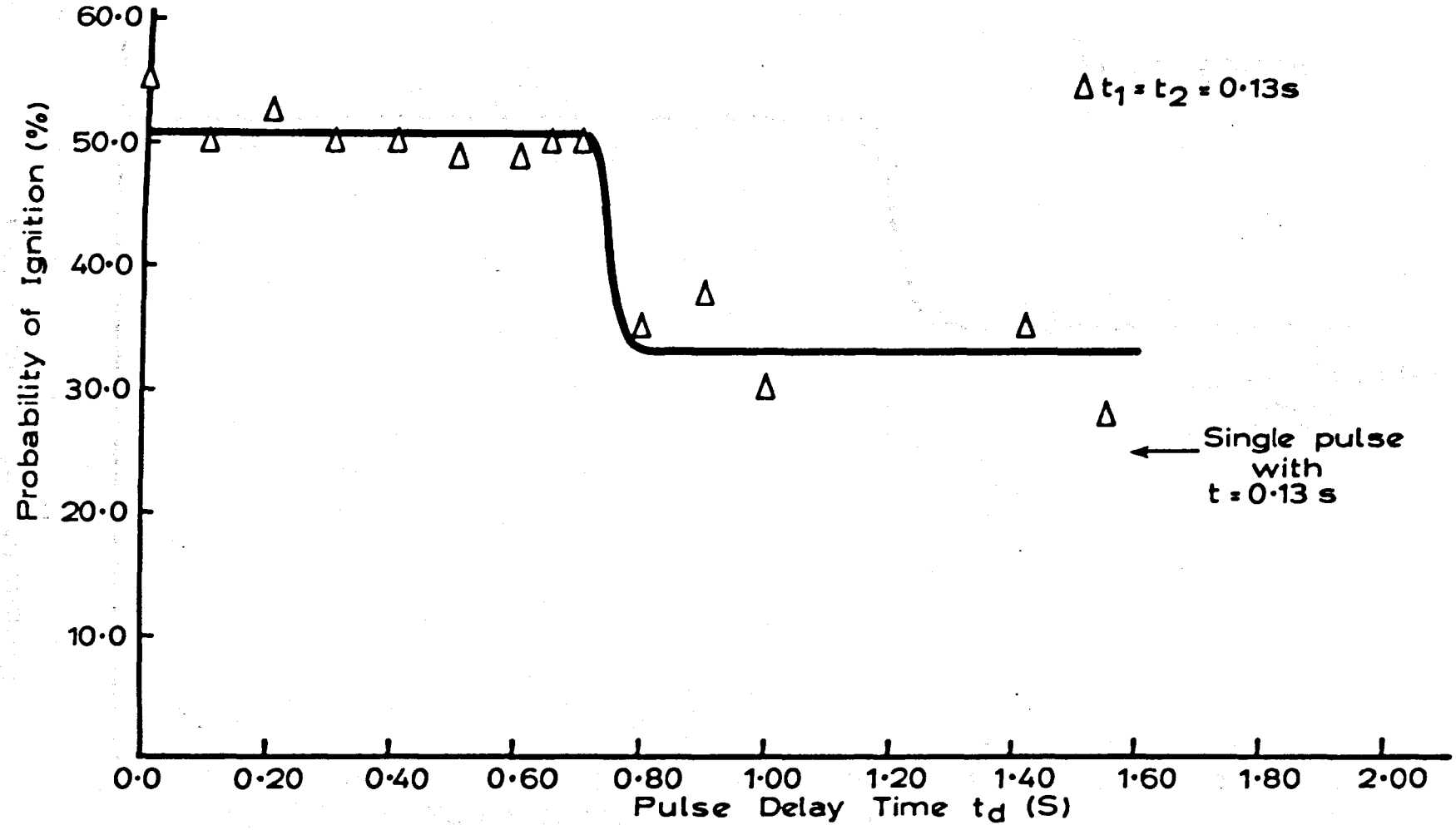

Fig. 6.9. Dual Pulse Test for an Electrical Input Power of 54.5W in Air at 3 atm.

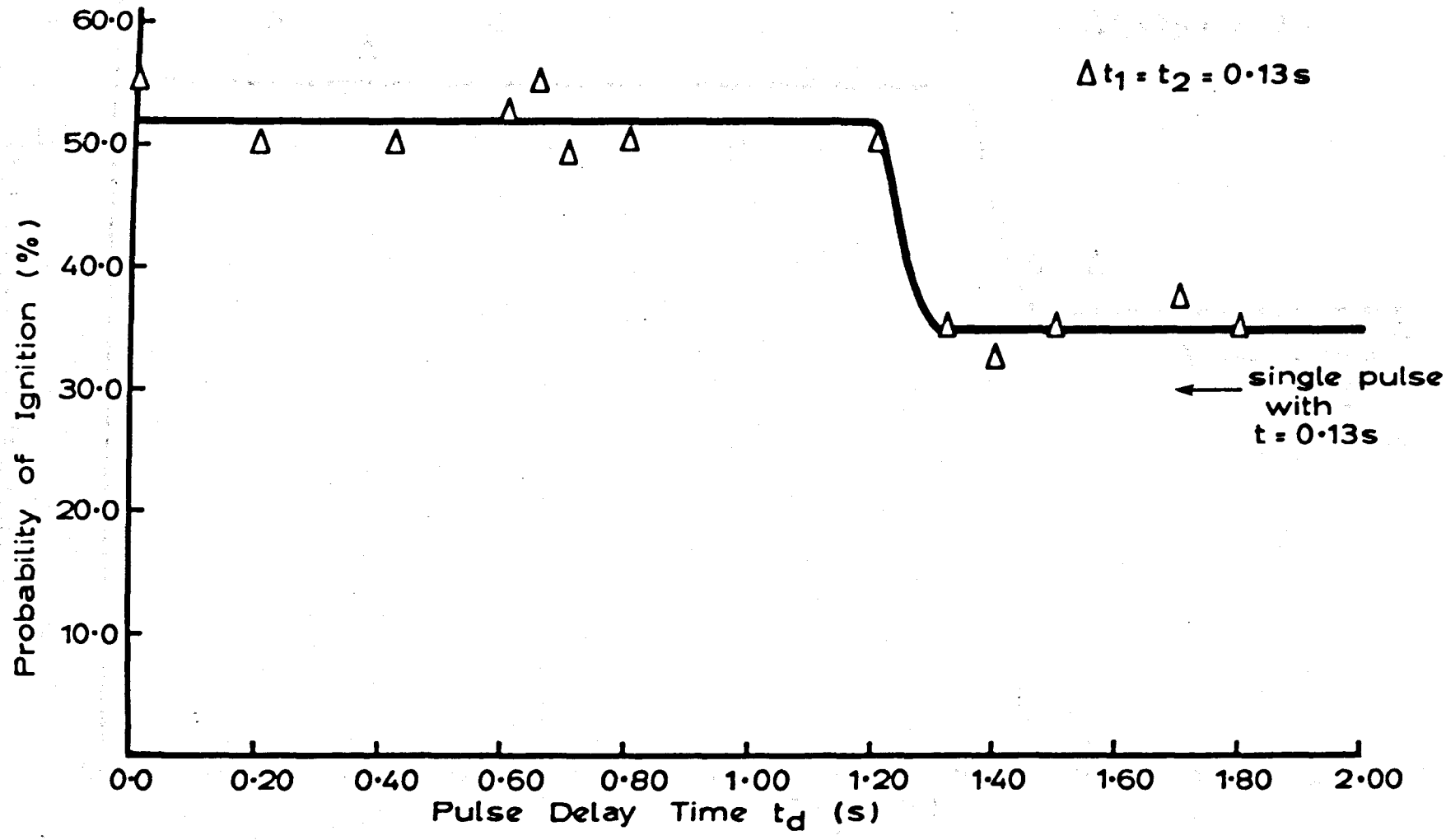

Fig. 6.10. Dual Pulse Test for an Electrical Input Power of 54.5W in air at 4 atm.

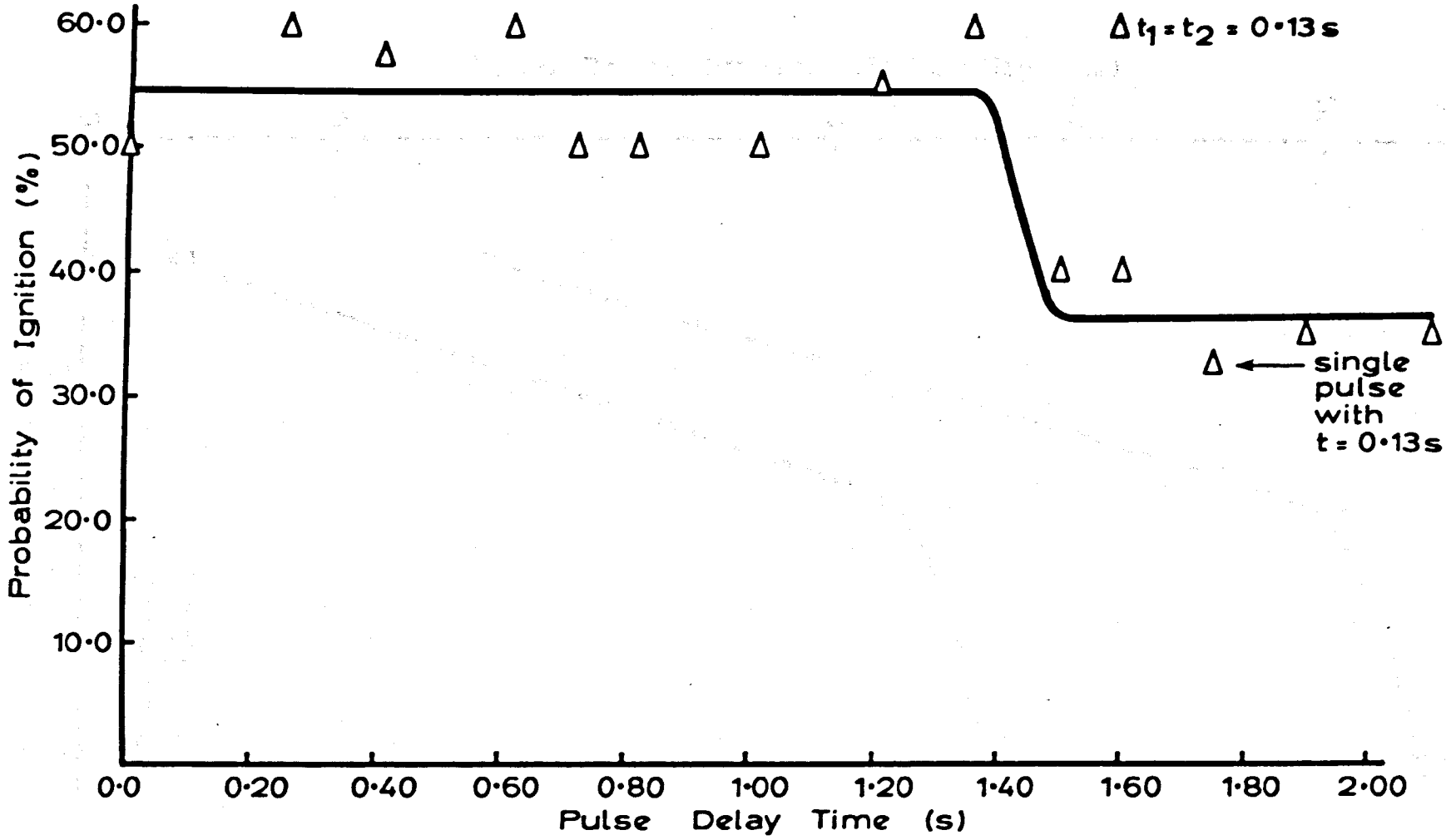

Fig. 6.11. Dual Pulse Test for an Electrical Input Power of 54.5W in Air at 5 atm.

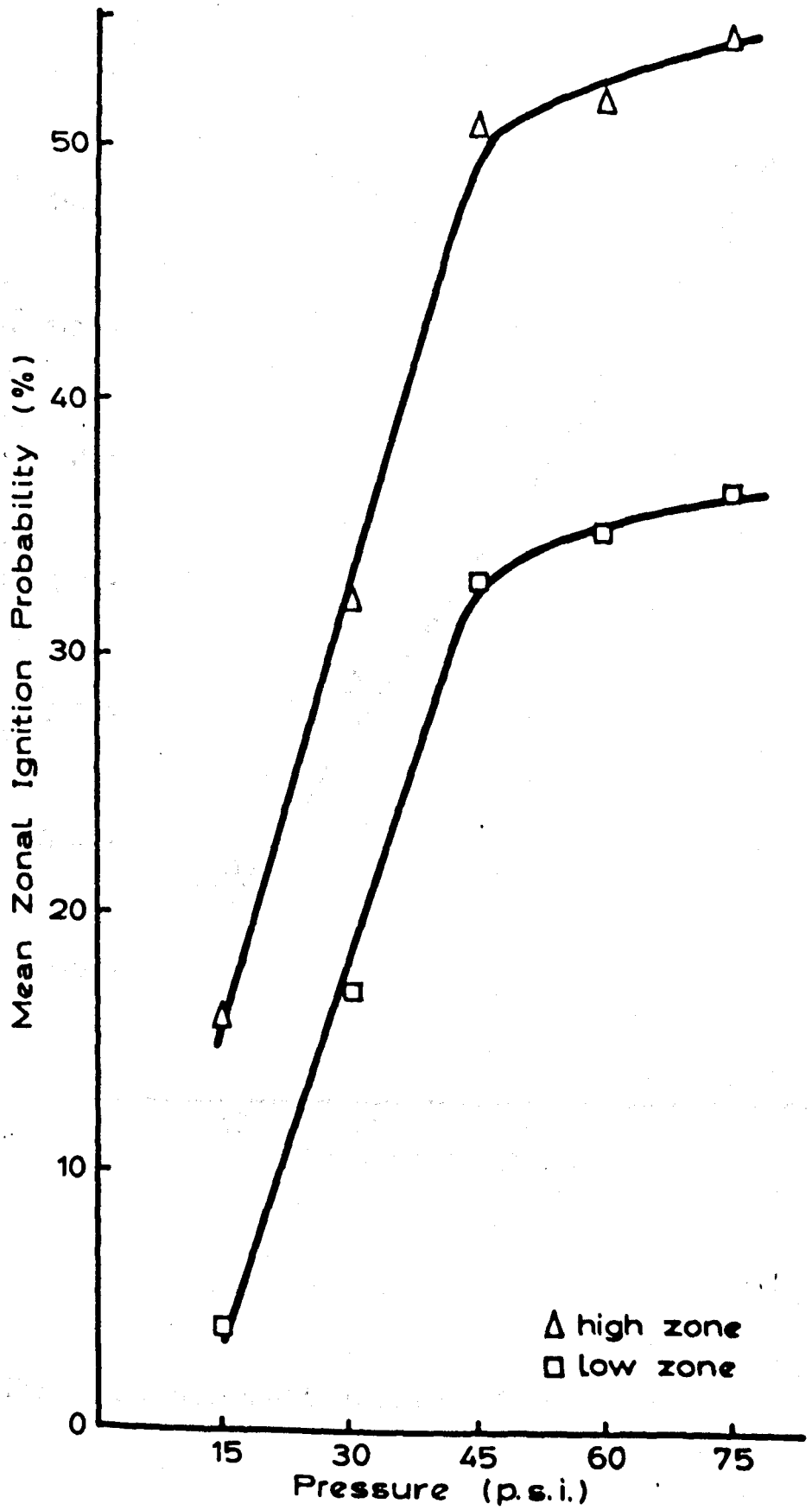

Fig. 6.12. Variation of Mean Ignition Probability for High and Low Zones with Pressure of Air.

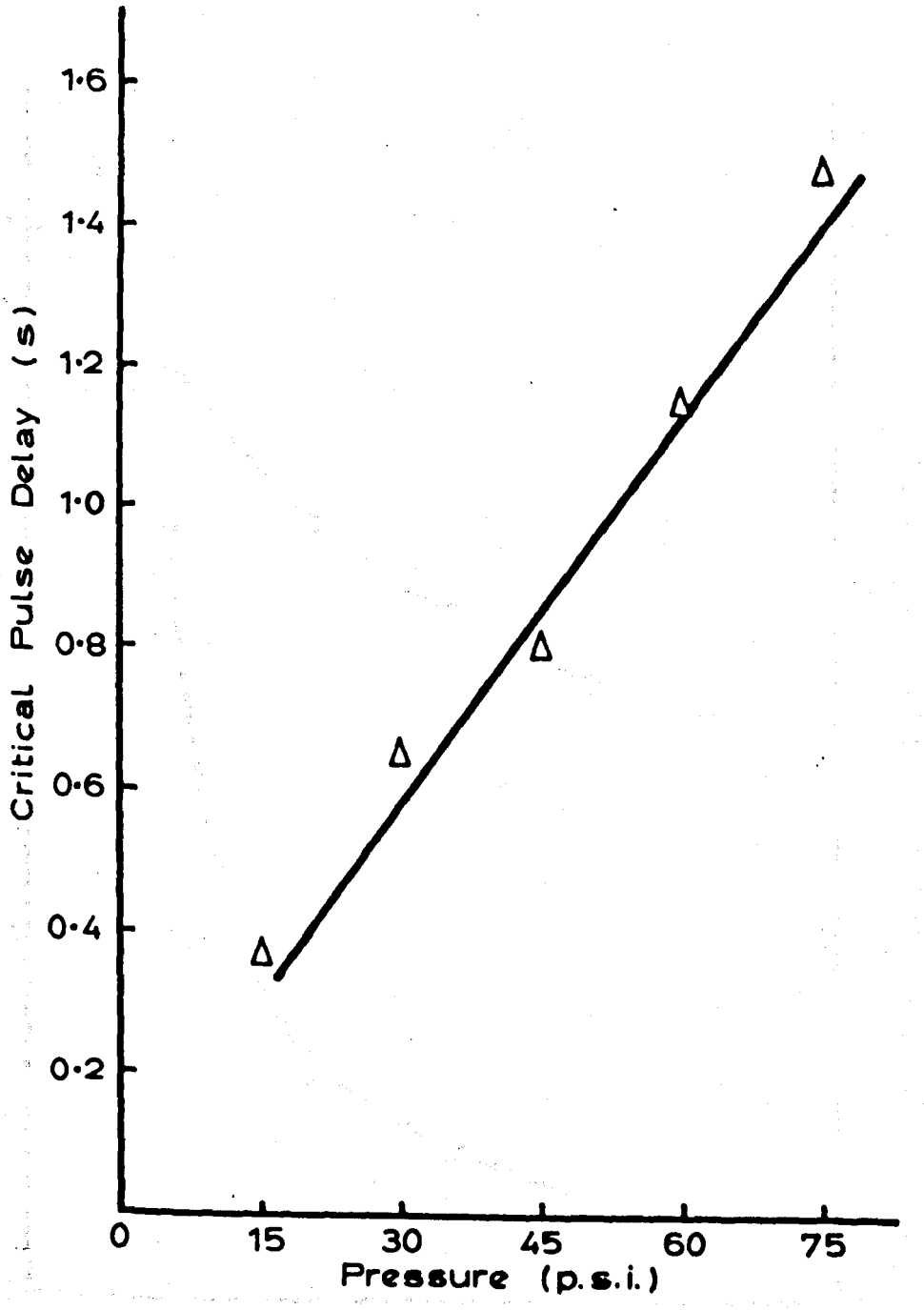

Fig. 6.13. Variation of Critical Pulse Delay with Pressure of Air.

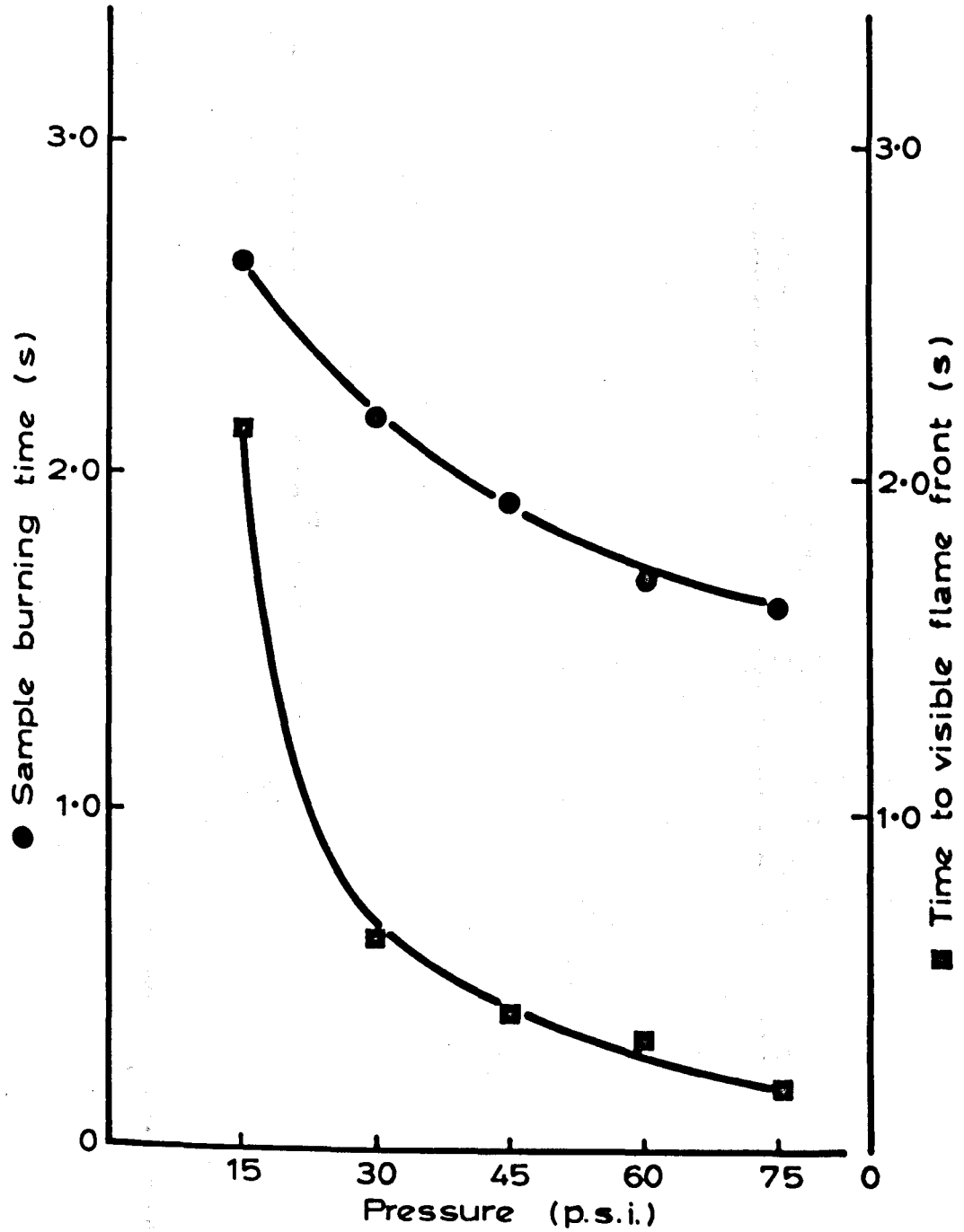

Fig. 6.14. The Effect of Pressure on Sample Burn Time and Time to Visible Flame Front in Air.

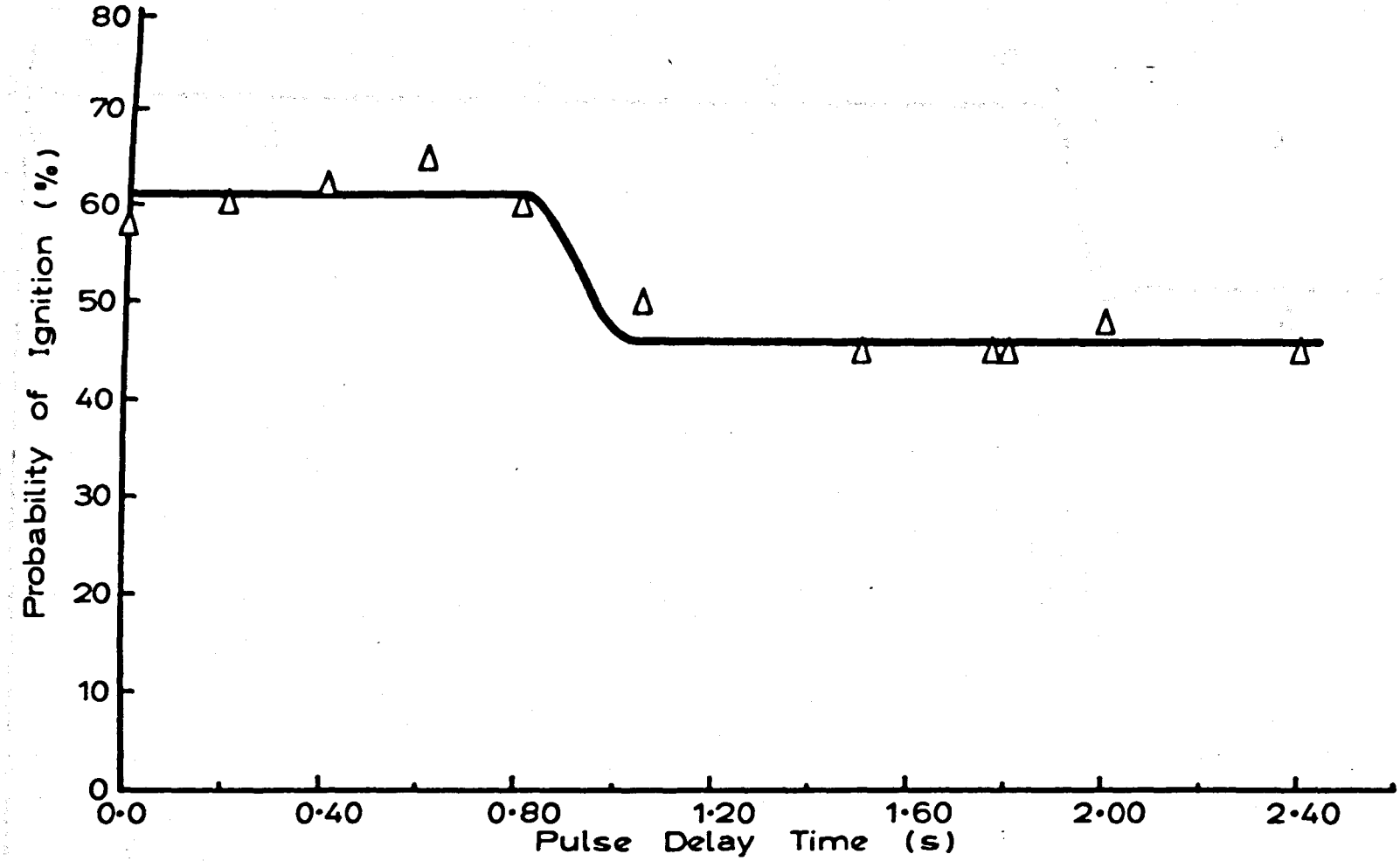

Fig. 6.15. Dual Pulse Test for an Electrical Input Power of 54.5W in 30% O_2/70% N_2 at 1 atm.

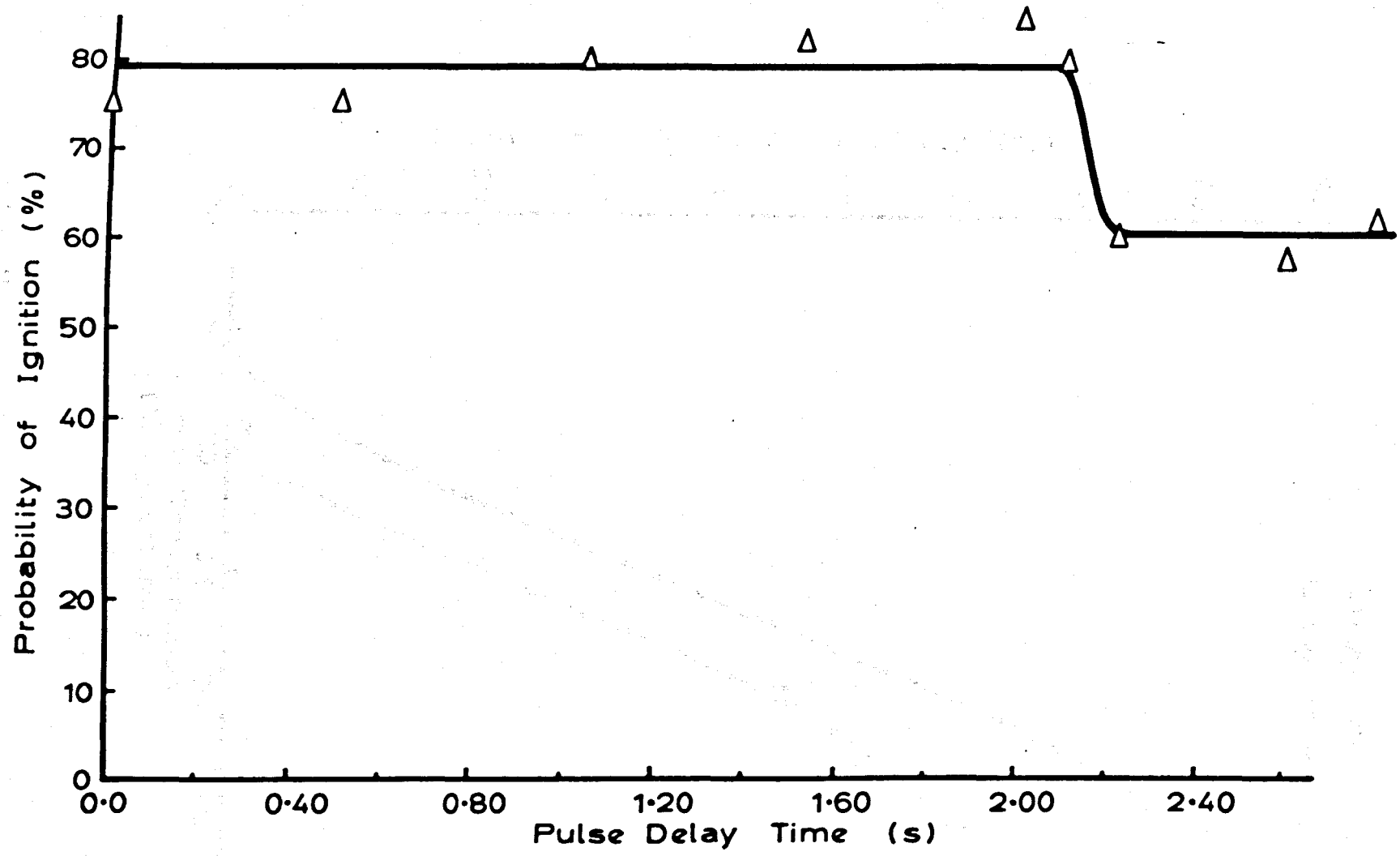

Fig. 6.16. Dual Pulse Test for an Electrical Input Power of 54.5W in 36% O_2/64% N_2 at 1 atm.

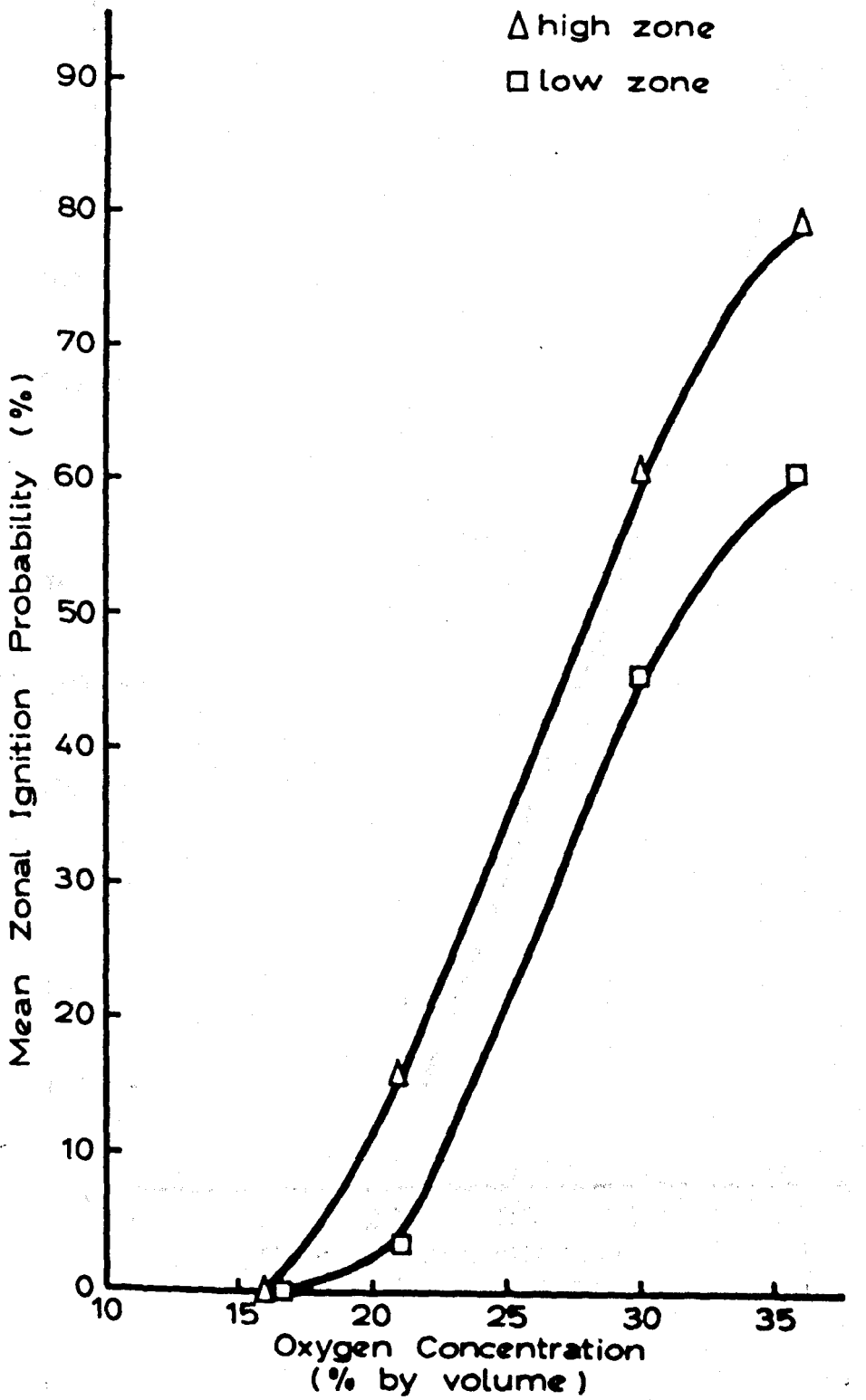

Fig. 6.17. Variation of Mean Ignition Probability for High and Low Zones with Oxygen Concentration at 1 atm.

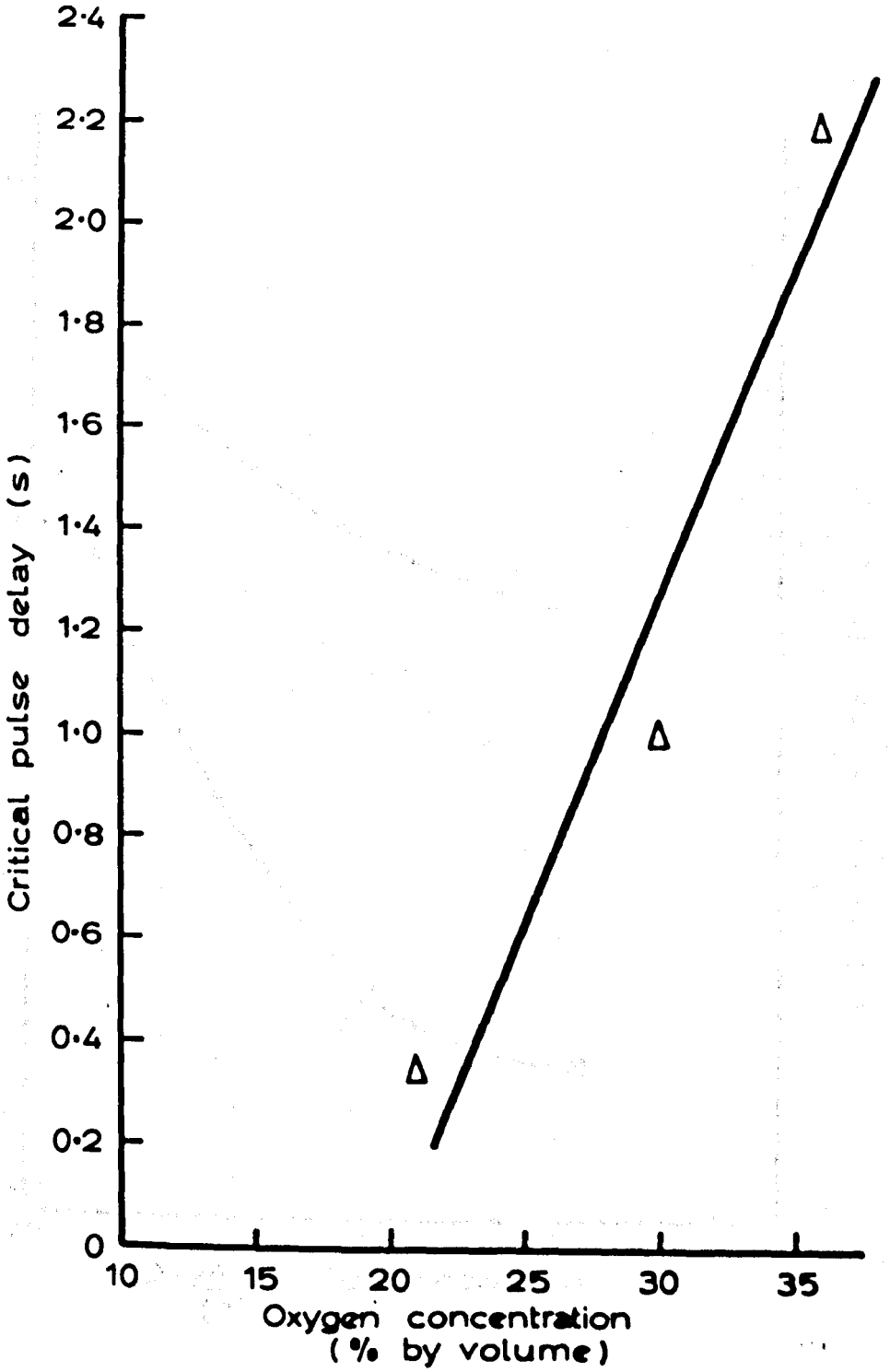

Fig. 6.18. Variation of Critical Pulse Delay with Oxygen Concentration at 1 atm.

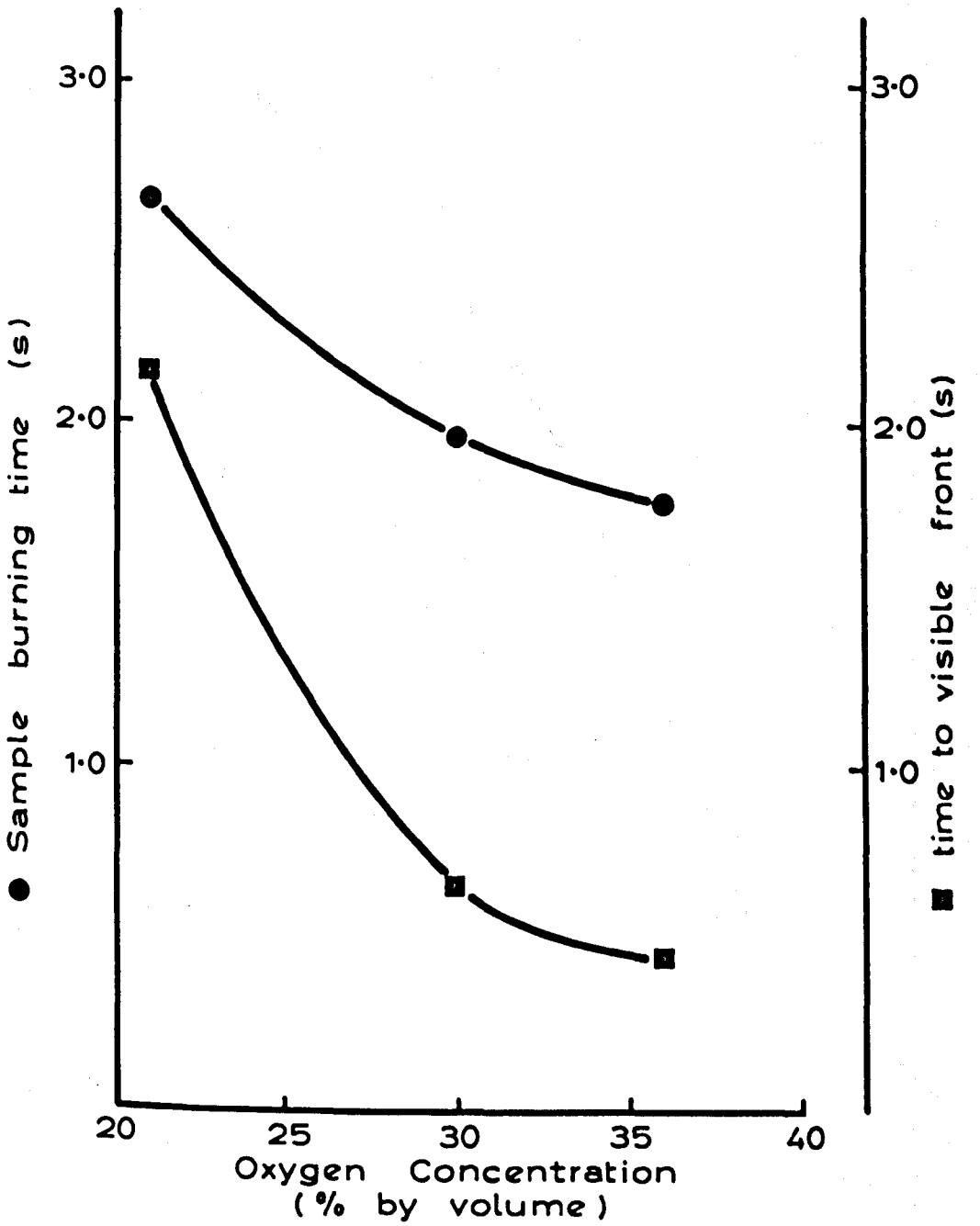

Fig. 6.19. The Effect of Oxygen Concentration on Sample Burn Time and Time to Visible Flame Front at 1 atm.

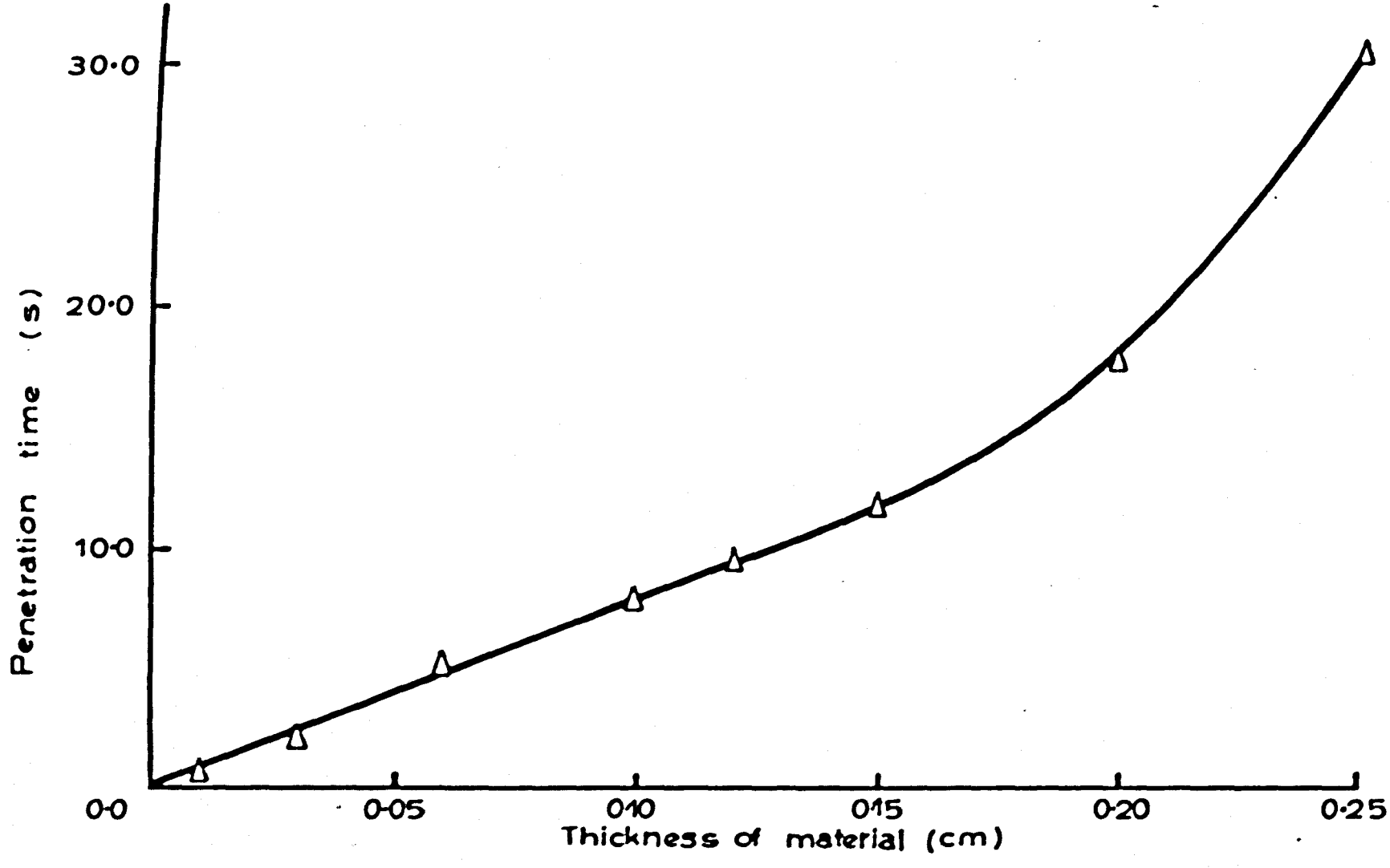

Fig. 6.20. Variation of Sample Penetration Time with Thickness of Sample for the Laser.

CHAPTER 7. CONCLUSIONS AND SUGGESTIONS FOR FUTURE WORK.

The principal aim of the work presented within this thesis has been to come to some understanding of the physical processes involved in the combustion of materials and to consider the implications for electrical fire safety in hazardous environments. To this end, a qualitative physical model of the combustion process has been developed based on the results discussed in chapter 6. There now follows a discussion of the model and a comparison of the arc and the laser as sources of ignition. Some suggestions are made for future experimental work and the implications of the results presented in this thesis for electrical safety in hazardous environments are discussed.

7.1 A PHYSICAL MODEL OF THE COMBUSTION PROCESS.

The model to be discussed postulates that the combustion process can be divided into three stages: the input stage, the growth-decay stage, and the sample consumption stage.

During the input stage let us consider a single pulse of electrical input power P_A and energy E. From the results discussed in chapter 6, section 2, it is the power (i.e. rate of energy supply) which determines the nature, rate of production, and composition of the gaseous volatile cloud produced from the surface of the sample during the pyrolysis of a material. An increase in power causes an increase in the volatile production rate and a tendency towards the production of lighter volatile species and hydrocarbons[1]. From the same results of section 6.2 it is the total energy of the pulse (provided that the energy is supplied at a rate which is sufficient to allow mixing of the volatiles with oxygen) that determines the concentration of volatile gas which is available for ignition. An increase in pulse energy gives an increase in sample flammability.

It is well documented[2,3] that the pyrolysis of a solid material proceeds as:

$$\frac{dm}{dt} \propto -m$$

where m represents the mass (or the concentration) of the solid material, and the above relationship represents an exponential decrease in concentration of solid fuel with time during the pyrolysis of that material. Thus the concentration of the volatile cloud during pyrolysis can be regarded

as increasing exponentially with time, making fuel available for mixing with the air near the surface and the onset of combustion reactions.

During this growth period the gaseous volatile cloud, having become concentrated at the surface, will begin to diffuse away from that surface and since[4],

$$\frac{\partial C}{\partial t} = \frac{1}{D}\frac{\partial^2 C}{\partial x^2}$$

where C is the concentration of the volatile cloud and D is the diffusivity of the gas, the amount of volatile gas in the mixing zone will decrease exponentially with time.

Thus we have two competing effects, one being volatile gas phase reactions which depend on the exponentially increasing concentration of gaseous volatiles produced by the radiant pulse; the other being a diffusion effect on the gas concentration which is a decaying exponential relationship with time, and depends, among other factors, on the mass of the volatile species.

From the above effects we can expect a critical flammable concentration which gives a flammability level which is dependent on the energy of the pulse initially incident on the material.

If now a second pulse of equal power and energy to that of the first pulse is applied to the material, at a variable delay after the first,the second pulse, acting alone, would have the same effect as pulse 1. A cloud of volatile gases having a similar composition to that produced by pulse 1, and a similar concentration, would be produced which would ex-

perience a growth stage and a diffusion influenced decay stage; see Fig 7.1.

It is postulated that if the decay between pulses is sufficiently short, the growth region of pulse 2 will add to that of pulse 1 and reinforce the concentration of flammable species produced by pulse 1, giving an increased flammability level - this is illustrated in Fig 7.1. If, however, the delay is such that the growth period of pulse 2 occurs at a point where pulse 1 is 'old' and the gaseous flammable concentration has gone into decay, pulse 2 will no longer be able to reinforce pulse 1 and the flammability will be in the region of that which would be produced by pulse 2 acting on its own. Thus, there must be some critical pulse delay for the system which corresponds to that point at which the concentration of volatiles for the gas phase combustion reaction is sufficiently in decay for the addition of the volatile cloud produced by pulse 2 not to cause reinforcement; this will be identified as a transition from a region of high ignition probability to a region of low ignition probability, and can be seen illustrated in Fig 7.1.

It is the power level of the individual pulses that determines the nature of the volatile species, and their respective masses. Thus, since the nature of the volatile species determines the type of chemical reaction occuring and hence the decay period due to chemical reactions producing non flammable species, and the mass of individual volatile species determines the diffusion rate, it is not unreasonable to expect a dependency of the critical pulse delay on input power. Indeed, as an increase of power results in the production of lighter volatile species, and hence an increase in the diffusion rate, it is likely that there is a decrease in the

critical pulse delay time with increase in power; this can be seen in Fig.6.7.

As postulated above, it is the input power, energy level and pulse delay in the input stage of the ignition model (under constant pressure and oxygen concentration) that determine the flammability of the material and the growth-decay balance of the combustion process. However, the time to visible flame front and the sample burning time appear independent of all three factors; it is postulated that flame spread phenomena are influenced principally by enviromnental conditions.

7.1.1 The Effect of Pressure on the Ignition Model.

The results presented in chapter 6, section 3, show an increase of sample flammability with increase of pressure for constant power and energy; this is consistent with the work of a number of investigators[5,6,7]. The pressure dependence of sample flammability can be explained in terms of the increase in the oxygen partial pressure associated with an increase of total gas pressure.

Since an increase of pressure corresponds to an increase of oxygen partial pressure, the concentration of flammable species, produced by the mixing of gaseous volatiles with increased oxygen content, will be increased leading to an increase of flammability for a particular value of pulse energy. The increase of flammability, for a particular pulse energy and power, with increase of pressure can be seen in Fig. 6.12. The effect

of pressure on the critical pulse delay can be seen in Fig. 6.13, with the critical pulse delay increasing with increase of pressure.

An explanation can be formulated by refering to the effect of an increase of pressure on the balance of the growth-decay stage seen in Fig. 7.2. Considering, first, the growth stage, an increase of total gas pressure resulting in a greater mixing of volatiles with oxygen (as mentioned above) will cause the leading edge of the growth curve to become steeper leading to an increase of sample flammability. This effect will, to some extent, be moderated by the increase of heat capacity of the bulk gas due to the increase of pressure, which will reduce the transfer of energy from the arc to the surface of the sample. Considering the decay stage, the increase of total gas pressure will result in a decrease in the diffusion rate of the flammable species causing the decay edge to flatten out.

The result of combining the above effects on the growth-decay characteristic will be to increase the period of time available for the second pulse to reinforce the first pulse and give rise to a higher sample flammability level. Thus the critical pulse delay, or reinforcement period before decay due to diffusion and chemical decay to less flammable species begins to dominate, can be expected to increase with increase of bulk gas pressure. This is consistent with the experimental data of Fig. 6.13.

From Fig. 6.14 the pressure has an effect on the time to visible flame front measured from the end of pulse 2. It is postulated that an increase of pressure accelerates the combustion reactions within the growth-decay cycle, without altering the balance, resulting in the decrease of time to visible flame front seen in Fig. 6.14.

sample burn time. This is consistent with the observations of previous investigators[5,6,7] who found that the burning rate increases with an increase of atmospheric pressure. This can be explained in terms of the increase in oxygen partial pressure with increase of total gas pressure, which provides an increase in the production of reactive flammable species by the advancing flame front. This results in an accelerated burning rate and hence a decrease in the burning time.

7.1.2 The Effect of Oxygen Concentration on the Ignition Model.

The results presented in chapter 6, section 4, show that the effect of increasing the oxygen concentration by volume, at constant pressure, is to increase the sample flammability and the critical pulse delay, and to decrease the time to visible flame front and sample burn time; each observation will now be discussed in terms of the physical ignition model outlined earlier in the chapter.

The flammability of the sample reaches zero as the oxygen concentration is reduced to 16% by volume (balance nitrogen) due to there being insufficient oxygen to allow mixing with the gaseous volatiles to a combustible level for the prescribed values of input power power, energy and pressure.

An increase of oxygen concentration by volume will cause an increase in the concentration of flammable species due to the improved mixing of the gaseous volatiles with the oxygen molecules. This will cause the gradient of the leading edge of the growth curve (see Fig. 7.3)

to increase, sending the sample to a higher flammability zone for one pulse. The dependence of sample flammability on an increase of oxygen concentration at constant pressure will be stronger than the dependence on an increase of oxygen concentration due to a change in total gas pressure. This will occur since, in the case of an increase of oxygen concentration at constant pressure, there is no moderating effect due to the change in thermal capacity of the gas with increase of total gas pressure.

As there is no increase of total gas pressure, no appreciable change in the diffusion rate of gas away from the surface of the sample can be expected (apart from that due to the change of mass of reactive species brought about by the change of oxygen content). However, the decay edge of the growth-decay balance will occur from a region of high concentration of flammable species; this will have the effect of prolonging the period of time available for the second pulse of energy to reinforce the first pulse before the balance of gaseous fuel concentration produced by the first pulse has decayed to a sufficiently low value; this is represented in Fig. 7.3. Thus the critical pulse delay will be increased; as seen in Fig. 6.18. As discussed previously, upon decreasing the oxygen concentration to 16% by volume, the gas is no longer oxygen rich and is insufficient for a flammable mixture to exist at the surface of the sample for the heating conditions prescribed for the present experimental programme; under these circumstances the concept of a critical pulse delay becomes meaningless.

The reduction of the time to visible flame front with increase of oxygen concentration can be explained by the rate of the combustion re-

actions after the input stage. It is postulated that an increase of oxygen concentration accelerates the combustion reactions of the growth-decay cycle of Fig. 7.1, without altering the balance, producing the decrease of time to visible flame front with increase of visible flame front seen in Fig 6.19.

The decrease of sample burn time with increase of oxygen concentration is due to the improved mixing of the volatiles liberated by the advancing flame front with the oxygen rich gas; so producing accelerated flame spread.

The observations of decrease of sample burn time and increase of sample flammability with oxygen enrichment at constant pressure are consistent with those reported by Johnson and Woods[5], Bartels and Howes[6], Tanaka and Ichikawa[8] and Brennan[7].

7.2 THE ARC AND THE LASER AS IGNITION SOURCES.

In order to compare the ignition properties of the arc and the laser, it is worthwhile considering the irradiances of the two sources i.e. the radiant flux per unit area.

Consider, first, the arc. For the majority of the results presented in chapter 6, the arc was used at an electrical input power of 51.5W which, when refering to Fig. 6.1., corresponds to a radiant flux of 3.3W. As the sample is vertical and to one side of the electrodes, we may regard one half of this power as 'wasted' power and assume that $\approx$ 1.6W of radiant flux is available for ignition of the sample. The geometry of the

electrodes is such that they are tapered to a diameter of 2mm with an electrode gap of 0.55mm; thus we may approximate the arc kernel to a cylinder of radius 1mm and side length 0.55mm. The irradiance of the arc is then:

$$E_a = \frac{1.6}{2\pi rl} = \frac{1.5}{\pi} \quad (W/mm^2)$$

Consider now the laser beam. As mentioned in section 6.3.1., the beam used in the experimental investigation had a peak output power of 5.0W with a gaussian beam waist at the sample of 2mm, at which radius the power has decayed to 0.7W. Assuming, then, that 4.3W of laser power is contained within a spot of radius 2mm, the irradiance of the beam is:

$$E_b = \frac{4.3}{\pi r^2} = \frac{1.1}{\pi} \quad (W/mm^2)$$

From the above calculations, the irradiances of the two ignition sources are very similar. However, as discussed in chapter 6, the two sources have very different effects on the combustion behaviour of the sample; the arc produces ignition with subsequent flame spread across the sample resulting in complete combustion of the sample; the laser produces vaporisation of a small area of sample, some charring, but a lack of flame spread and non-combustion of the sample.

The explanation for the different effects produced by the two sources must clearly lie in the properties of the radiation supplied by the two sources.

The radiation produced by the arc has a bandwidth of wavelengths from the ultra-violet to the infra-red. The radiation produced by the laser

is in a very narrow range of wavelengths, centred at 10.6 microns. A further difference is that while the radiation from the arc is approximately uniformly spread over the target area, the power output from the laser has a gaussian profile and thus is variable across the beam waist - falling from 5.0W at the centre to 0.7W at a radial distance of 2mm from the centre of the beam.

The combustion model described in this chapter has as its principal component a unique concentration of flammable species which experiences a growth/decay balance. Thus, in order for a sample to ignite, a flammable mixture must exist near the surface in sufficient quantity to enable the growth stage to reach a level at which the combustion reactions proceed before the decay stage (due to diffusion and secondary chemical reaction) can dominate.

The power level of the incident radiation determines the composition of the volatile cloud and the type of combustion reactions that occur upon mixing with oxygen. The power level also has an effect on the diffusion rate of the gas cloud, since an increase of power results in a tendency for the production of lighter volatile species and hence increases the diffusion rate.

It is proposed here that the spatially uniform nature of the arc source acts so as to produce a volatile cloud which has a uniform concentration of unique volatile species (determined by the power of the arc) which can combine with oxygen to produce combustion reactions. The laser beam, however, has a spatially dependent power output and, at each point along the beam radius, a different balance of volatile species is produced. Thus the growth/decay balance of flammable species is vari-

able along the beam radius, which does not allow the required flammable species to be produced in a sufficiently high concentration for combustion reactions to occur: only a small area of sample is vaporised.

The dependence of the combustion of the samples on wavelength is another factor worthy of consideration. The arc produces radiation from U.V. to I.R. as well as transfering energy through ion transfer and the transportation of electrode material[9]. The laser has only one wavelength in the I.R. portion of the electromagnetic spectrum. As discussed in chapter 2, wavelengths in the U.V. band of the spectrum have an important role to play in the degradation of cellulose[10], and thus limiting the ignition source to a single wavelength limits the 'ignitability' of that particular source.

7.3 SUGGESTIONS FOR FUTURE WORK.

Having developed a laser system for the investigation of the combustion behaviour of solid materials, it would be desirable to interface the system to the pressure chamber used in the arc experiments. The Dual Pulse Test results presented in chapter 6 could then be duplicated to observe the effect of limiting the wavelength of the ignition source to a single value. There are, however, several problems.

As discussed above, although the irradiance of the laser is similar to that of the arc, the power distribution of the beam is variable across its radius, resulting in non-combustion of the sample under test. This can be overcome by the use of a beam expander[11] which will eliminate the

gaussian profile of the beam, producing a spot of uniform power - this can then be compared directly to the arc source.

The type of interface to the chamber is also a problem. Location of the laser within the chamber would require major structural alterations to the chamber itself; clearly such alterations would be undesirable. An alternative would be to replace the glass of the viewing port with germanium strengthened to withstand a pressure in excess of 6 atm. This substance will transmit I.R. radiation with a negligible amount of attenuation, thus allowing the effect of the variations of environmental conditions (described in chapter 6 in relation to the arc apparatus) on the combustion behaviour of the sample during laser irradiation to be investigated.

A mass spectrometer with capillary sampler in the volatile cloud, close to the surface of the sample during heating, would also provide valuable information and would allow the ideas postulated earlier, concerning the variation of flammable species under differing heating conditions and the existence of a growth/decay balance, to be tested.

7.4 THE IMPLICATIONS FOR INTRINSIC ELECTRICAL SAFETY.

The present experimental programme has gone some way to identifying the physical processes involved in the combustion of a solid material and the effect parameters such as electrical input power, energy, total gas pressure, oxygen concentration and sample thickness have on the combustion characteristics of that material. The results presented

and discussed within this thesis have far reaching implications for electrical safety in hazardous environments, particularly when the existence of a critical pulse delay is considered.

Previous work by Brennan[7] was concerned with employing a single pulse of known power and energy to obtain values for the minimum ignition energy for a cellulosic material. The existence of a critical pulse delay as shown in the present work must modify our concept of the minimum ignition energy, as we now have to consider the distribution of the pulse of energy with time; particularly for circumstances where an intermittent electrical fault giving rise to a sequence of sparks exists. If the electrical fault under consideration supplies energy for ignition at a certain power level and in a single pulse, previous thinking would have us believe that safety would not be compromised if the energy of this pulse was below a minimum ignition level. However, if a second pulse is supplied within the critical delay time for the material in close proximity to the fault, it may reinforce the first pulse giving rise to ignition of the material. Specifying safe limits for the power level and energy of a single spark is no longer adequate. Lower limits must be specified if the spark (pulse) is repeated within the critical delay time.

The critical delay time for electrical ignition decreases with increase of power level, and thus the level of source power is essential when considering safe conditions for the system under consideration. The critical delay is also increased with increase of pressure and oxygen concentration, as is the absolute flammability level of the material; an increase in sample flammability also accompanies an increase of source energy. Thus reductions in one or all of the source power, energy, total pressure and oxygen concentration, will decrease the critical delay for electrical ignition and the material flammability, and will lead to a system which can be regarded as intrinsically safe.

The safety considerations for working with a system which produces a train of sparks, such as with the armature of an electrical machine, will be affected by the existence of the critical pulse delay. The source will produce sparks at a particular frequency, which depends on the rate of revolution of the armature, and hence with a particular delay between successive sparks.

Figure 6.2 specifies that, for air at 1 atm. pressure, if an individual spark has a power level of 55W and an energy of 5J then the system will have a critical pulse delay for the electrical ignition of cellulosic materials of 0.36s. Thus the system is safe for delays greater than 0.36s and any increase in spark frequency which produces a spark delay below the critical value of 0.36s will result in an increased likelihood of ignition for the system. Under these circumstances the system which was previously considered to be safe can no longer be regarded as such.

With the above operation in mind it would be desirable to develop a system for the control of arcing safety. One way in which to achieve this would be to observe the white noise produced by the arc by the use of a high pass filter circuit. The frequency of arcing could be monitored until it increased above a level which corresponds to the critical arc delay. At this point an emergency shutdown facility or a speed reduction operation could be employed to reduce the arcing frequency and hence increase the delay between successive pulses to a value above the critical pulse delay, resulting once again in safe operating conditions.

Figure 6.8 shows that this safe level would be increased from 0.36s to 0.62s for an increase of air pressure from 1 atm. to 2 atm., thus any safety control system would have to allow for the variation of ignition safety with pressure and oxygen concentration as described in chapter 6.

Chapter 6 has, at its heart, the experimental investigation of the ignition safety of materials subject to energy in the form of an electrical arc and a carbon dioxide laser. The effects of oxygen concentration, pressure, source power, energy and in particular the existence of the critical pulse delay (as discussed above) are considered in relation to ignition safety.

As mentioned in section 7.3 one particular property of the incident radiation, that of wavelength, was not investigated experimentally during the present programme and is worthy of future work. It was found that the arc and the laser had different effects on the sample for similar levels of irradiance; one explanation for this may be that whilst

the radiation from the arc consists of a wide bandwidth of wavelengths, the laser is centred on the infra red.

A method for investigating the effect of the source wavelength on the composition of the growth-decay gas balance (and hence combustion behaviour) of the sample, would be to employ several sources of energy each producing radiation having different characteristic wavelengths. The decomposition products could be monitored using a mass spectrometer for each source and the effect of wavelength on the nature of the growth -decay balance and hence the combustion characteristics of the sample could be investigated. some possible sources of radiation could be: the carbon dioxide laser (10 microns), a YAG laser (0.4 microns), an EXCIMER laser (0.4 microns), a microwave source, and the electric arc.

PAGE NUMBERING AS ORIGINAL

7.5 REFERENCES.

[1] Lincoln, K.A., "Flash Pyrolysis of Solid Fuel Materials by Thermal Radiation." Pyrodynamics, 2, pp.133-143. (1965)

[2] Shivadev, U.K., and Emmons, H.W., "Thermal Degradation and Spontaneous Ignition of Paper Sheets in Air by Irradiation." Combustion & Flame, 22, pp.223-236. (1974)

[3] Drysdale, D., "Introduction to Fire Dynamics." Wiley Press. (1985)

[4] Kreysig, E., "Advanced Engineering Mathematics." 5th Edition, Wiley Press. (1983)

[5] Johnson, J.E., and Woods, F.J., "Flammability in Unusual Atmospheres, Part 1. Preliminary Studies of Materials in Hyperbaric Atmospheres Containing Oxygen, Nitrogen, and/or Helium." NRL. Report 6470. (Oct. 1966)

[6] Bartels, A.L., and Howes, J.A., "The Variation of Minimum Igniting Currents withn Pressure, Temperature and Oxygen Enrichment." Electrical Research Association Report. (March 1971)

[7] Brennan, J.F.M., "Ignition of Materials Under Conditions of Hyperbaric High Oxygen Concentration." PhD. Thesis, Liverpool University. (1987)

[8] Tanaka, T., and Ichikawa, K., "Ignition of Materials by Electrical Discharges Under Artificial Atmospheres." 2nd International Conference on Electrical Safety in Hazardous Environments. (Dec. 1975)

[9] Ryalkin, N.N., Kulagin, I.D., and Nikolaev, A.V., "Vaporised Electrode Material and Energy Balance in Welding Arcs." A Symposium, The Institute of Welding. (1962)

[10] Flynn, J.H., Wilson, W.K.,and Morrow, W.L., "Degradation of Cellulose in a Vacuum with Ultra-Violet Light." Journal of Research-N.B.S., 60, pp.229-233. (1958)

[11] Melles-Griot, ""Optics Guide 3." pp.331-343. (1985)

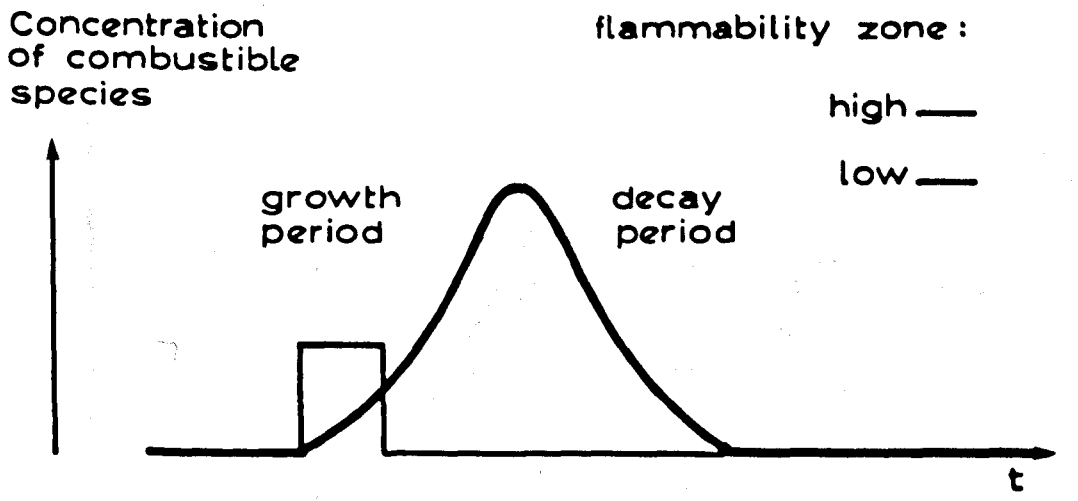

Growth-Decay Curve for a Single Pulse.

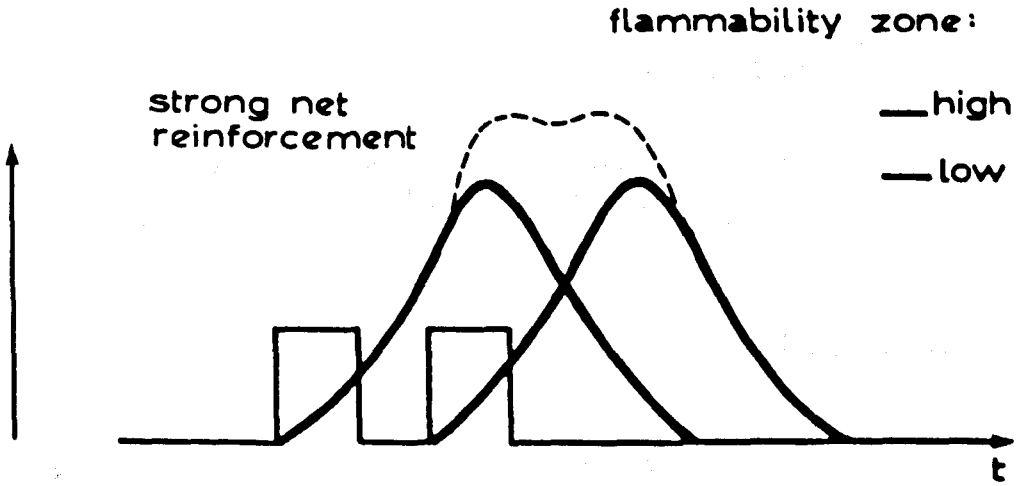

Growth-Decay Curve for Dual Pulse Delay < Critical Delay

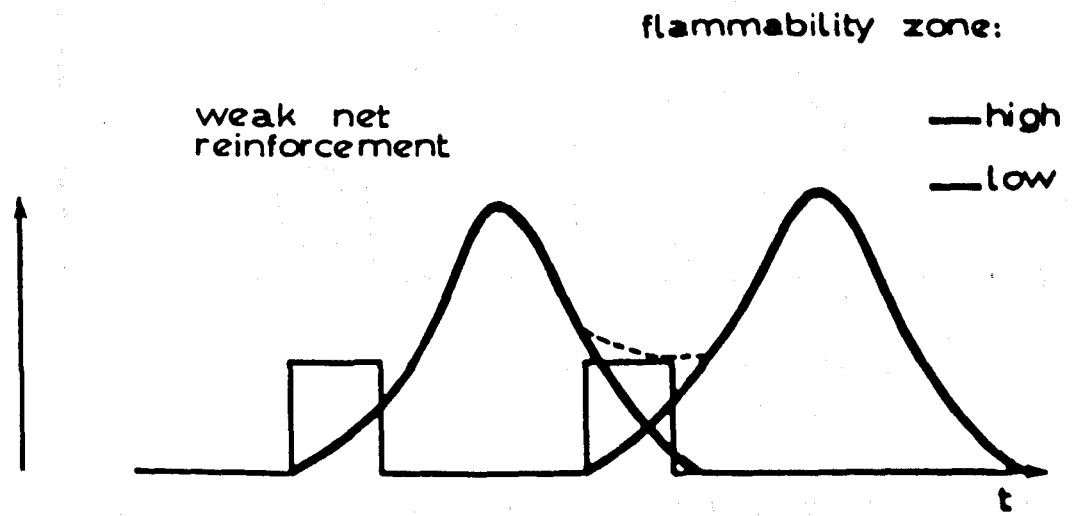

Growth-Decay Curve for Dual Pulse Delay > Critical Delay.

Fig. 7.1. Concentration of Flammable Species Produced During Dual Pulse Test.

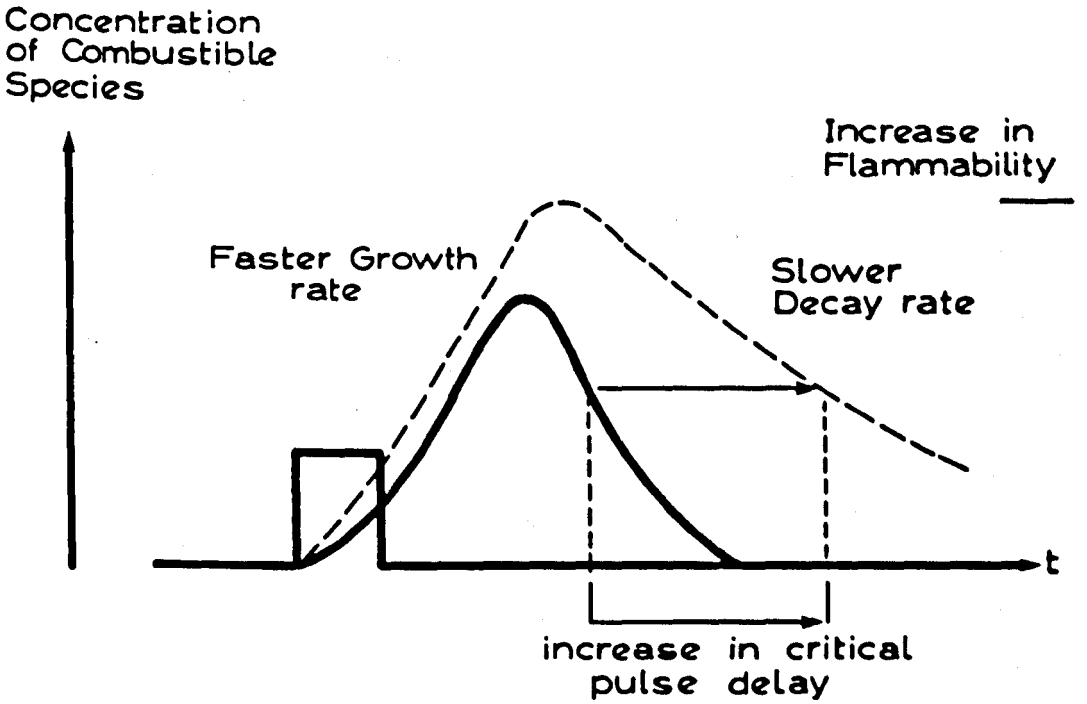

Fig. 7.2. The Effect of an increase of Pressure on the Growth-Decay Curve.

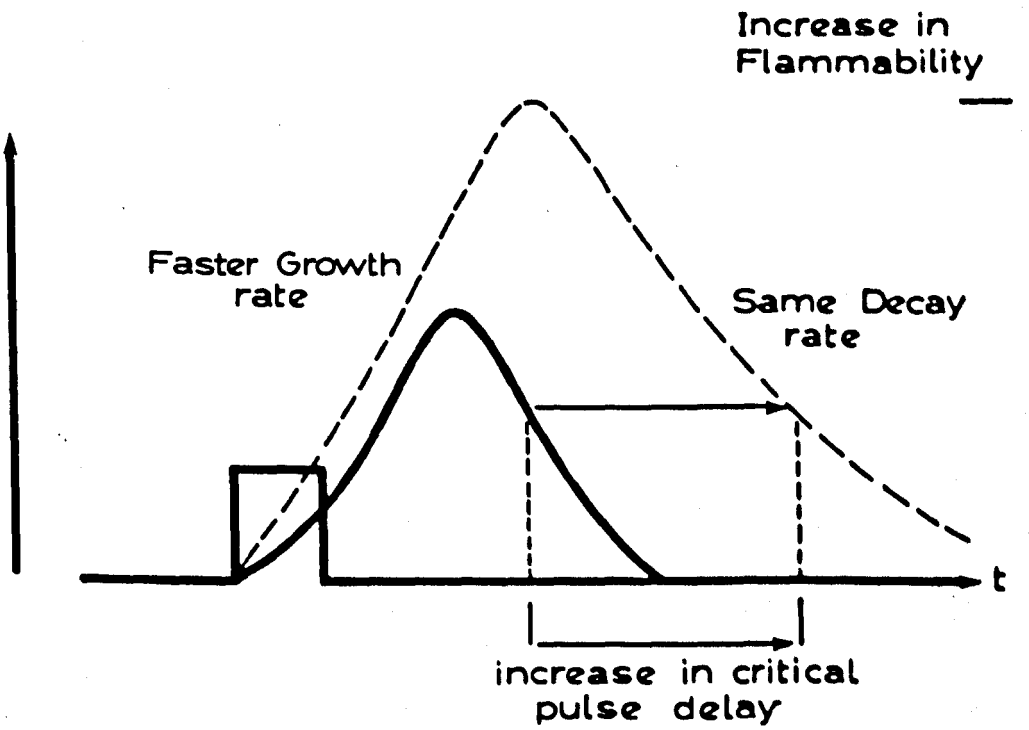

Fig. 7.3. The Effect of an Increase of Oxygen Concentration on the Growth-Decay Curve at Constant Pressure.

APPENDIX A. EXPERIMENTAL ERRORS AND STATISTICAL ANALYSIS.

A.1 ERROR ON A MEASUREMENT.

The measurement of any experimental quantity has an associated error. This may be in the form of a 'random error' in which the inaccuracy is due to the random nature of the observer or experimental conditions, or a 'systematic error' in which the inaccuracy is due to the particular measuring instrument being employed in the experiment. An indication of the error involved with a measurement is given the form;

$$X = A \pm \Delta A \quad \text{Units}$$

where A is the measured experimental parameter and ΔA is an assessment of the degree of accuracy with which the observer is confident of measuring.

A.1.1 Systematic Errors.

The criterion for systematic error assessment used by the observer in the present research programme is normally one-half of the smallest scale division of the measuring instrument employed in a particular experimental situation.

Let us consider the measurement of distance during the present investigation. The diameter of the pressure chamber is measured using a ruler which has a smallest scale division of 0.1cm; thus the diameter is quoted as 19.60 ± 0.05 cm i.e. one half of the smallest division. Similarly the length of the sample is quoted as 2.00 ± 0.05 cm. If we consider the measurement of the electrode gap, d, a feeler gauge is used and thus $d = 0.55 \pm 0.05$ mm; similarly the precision of the Hardinge-Collet lathe, used by the mechanical workshop to manufacture the electrodes, dictates an accuracy of diameter of ± 0.05 mm.

If we consider the accuracy of the pressure gauge attached to the pressure chamber, the smallest scale division is 5 p.s.i. However, it is estimated that the gauge can be read accurately to within ± 1 p.s.i.

The systematic error associated with time measurement during the investigation, such as pulse delay and time to ignition, is due to the accuracy of the scale on the oscilloscope, which varies with any change in the time/div sensitivity.

A.1.2 Random Errors.

The anode and cathode voltages used in the calculation of input power and arc current are subject to a systematic error associated with the storage oscilloscope, however the measurements are principally affected by a random error due to noise on the respective waveforms.

The systematic error involved with each measurement would have been $V_A = 45.0 \pm 2.0$ V and $V_C = 7.5 \pm 0.2$ V, however the dominating

random error gives a more realistic estimate of $V_A = 45.0 \pm 4.0$ V and $V_C = 7.5 \pm 0.4$ V. The calculation of arc voltage, arc current, input power and energy, involves a combination of quantities, all of which have inherent errors. The consequence of these 'compound' errors is resolved by the use of standard error formulae and will be discussed later.

A considerable random error is involved in the measurement of radiant power using the thermopile - due mainly to the variability of the arc energy supply. Refering back to chapter 5, plate 6 shows a typical example of the voltage output of the thermopile, giving a measurement of 2.0 ± 0.3 mV; a 15% error which may be regarded as large, however the output is variable and the present observer believes that such an error estimate is justified in this particular case.

The measurement of probability of ignition and the subsequent measurement of critical pulse delay and zonal probability are subject to statistical errors which will be discussed later with the aid of a specific table of results.

There now follows a discussion of the errors involved with a calculation in which the quantities used possess an independent error.

A.2 ERROR ON A CALCULATION - COMPOUND ERRORS.

It has been shown above that a single measurement has an inherent error, expressed in the form $X = A \pm \Delta A$ units. However, during the present period of research it has been necessary to perform calculations such as arc voltage, arc current, power and energy, in which several

measurements are used, each having an associated individual inaccuracy. The subsequent error analysis is more complex and involves the use of the following standard formulae:

Let $X = A \pm \Delta A$ and $Y = B \pm \Delta B$, be two independent quantities. If $Z = X - Y$ or $Z = X + Y$, then

$$\Delta Z = \pm \sqrt{(\Delta A)^2 + (\Delta B)^2}$$

If $Z = X.Y$ or $Z = \frac{X}{Y}$, then

$$\frac{\Delta Z}{Z} = \pm \sqrt{\left(\frac{\Delta A}{A}\right)^2 + \left(\frac{\Delta B}{B}\right)^2}$$

If $Z = nX$, where n is a constant, then

$$\Delta Z = n\Delta A$$

If $Z = X^2$, then

$$\Delta Z = 2A\Delta A$$

Thus the errors associated with arc voltage, arc current, input power and radiant energy quoted in the course of this thesis have all been obtained using a combination of the above formulae.

A.3 STATISTICAL ERRORS.

The main body of the results contained within this thesis are concerned with the change of zonal ignition probability and critical ignition

delay with varying experimental conditions; results which are subject to statistical variations. The statistical treatment of the results is based on a 'normal distribution' (see Fig A.1) and it will be necessary to establish several definitions before analysing a typical table of results.

A.3.1 The Arithmetic Mean.

The arithmetic mean represents the mid-point of a group or distribution of test scores and is defined as,

$$\bar{X} = \frac{\sum X}{n}$$

where $\sum X$ is the sum of the individual scores, and n is the total number of individual scores.

A.3.2 The Standard Deviation.

The standard deviation is a measure of the average variability around a mean score and gives an idea of the variability of a set of experimental results. It is defined as,

$$\sigma_n = \sqrt{\frac{(X - \bar{X})^2}{n}}$$

In the present programme of research σ_{n-1}, defined as

$$\sigma_{n-1} = \sqrt{\frac{(X - \bar{X})^2}{n - 1}}$$

is prefered to σ_n as the number of tests is not large and $(n - 1)$ provides an unbiased estimate of the spread of results.

A.3.3 The Variability of a Single Ignition Probability.

Table A.1 is an example of the statistical variation observed when repeating a particular test 10 times. The experimental conditions are; air at 1 atm. pressure, for a dual pulse test having $t_1 = t_2 = 0.13s$ and $t_d = 0.32s$. It can be seen that the average ignition probability is 19.0% with a variability of $\sigma_{n-1} = \pm 2.1\%$. This is typical of the statistical variation of a single probability occuring in the high probability zone under conditions of repeated measurement.

A typical example of the statiatical variation of a single ignition probability occuring within the low probability zone can be seen in table A.2. The conditions are the same as above, except that $t_d = 0.37s$. The average probability is 4.8% with a variability of $\sigma_{n-1} = \pm 1.4\%$.

A.3.4 The Variability Over High and Low Probability Zones.

Table A.3 shows a set of results for Fig 6.2, typical of the main body of the results contained within this thesis. From the table and the graph it can be seen that there are two distinct probability zones, with

the transition point between the two dependent upon some critical pulse delay time. The problem encountered is whether or not the transition point is sufficiently independent of the statistical fluctuations within each zone in order to be regarded as a significant change.

Let us consider the high probability zone. The mean probability is 16.0% with a variability of $\sigma_{n-1} = \pm 2.4\%$. A normal distribution is such that 99.6% of values will lie within $\pm 2\sigma$ from the mean, thus any change of ignition probability, from the mean value, greater than $\pm 7.2\%$ can be regarded as a significant event. Similarly within the low probability zone the mean probability of ignition is 4% with a variability of $\sigma_{n-1} = \pm 1.4\%$. In this case a change of ignition probability greater than $\pm 4.2\%$ can be regarded as significant.

As the change in mean probability from high to low is 12%, this can be regarded as a significant event and the pulse delay can justifiably be termed a 'critical' pulse delay.

All of the results concerning the dual pulse test contained within this thesis are treated using the same rigorous statistical analysis described above. It is worth noting that the high and low probability zones are represented by a single line through the mean probability of ignition in order to identify the significant change that is the signature of the critical pulse delay. This is for convenience only and is not meant to mislead or imply that there is no statistical fluctuation within each zone - indeed there is a variability within each zone as described earlier, however it is relegated to second order status in order to identify the critical change described above.

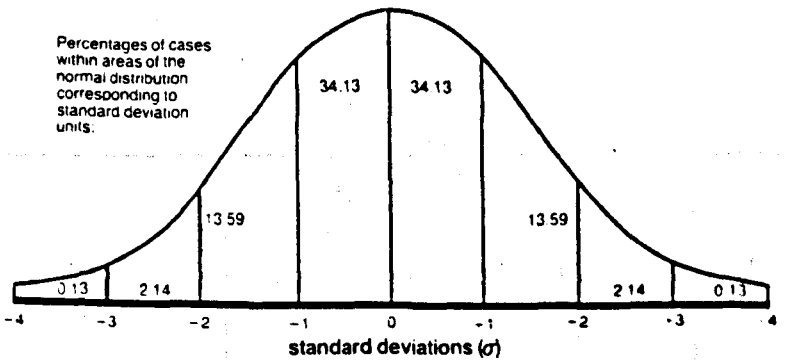

Fig A.1 A Normal Probability Distribution.

Test	1	2	3	4	5	6	7	8	9	10
% Prob	17.5	22.5	20.0	17.5	15.0	20.0	20.0	20.0	20.0	17.5

High Zone: $\overline{X} = 19.0\%$, $\sigma_{n-1} = 2.1\%$.

Table A.1 Variability of a Single Ignition Probability in the High Zone.

Test	1	2	3	4	5	6	7	8	9	10
% Prob	5.0	5.0	2.5	5.0	5.0	7.5	5.0	5.0	5.0	2.5

Low Zone: $\overline{X} = 4.8\%$, $\sigma_{n-1} = 1.4\%$.

Table A.2 Variability of a Single Ignition Probability in the Low Zone.

t_1 (s)	t_2 (s)	t_d (s)	% Ignition
0.13	0.13	0.00	20.0
0.13	0.13	0.02	15.0
0.13	0.13	0.04	15.0
0.13	0.13	0.06	15.0
0.13	0.13	0.08	15.0
0.13	0.13	0.10	15.0
0.13	0.13	0.12	12.5
0.13	0.13	0.14	12.5
0.13	0.13	0.16	15.0
0.13	0.13	0.20	17.5
0.13	0.13	0.28	17.5
0.13	0.13	0.32	20.0
0.13	0.13	0.34	17.5
0.13	0.13	0.37	5.0
0.13	0.13	0.40	5.0
0.13	0.13	0.50	5.0
0.13	0.13	0.90	2.5
0.13	0.13	1.30	2.5

High Zone: $\overline{X} = 16.0\%$, $\sigma_{n-1} = 2.4\%$.

Low Zone: $\overline{X} = 4.0\%$, $\sigma_{n-1} = 1.4\%$.

Table A.3 Variability over High and Low Ignition Probability Zones.

APPENDIX B. CONTROL PROGRAMS.

PROGRAM DUALI

```
 10 *KEY1 GOTO 130|M
 20 *KEY2 GOTO 570|M
 30 *KEY3 GOTO 770|M
 40 END
 50 REM program for the control
 60 REM of a pulsed discharge
 70 REM with variable duration.
 80 REM a stepper motor is employed
 90 REM for multiple sample testing
100 REM discharge duration is
110 REM controlled by means of
120 REM BBC. internal timer
130 INPUT " Duration of Pulse 1 = ",X1," Centiseconds "
140 INPUT " Pulse Delay = ",X2," Centiseconds "
150 INPUT " Duration of Pulse 2 = ",X3," Centiseconds "
160 REM all port b pins are outputs
170 REM and sent low
180 ?&FE62=&FF
190 ?&FE60=&00
200 REM pre-discharge delay of 5 secs
210    X = 500
220 PROCDELAY(X)
230 REM pin 0 high starting pulse 1
240 ?&FE60=&01
250    X = X1
260 PROCDELAY(X)
270 REM pin 1 sent high, also,
280 REM stopping Pulse 1
290 ?&FE60=&02
300    X = 1
310 PROCDELAY (X)
320 ?&FE60=&00
330 REM inter-pulse period
340    X = X2
350 PROCDELAY(X)
360 REM pin 0 high starting pulse 2
370 ?&FE60=&01
380    X = X3
390 PROCDELAY(X)
400 REM pin 1 sent high, also,
410 REM stopping Pulse 2
420 ?&FE60=&02
430 REM delay of 4 secs. Time for
440 REM which 120V supply is off
450    X = 400
460 PROCDELAY(X)
```

```
470 REM all output pins sent low
480 ?&FE60=&00
490 PRINT " END OF DUAL PULSE TEST "
500 END
510 DEF PROCDELAY(X)
520 DELAY=TIME
530 REPEAT UNTIL TIME-DELAY>X
540 ENDPROC
550 REM this program controls
560 REM the stepping motor
570 ?&FE62=&FF
580 REM lines 600 to 720 generate
590 REM 20 pulses to rotate the
600 REM motor through 36 degrees
610 Z = 20
620 ?&FE60=&04
630 REPEAT
640 ?&FE60=&00
650    X = 1
660 PROCDELAY(X)
670 ?&FE60=&04
680    X = 10
690 PROCDELAY(X)
700 Z = Z-1
710 UNTIL Z = 0
720 PRINT " SAMPLE IN POSITION "
730 END
740 REM this program allows
750 REM fine adjustment of sample
760 REM position
770 ?&FE62=&FF
780 Z = 02
790 ?&FE60=&04
800 REPEAT
810 ?&FE60=&00
820    X = 1
830 PROCDELAY(X)
840 ?&FE60=&04
850    X = 10
860 PROCDELAY(X)
870 Z = Z-1
880 UNTIL Z = 0
890 PRINT " FINE ADJUSTMENT COMPLETED "
900 END
```

PROGRAM LASERI

```
 10 *KEY1 GOTO 80|M
 20 *KEY3 GOTO 270|M
 30 END
 40 REM program for the control
 50 REM of the laser.
 60 REM STRIKE SEQUENCE:
 70 REM all output pins low.
 80 ?&FE62=&FF
 90 ?&FE60=&00
100    X = 500
110 PROCDELAY(X)
120 REM LASER INHIBITED:
130 REM pin 0 high.
140 ?&FE60=&01
150    X = 200
160 PROCDELAY(X)
170 REM SAMPLE IRRADIATION:
180 REM all output pins low.
190 ?&FE60=&00
200 END
210 DEF PROCDELAY(X)
220 DELAY=TIME
230 REPEAT UNTIL TIME-DELAY>X
240 ENDPROC
250 REM laser inhibition after
260 REM sample combustion.
270 ?&FE60=&01
280 PRINT "EXPERIMENTAL RUN COMPLETED"
290 END
```

APPENDIX C. THE ELECTROMAGNETIC SCREENING OF THE EXPERIMENTAL APPARATUS.

During the period of research encompassed by this thesis it was found that the BBC microcomputer controlling the experiment and also several IBM PCs being used in adjacent laboratories had a tendency to 'crash' when the arc was being operated. This was correctly attributed to electromagnetic interference caused by the high voltage initiating spark and, after monitoring the mains supply and through the use of mains filters, it was concluded that the interference was airborne.

Several steps were taken in order to minimise the effect of this airborne interference:

1. The position of the equipment was varied in order to increase the distance between the chamber and adjoining laboratories.

2. The experimental apparatus was completely re-wired with major links being screened using sections of copper braide which were earthed to a central 'star point' (this can be seen in the centre of plate 8).

3. The star point was used as an earth reference for the pressure chamber.

4. The arc initiation circuit was enclosed in a box which was also earthed to the star point.

5. The whole apparatus was screened using an earthed partial Faraday cage (part of which can also be seen in plate 8.

These steps solved the problem associated with the IBM PCs: Fig C.1 shows two spectra of the airborne interference taken using a Hewlett-Packard 3582A spectrum analyser, a) with the chamber lid off, and b) with the chamber lid on and the apparatus earthed. It is worthy of note that the above screening process has removed frequencies around the 8MHz level - which is a clock frequency for the IBM PC central processing unit.

This screening process did not entirely solve the problem associated with the BBC microcomputer; this was finally solved by placing the computer within a screened aluminium box which was earthed to the central star point mentioned above.

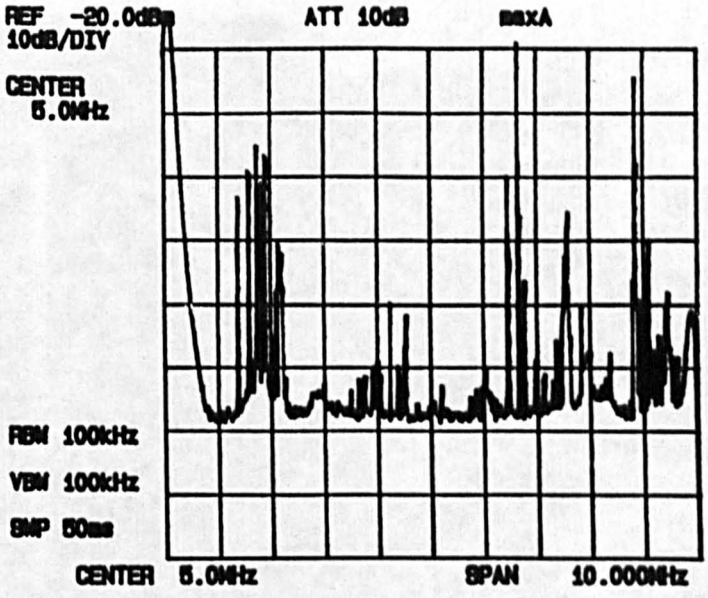

a) Chamber Lid Removed.

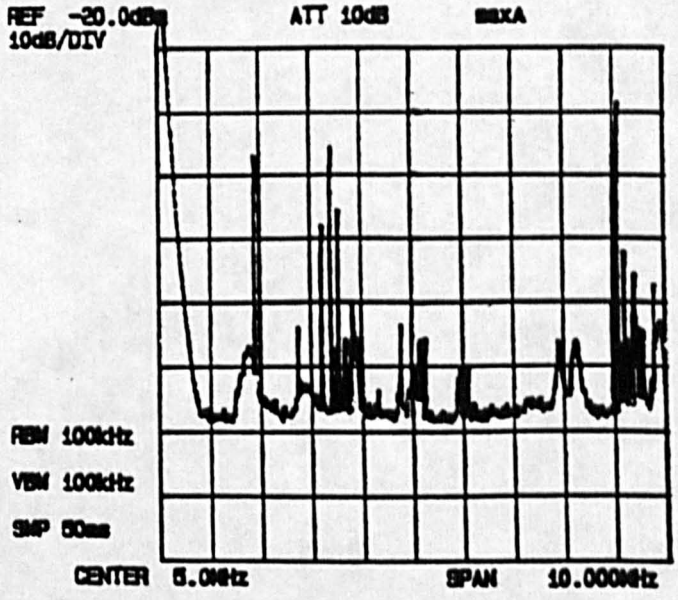

b) Chamber Lid in Position and Apparatus Earthed.

Fig. C.1. Spectra of Airborne Interference.

Plate 8. Electromagnetic Screening of Arc Apparatus.

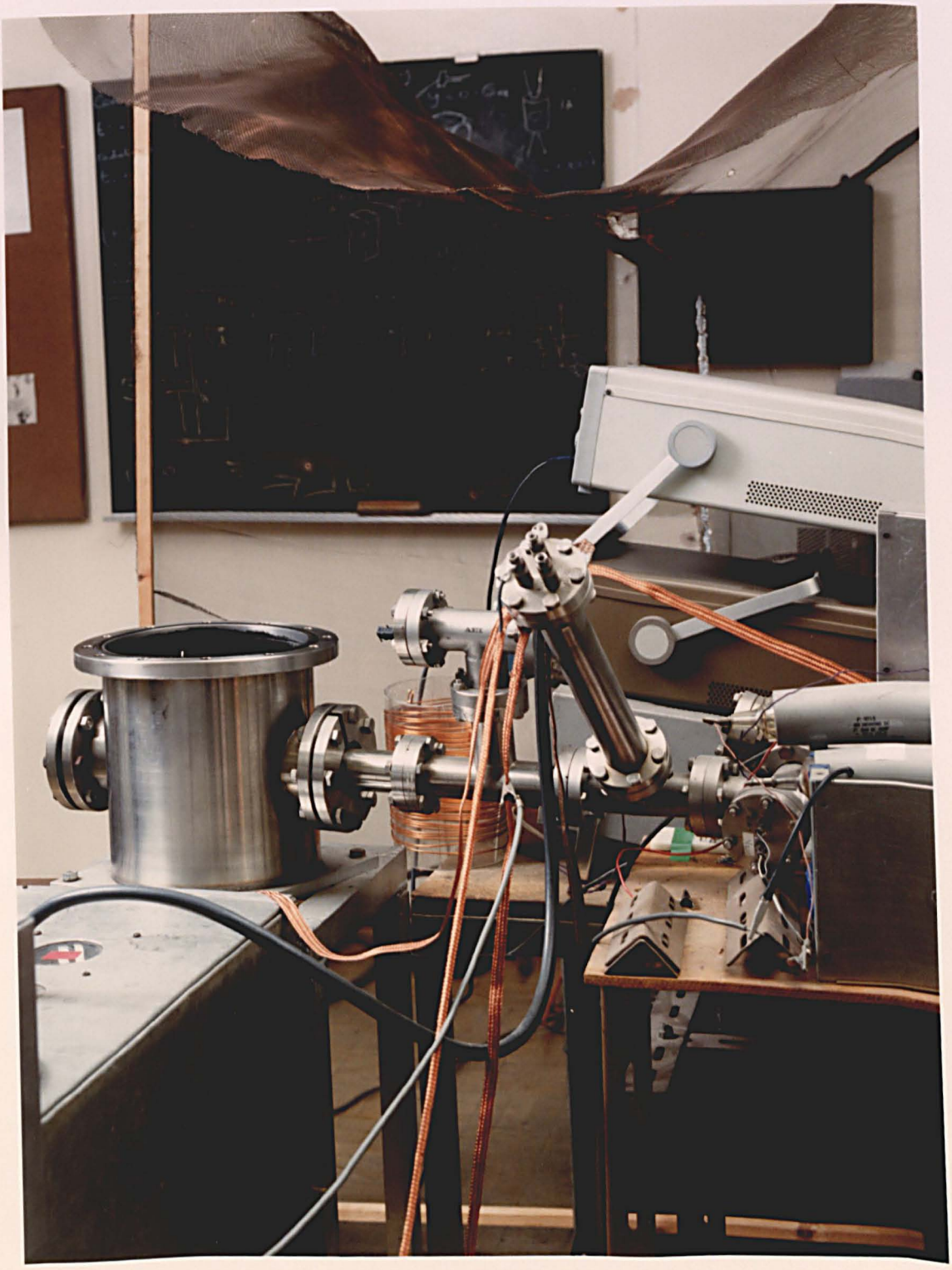

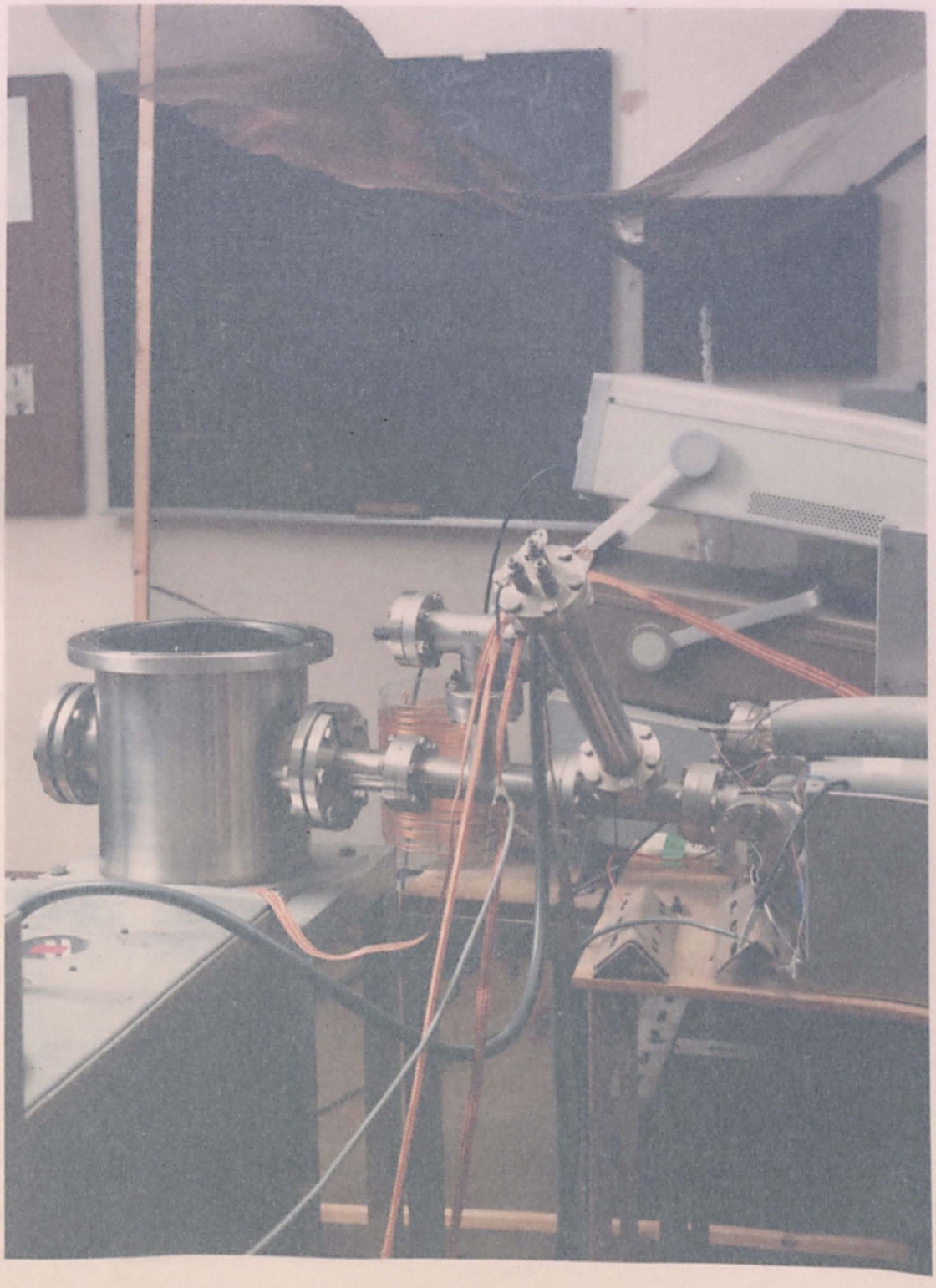

Plate 8. Electromagnetic Screening of Arc Apparatus.